STRATIGRAPHIC SETTING OF SOME NEW AND RARE PHOSPHATE MINERALS IN THE YUKON TERRITORY

A Thesis

Submitted to the Faculty of Graduate Studies and Research in

Partial Fulfilment of the Requirements

For the Degree of

Master of Science

in the

Department of Geological Sciences

University of Saskatchewan

by

Benjamin Telfer Robertson

Saskatoon, Saskatchewan

May, 1980

The author claims copyright. Use shall not be made of the material contained herein without proper acknowledgement, as indicated on the following page.

8020000160727

The author has agreed that the Library, University of Saskatchewan, may make this thesis freely available for inspection. Moreover, the author has agreed that permission for extensive copying of this thesis for scholarly purposes may be granted by the professor or professors who supervised the thesis work recorded herein, or, in their absence, by the Head of the Department or the Dean of the College in which the thesis work was done. It is understood that due recognition will be given to the author of this thesis and to the University of Saskatchewan in any use of the material in this thesis. Copying or publication or any other use of the thesis for financial gain without approval by the University of Saskatchewan and the author's written permission is prohibited.

Requests for permission to copy or to make other use of material in this thesis in whole or in part should be addressed to;

Head of the Department of Geological Sciences
University of Saskatchewan
Saskatoon, Saskatchewan

ABSTRACT

The Big Fish River - Rapid Creek phosphatic iron formation, in the Richardson Mountains, Yukon, is a unique sedimentary deposit of lowermost Albian age. It had an unusual post-depositional history which led to the development of a spectacular phosphate occurrence.

Strata were deposited in an environment without currents but of relatively shallow depth, probably just below storm-wave base. The deposit formed on the west side of the penecontemporaneous Cache Creek High. Fluctuations in sea level, tectonic instability, or a progradational sediment system caused coarsening-upward sequences capped by conglomeratic slump deposits in the lower part of the formation in the Rapid Creek area. The rest of the section in this area represents relatively stable conditions. In the Big Fish River and Boundary Creek areas, differential deposition of autochthonous minerals has resulted in gradational mudstone-shale couplets.

Most rocks of the formation are texturally similar to other phosphate and iron deposits. They are broadly categorized as shale, mudstone, siltstone and sandstone. They are composed of four basic components: pellets and granules, detrital quartz grains, skeletal fragments, and siderite matrix. Mixed phosphate-siderite pellets (as well as granules) and matrix constitute a spectrum from sandstone to mudstone and comprise the major part of the formation.

The rocks were originally composed of detrital quartz and clay minerals and autochthonous siderite, pyrite, and a mixed Ca-Fe-Mg phosphate of uncertain identity. Metamorphism altered the phosphate minerals and remobilized the siderite. In non-pelletal phosphate mudstone, the primary Ca-Fe-Mg phosphate is altered to carbonate-apatite, which occurs together with siderite as pseudomorphs in star-shaped concretionary bodies. In coarser-grained rocks, the primary Ca-Fe-Mg phosphate is altered to satterlyite ($(Fe,Mg)_2 PO_4 (OH)$) which in turn is altered to arrojadite ($K(Na,Ca)_5(Fe,Mn,Mg)_{14} Al(OH,F)(PO_4)_{12}$). Gormanite-souzalite ($(Fe,Mg)_3 (Al,Fe)_4 (PO_4)_4 (OH)_6 \cdot 2H_2O$) is a common alteration (or replacement) in both.

The four major epigenetic, fracture-filling mineral associations are categorized by the persistent occurrence or dominance of one or two characteristic elements in one or more minerals. They are related to particular host rocks: Ca-rich association with phosphate mudstone, Ba-rich with conglomeratic slump deposits, Fe-Mg-rich with siderite sandstone, and Na-bearing with phosphate sandstone. Simple mineral associations (three minerals, or fewer) are related to particular host rocks or represent local accumulations of a restricted number of elements.

The mineralization in the Big Fish River and Boundary Creek areas is largely confined to spherulitic recrystallized replacements of ammonites and pelecypods. Moreover, concretionary

phosphate nodules are present. The minerals in both comprise pyrite, wolfeite ($(Fe,Mg)_2PO_4(OH)$), satterlyite, maricite ($NaFePO_4$), vivianite-baricite ($(Fe,Mg)_3(PO_4)_2 \cdot 8H_2O$), varulite ($(Na,Ca)(Mn,Fe)_2(PO_4)_2$), and their alteration products.

Nahpoite (Na_2HPO_4), a new mineral which occurs as a white powdery alteration product of maricite in some nodules at Big Fish River, was identified for the first time during this study.

TABLE OF CONTENTS

PAGE

PAGE

* for logistic reasons, the diacritical mark in 'baricîte' and 'maricîte' has been deleted in the text.

List of Tables

List of Figures

PAGE

List of Plates

INTRODUCTION

Purpose of investigation

The Big Fish River - Rapid Creek phosphatic iron formation has aroused great interest among mineralogists in recent years because of its spectacular phosphate minerals. Attention was first drawn to this area when F. A. Campbell (1962) identified lazulite, a hydrous magnesium, iron, aluminum phosphate, in samples recovered by B. Cameron from the bed of Blow River.

Regional geological mapping was carried out intermittently from 1970 to 1976 by F. G. Young (1977), formerly of the Geological Survey of Canada. His first detailed report (1972) showed the existence of an extensive iron formation in the region. This led Welcome North Mines to claim large tracts of land in the area. In the process of staking claims, several macroscopically well crystallized phosphates were noted by A. Kulan, who led the company field party. He later staked his own claims and began mining the minerals for sale to collectors and museums. During this work, Kulan was joined by members of the staff of the Royal Ontario Museum who helped with the identification of the minerals found there. Since then, J. A. Mandarino and B. D. Sturman (1976, 1977, and 1978) have identified seven new mineral species. Full descriptions of five of these have already been published. As well as the new

minerals, a number of other rare phosphates occur in the area in exceptionally well crystallized forms.

So far, no attempts have been made to correlate the mineral occurrence of the area with its geology. This study was undertaken to provide an understanding of the stratigraphy and petrography of the phosphatic iron formation that contains these rare minerals. It is hoped that from this a groundwork can be laid for future formal nomenclature and that some understanding can be obtained of the origin of these minerals and the reason for the localization of their occurrence within particular strata.

Geography

The eastern flank of the Richardson Mountains is characterized by relatively low, rounded hills trending north-south in a rolling plateau. The highest peak in the study area is Mount Davies Gilbert at 821 m (2693 ft.). The plateau ranges from 150 m (500 ft.) to 300 m (1000 ft.) in elevation. The area is dissected by several meandering creeks and rivers which cut 150 m into the surrounding plateau. The principal outcrops are located along three streams: Rapid Creek (and its tributaries), Big Fish River, and Boundary Creek (Figure 1).

Alpine tundra covers most of the plateau and hills. In the stream valleys on stable sand and gravel bars, willows sometimes take root and provide the tallest vegetation in the area. From

Figure 1

Location map. The areas delineated in rectangular outline are enlarged in other illustrations; 1 = Figure 7, 2 = Figures 5 and 10, and 3 = Figure 9. The letters A, B1, B2, and C denote the main sites of this investigation; Cross-cut Creek and lower Rapid Creek, the 'Big Bend' on Big Fish River, Boundary Creek, and upper Rapid Creek, respectively. Site C is also referred to as Area 7 in the text.

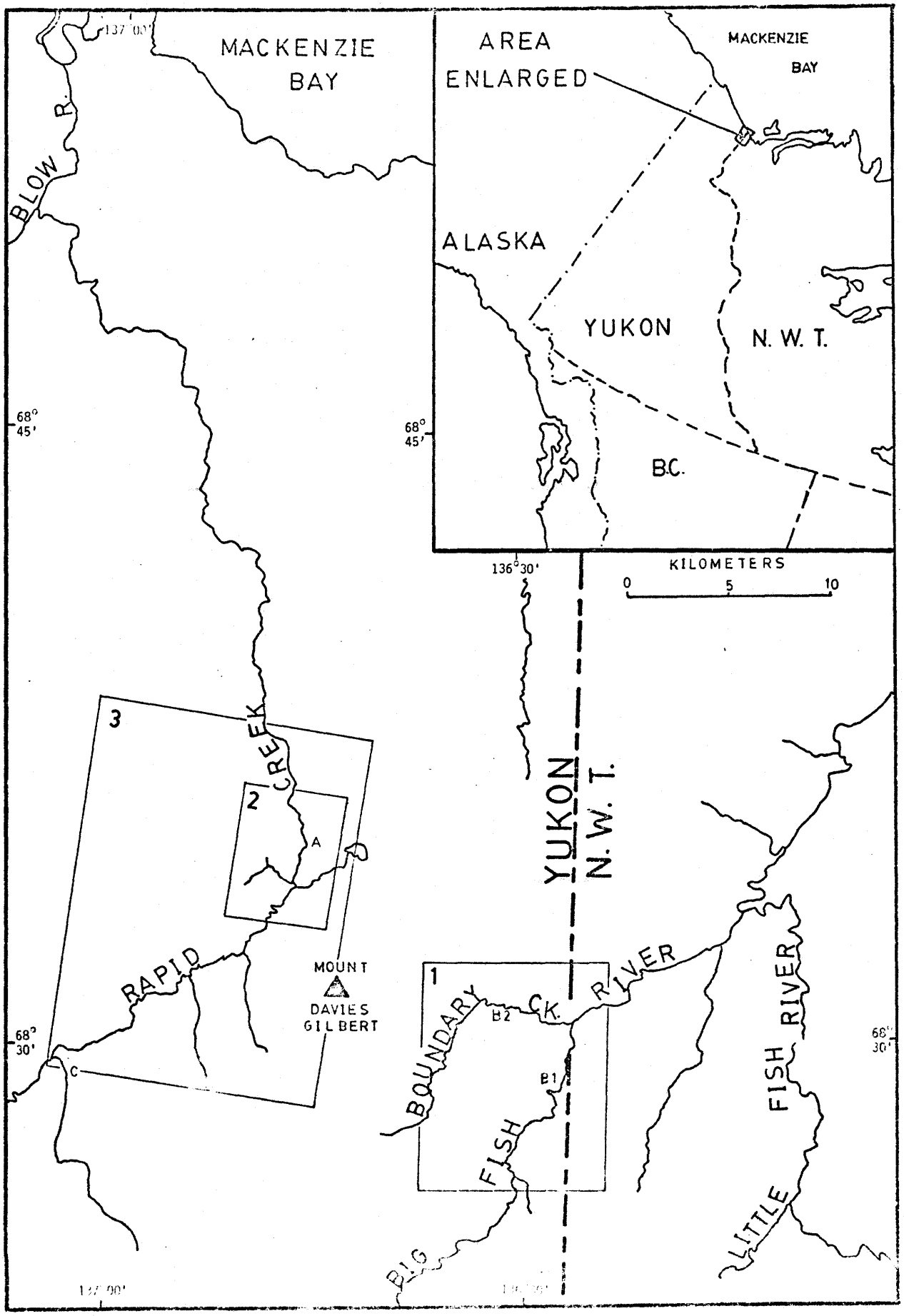
MACKENZIE BAY
AREA ENLARGED
MACKENZIE BAY
ALASKA
YUKON
N. W. T.
B.C.
BLOW R.
137° 00'
68° 45'
136° 30'
KILOMETERS
0 5 10
YUKON
N.W.T.
3
2
1
CREEK
A
RAPID
MOUNT
DAVIES
GILBERT
C
68° 30'
BOUNDARY
CK.
B2
B1
RIVER
FISH
FISH RIVER
LITTLE
BIG
137° 00'

early June to late August the weather permits field work with twenty-four hour daylight. Precipitation is generally light. Snow may occur in early June but the temperatures in mid-July may reach as high as 30°C. There are several permanent snow drifts in the area, particularly in the deep and narrow parts of stream valleys.

At present, the only means of access is a forty-five minute flight from Inuvik, N.W.T., by charter helicopter or by float-equipped fixed-wing aircraft to one of the few small lakes. Seismic crews have driven as far as Rapid Creek, but only after freeze-up.

General Geological Setting

For a complete review of the general geology of the Beaufort-Mackenzie Basin, see Young et al. (1976).

The pericratonic Beaufort-Mackenzie Basin is located at the very northwestern part of the Canadian continental margin. It is bounded by that margin in the north, by the Romanzoff Uplift in the west, and the Aklavik Complex in the southeast. It underlies the MacKenzie Delta, Tuktoyaktuk Peninsula, Yukon Coastal Plain, and northern Richardson Mountains and encloses about 155,000 km^2 (60,000 sq. mi.). The basin has been classed as a Mesozoic and Cenozoic 'successor' basin which is stratigraphically and structurally discordant above pre-Mesozoic rocks and displays a classical geosynclinal character in the

depositional phases of the clastic terrigenous rocks from Triassic to the present (Young et al., 1976).

The Keele-Old Crow Landmass (Figure 2) (Jeletzky, 1971a and 1972) is a Late Jurassic to Early Cretaceous eastward extension of the Brooks Range of Alaska. It abuts against the north trending Blow Trough, termed 'Porcupine Plain-Richardson Mountains Marine Trough' by Jeletzky (1975b), which, through the Keele-Kandik Trough, connects with the east-central Alaska Kandik Basin (Young et al., 1976).

The Cache Creek High is part of the Aklavik Arch Complex (Yorath and Norris, 1975) which was first termed 'Aklavik Arch' by Jeletzky (1961). During Jurassic and Early Cretaceous time, it was a positive element and strongly influenced sediment distribution in the Beaufort-MacKenzie Basin.

The Rapid Fault Array (Norris, 1974; Yorath and Norris, 1975) is probably an extension of the large right-lateral strike-slip Kaltag-Porcupine Fault. It consists of a number of surfaces along which there have been substantial vertical movements with probable right-lateral components. Young (1974) has shown that pre-Aptian activity in part of this array (the Blow Fault Zone) was responsible for early vertical movements in the Blow Trough. Young et al (1976) believe that the Rapid Fault Array persisted as a major tectonic element and strongly influenced Aptian and Albian sedimentation in the trough. The

Figure 2

Tectonic elements. Dashed line = arch axis, solid line = uplift margin, dotted line = trough axis, and dashed wiggly line = fault trace (from Young et al, 1976, p. 4 and 5, Figures 2 and 3).

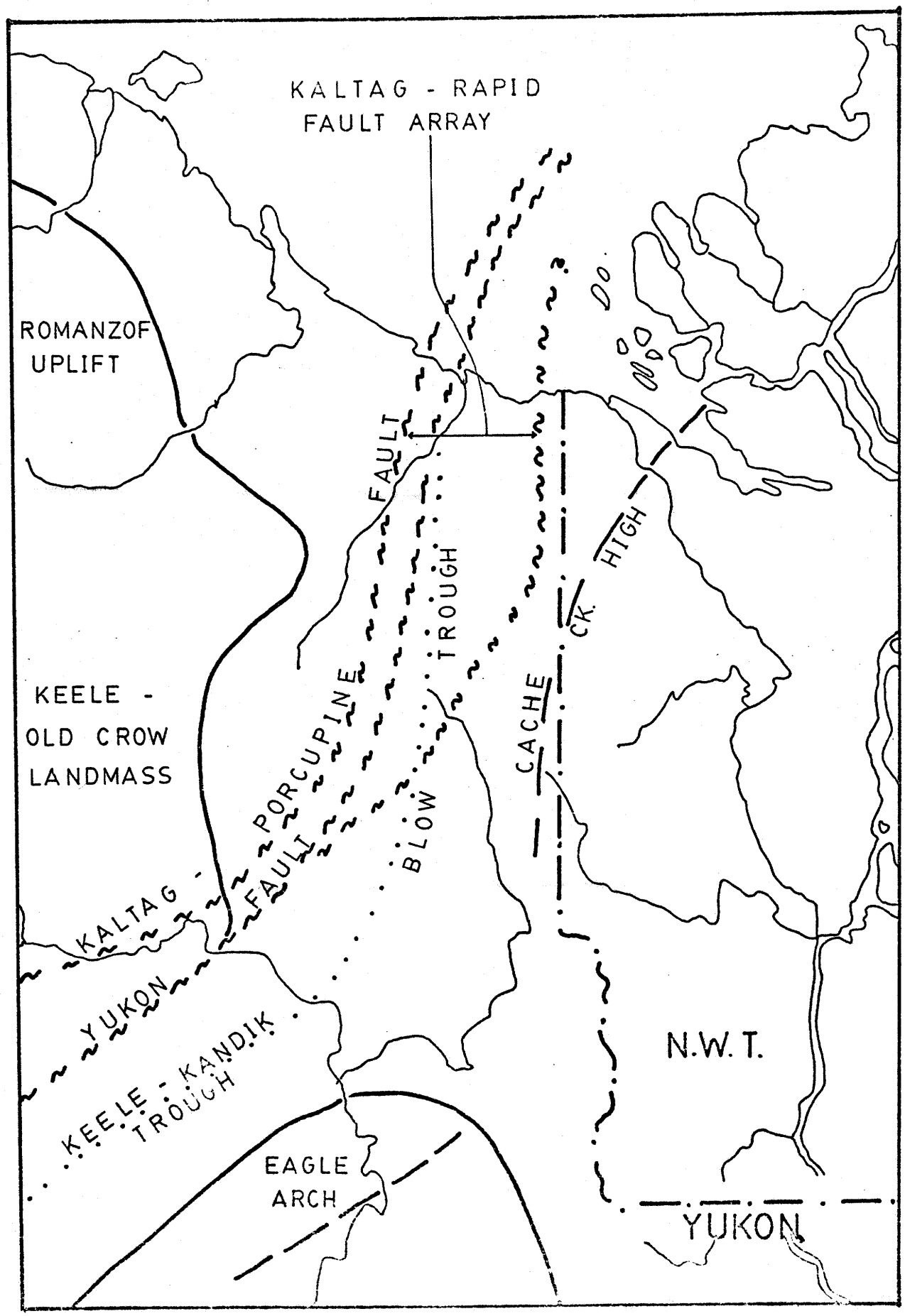
KALTAG - RAPID
FAULT ARRAY
ROMANZOF
UPLIFT
FAULT
TROUGH
HIGH
CK.
CACHE
BLOW
PORCUPINE
FAULT
KALTAG -
KEELE -
OLD CROW
LANDMASS
YUKON
KEELE - KANDIK
TROUGH
EAGLE
ARCH
N.W.T.
YUKON

array was reactivated during Laramide tectonism with the addition of the Yukon Fault.

In Early Albian time, the Beaufort-MacKenzie Basin was the site of major marine transgression which spread far into the North American interior along the Western Canada Seaway (Jeletzky, 1971b). During this time the Brooks Range Geanticline was being uplifted and the Blow Trough downwarped. The geanticline, represented by the Keele-Old Crow Landmass, shed great volumes of sediment eastward which resulted in the deposition of a thick flyschoid sequence in the Blow Trough (Figure 3). The flyschoid sequence thins rapidly eastward onto the Cache Creek High where its equivalent consists of shale and phosphatic iron carbonate rocks (Young, 1975). Subsequent to filling, the trough was elevated and later structurally deformed.

The Cache Creek High was reactivated by Laramide tectonic activity and resulted in the present day Richardson Mountains. Young (1977) has divided the northern Richardson Mountains into four structural blocks along major north-trending vertical faults which make up part of the Rapid Fault Array. The phosphatic iron formation is present in three of these; Rapid Creek, Mount Davies Gilbert, and Big Fish River; but only the latter two blocks were examined in this study. Within these blocks, relatively minor northeast-trending faults further dissect the moderately folded strata.

Figure 3

Albian paleogeography. The cross-hatched area indicates the approximate location of phosphate-rich sediments.

1 = dominantly shale

2 = interbedded shale and sandstone

3 = dominantly sandstone

4 = greater than 10% conglomerate

5 = interbedded shale and sideritic mudstone

(modified from Young et al., 1976, p. 27, figure 11)

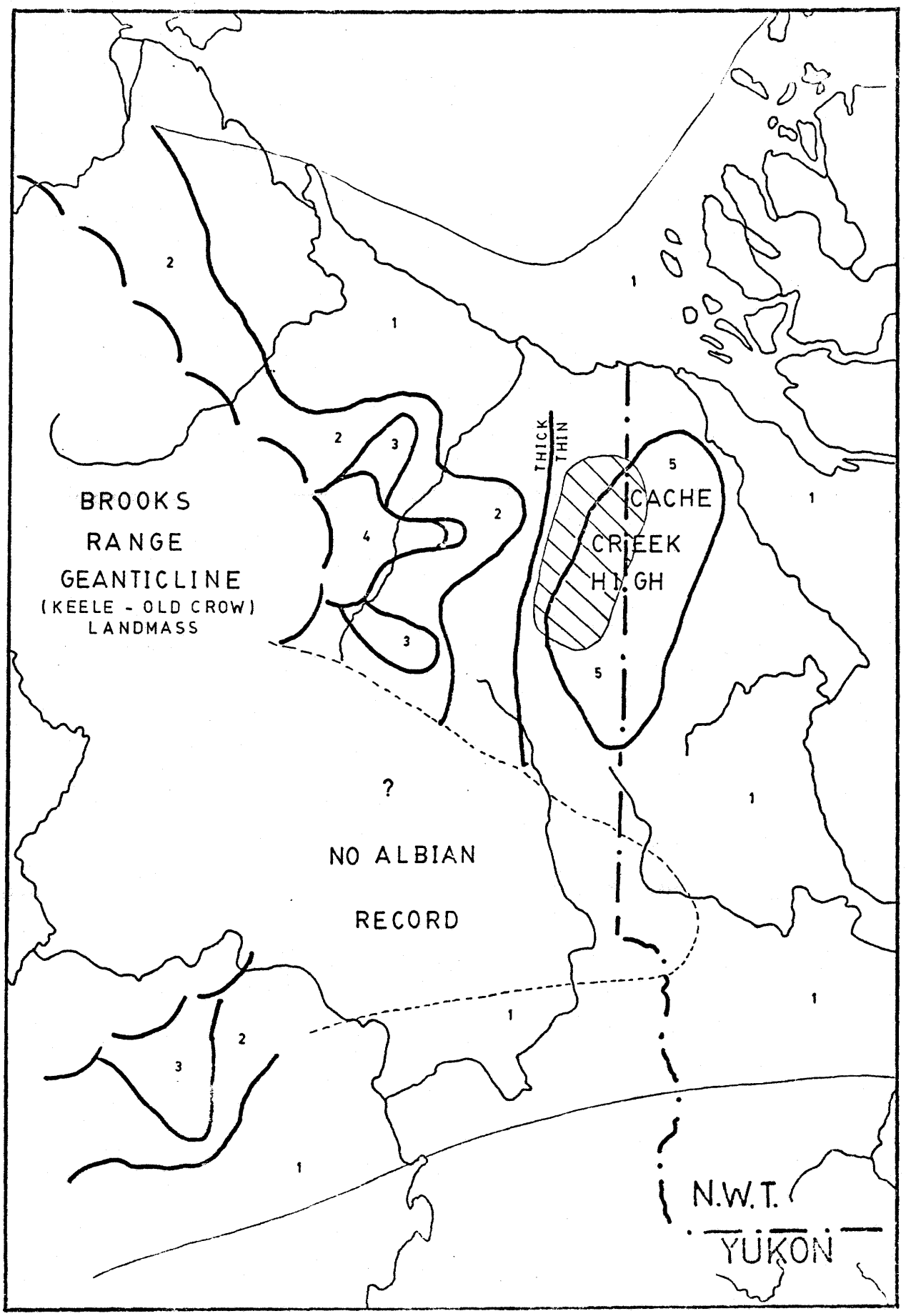
BROOKS
RANGE
GEANTICLINE
(KEELE - OLD CROW)
LANDMASS
THICK
THIN
CACHE
CREEK
HIGH
?
NO ALBIAN
RECORD
N.W.T.
YUKON

Figure 4

Correlation chart (modified from Young et al., 1976, p. 8 and 9, Table 1 and scaled with respect to stage boundaries according to Van Hinte, 1976).

The Upper Shale-Siltstone division is more commonly referred to as the Upper Siltstone Division.

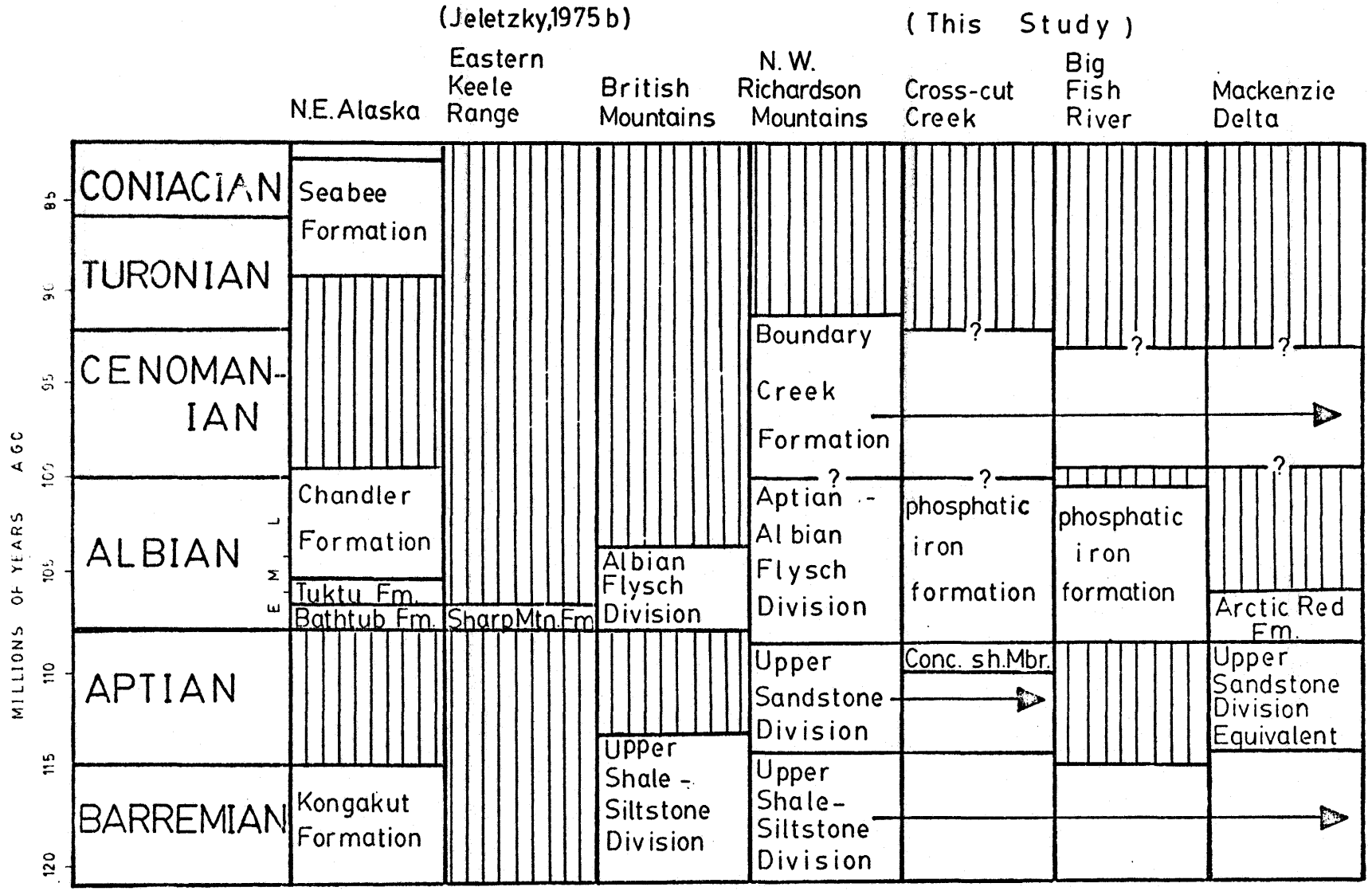
(Jeletzky,1975 b)
(This Study)
N.E. Alaska
Eastern Keele Range
British Mountains
N. W. Richardson Mountains
Cross-cut Creek
Big Fish River
Mackenzie Delta
MILLIONS OF YEARS AGO
CONIACIAN
TURONIAN
CENOMAN-IAN
ALBIAN
APTIAN
BARREMIAN
E M L
Seabee Formation
Chandler Formation
Tuktu Fm.
Bathtub Fm.
Kongakut Formation
Sharp Mtn. Fm
Albian Flysch Division
Upper Shale - Siltstone Division
Boundary Creek Formation
Aptian - Albian Flysch Division
Upper Sandstone Division
Upper Shale - Siltstone Division
phosphatic iron formation
Conc. sh. Mbr.
phosphatic iron formation
Arctic Red Fm.
Upper Sandstone Division Equivalent

The phosphatic iron formation correlates with the Aptian-Albian Flysch Facies (Young, 1972) to the west (Figure 4). It grades into the Arctic Red Formation on the east side of the Cache Creek High. The entire Albian record is eroded and missing to the south except in the Porcupine River region where the Sharp Mountain Formation is equivalent in age (Jeletzky, 1975a).

Acknowledgements

This thesis is submitted to the University of Saskatchewan in partial fulfillment of the requirements for the Master's degree. Financial support was provided by the Institute for Northern Studies, in the form of a scholarship to the author and a grant to L. C. Coleman. The Western Canada Scientific Research Center, a foundation supported by D.I.N.A.-N.W.T., provided field equipment and in-transit services. The Polar Continental Shelf Project provided some equipment and helicopter support and much appreciated radio contact. The Department of Indian and Northern Affairs (Geology Section - Yukon) and Petro-Canada both provided considerable helicopter support. The Department of Geological Sciences, University of Saskatchewan, provided funds for chemical analyses.

The study was carried out under the supervision of Professor L. C. Coleman. His guidance, critical reading of the manuscript, and advice in the field are greatly appreciated.

Other faculty in the Department of Geological Sciences, University of Saskatchewan, particulary N. T. Arndt, H. Hendry, W. K. Braun, and R. W. Forester, provided valuable advice during the course of the work.

The writer wishes to thank B. D. Sturman, for his instruction in the mineralogy of this area, both in the field and at the Royal Ontario Museum, and for supplying a probe standard; H. G. Ansell (Geological Survey of Canada) for his advice and comment in the field; P. B. Moore (Univerity of Chicago) for several excellent probe standards; and F. G. Young (Home Oil - formerly of the Geological Survey of Canada), for suggesting this area for study and acting as a useful sounding board throughout its progress.

The writer also wishes to acknowledge the support from his wife, Alyson, who prepared and drafted many of the figures in this text; and Debbie Jones who prepared the manuscript.

METHODS

Field Work

In the summer of 1978, after an initial week reconnoitring the area in the company of B. D. Sturman and R. Ramik of the Royal Ontario Museum, the writer spent five weeks logging and sampling the section at both Big Fish River and Rapid Creek and in detailed examination of the vein type phosphate occurrences in the Rapid Creek area. Another three weeks were spent in the Big Fish River and Rapid Creek areas in 1979 reexamining portions of the section and carrying out further sampling. During that time the section at Boundary Creek was examined and sampled for nodules during two visits.

The sections at Big Fish River and Cross-cut Creek were measured, described, and sampled at about one meter intervals. Besides this, rock and mineral samples from six other areas (Figure 5) were collected but, because of incomplete or disturbed strata, the sections in these areas were not logged. Shale samples for micropaleontological study were collected over five meter intervals from the Cross-cut Creek section. These were obtained for part of another study being carried out at the University of Saskatchewan by S. Fowler (results not available to date). Sampling for petrographic study was generally confined to the competent beds of sandstone and varieties of

Figure 5

Location of sampling areas. Circled areas along Cross-cut Creek refer to mineralized zones 1 to 3, respectively, from west to east. Other areas (1 to 6) are denoted with numbers. Area 7 is not shown but is denoted with a 'C' on Figure 1.

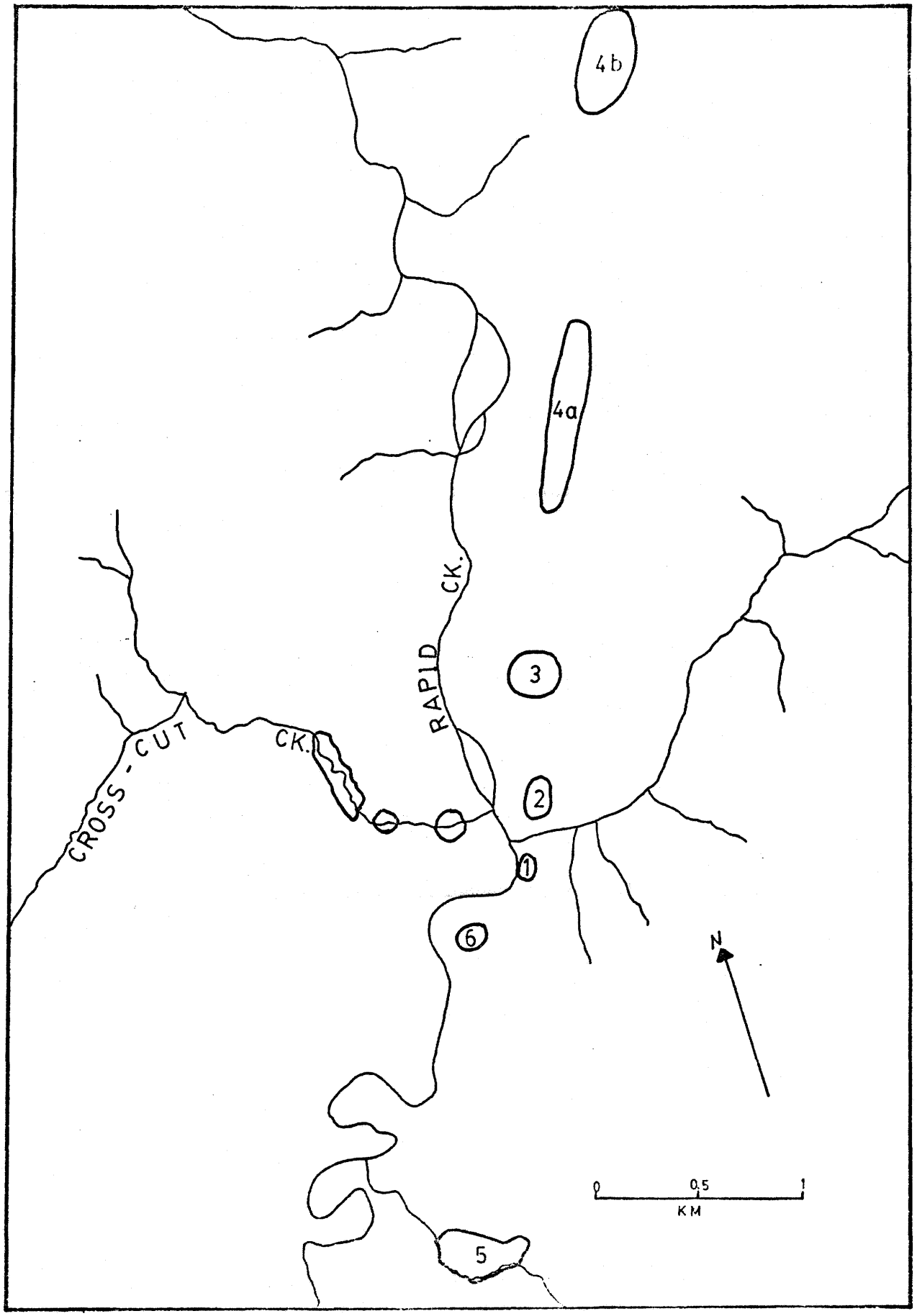
4b
4a
3
2
1
6
5
RAPID CK.
CROSS-CUT CK.
N
0
0.5
1
KM

mudstone. Occasionally other rock types were sampled throughout the sections.

In each area studied, a complete suite of minerals was collected. In cases where a given mineral displayed different habits in different veins or where it occurred with different associations in the same area, specimens were collected that were related to these varied aspects.

Laboratory Work

Initially, over 200 thin sections were examined. These represented specimens at five meter stratigraphic intervals for most of the section, specimens collected at approximately one meter intervals for portions of the section of particular interest, specimens of all types of phosphate nodules (approximately 30 thin sections) and some of the vein-type phosphate occurrences. Samples used for oxygen and carbon isotopes, elemental migration studies and for whole rock analyses were also examined in thin section.

Mineral specimens which had been tentatively identified macroscopically in the field were later examined in more detail in the laboratory with a binocular microscope and the identities of selected grains and crystals were confirmed by x-ray diffraction. The prime constituents of finer-grained materials were also identified by x-ray diffractometry.

Since many of the minerals in this occurrence are solid solution series, compositions of specific samples were determined by electron microanalysis. The details of this procedure and results are given in Appendix II. The composition of several minerals in the coarser grained rocks was also determined with the microprobe.

Whole rock analyses were made at the University of Regina by B. Watters. Major and minor elements, Si, Ti, Al, Fe, Mg, Ca, P, Ba, Sr, Zn, Cu, V, and Y, were determined by inductively coupled argon plasma spectrometry. These values have a 2% error for the value quoted. Other elements, Mn, Na, K, and Rb, were determined by atomic absorption spectrometry and have an error of about 3%, for the first three, and about 5 ppm, for Rb. In all analyses, determined values are well above the detection limits.

An investigation of the carbon and oxygen isotopes of siderite from rock samples was initiated during this study. A procedural problem, however, has precluded the presentation of final results in time for this dissertation but will be published at a later date. Preliminary results are presented in the text where they are applicable.

An investigation of fluid inclusions in vein-quartz from both the Big Fish River and Boundary Creek areas was attempted in order to determine a minimum temperature of vein-mineral

formation. The size of these fluid inclusions was deemed too small for quantitative analysis (J. Hoeve, Saskatchewan Research Council, pers. comm.).

P A R T I

STRATIGRAPHY

Introduction

New and rare phosphate minerals occur in an Albian phosphatic iron formation in the northeastern Richardson Mountains. Two complete sections of the phosphatic iron formation were examined in this study: the first on the "Big Bend" of Big Fish River (Lat. 68°28'N and Long. 136°29'W), in the middle of the Big Fish River structural block (Young, 1977) and at approximately the center of the penecontemporaneous Cache Creek High; the second along the informally named "Cross-cut Creek" (Lat. 68°46'N and Long. 136°34'W), a tributary to Rapid Creek, in the middle of the Mount Davies Gilbert structural block (Young, 1977) and on the western flank of the high. Other areas examined include Boundary Creek (Lat. 68°31'N and Long. 136°32'W) and on Rapid Creek (Lat. 68°30'N and Long. 136°58'W). In the study area, the phosphatic iron formation comprises the total equivalent of the Atpian-Albian Flysch Division (Young, 1977). Because only two complete sections of the formation have been studied, no attempt has been made to formalize the nomenclature of these strata.

Several terms used in this section are defined on pages 55 to 59.

Age and correlation

Inoceramus ex gr. and I. anglicus-cadottensis, both pelecypods, and ?Sonneratia n. sp., an ammonite, found by Young (1977) in the Big Fish River area and identified by J. A. Jeletzky, indicate an Early Albian age for this strata.

Only very poorly preserved ammonites and pelecypods, completely replaced by phosphate minerals or pyrite, were found during the present investigation in the lower 30 m of the Big Fish River section or in talus derived from the lower 30 m (Figure 6). Dr. Jeletzky of the Geological Survey of Canada identified Sonneratia (s. lato)? sp. ex aff., Sonneratia (s. lato)? n. sp. indet. A of Jeletzky (1964), Inoceramus anglicus Woods, I. cf anglicus Woods and Pholadomya sp. indet. and stated that this assemblage is widespread in the lower Albian of Western Canada (Jeletzky, pers. comm.). He states further that the Sonneratia A Zone correlates with the very lower part of the Leymeriella tardefurata Zone of Europe and thus is assigned an Earliest Albian age.

A single vertebra found in talus derived from the lower 30 m of the Big Fish River section was identified by T. SkwaraWoolf (pers. comm.) as a posterior (one of the last lumbar or one of the first caudal) vertebra of a member of the family Mosasauridae.

Samples collected from this section yielded meagre microfauna. A fish scale, genus unknown, was obtained from the

top of the lower ironstone unit of the Big Fish River section (78 m from base).

Big Fish River

At Big Fish River, the Albian phosphatic iron formation is easily distinguished from other units by its cliff-forming character and white coating of dypingite. The measured section is located on one of the few accessible ridges at the northeastern corner of the "Big Bend" (Figure 6). The area (Figure 7) has several moderate normal faults with less than one hundred meters displacement and one minor thrust fault with a few tens of meters displacement. There are several large slump blocks present and virtually every accessible outcrop shows signs of small-scale faulting with displacements ranging from a few millimeters to several centimeters.

The section between the base of the lowest bed of phosphatic mudstone and the top of the uppermost ironstone bed is 160 meters thick (Figure 8). The upper contact with the Boundary Creek Formation (Young, 1975) appears to be transitional at most outcrops. At one outcrop, open folds in the uppermost beds of the iron formation have been truncated by later strata. There may be an angular unconformity with the Boundary Creek Formation, or the top of the phosphatic iron formation may be slumped. The lower contact is unconformable but is not immediately apparent in outcrop. It is observed best

Figure 6

The 'Big Bend' on Big Fish River and measured section location. Numbers refer to fossil locations:

1 = vertebra

2 = ammonites and pelecypods in talus derived from the lower 30 m of the iron formation

3 = same as 2, but ammonites only

4 = same as 3 but located 30 m from the base of the measured section

5 = fish scale found at the top of the lower ironstone

6 = plant remains at the top of the iron formation

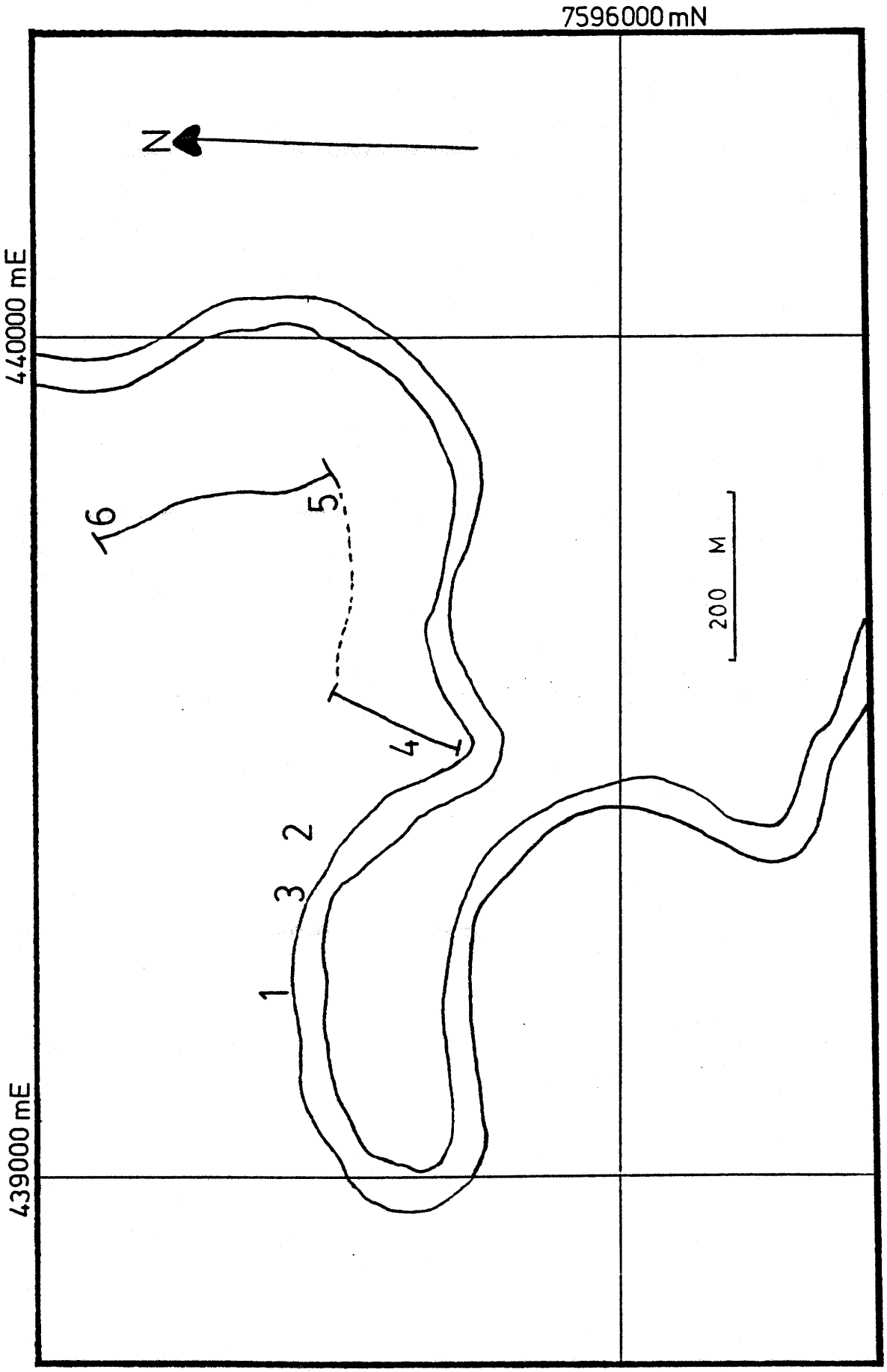
7596000 mN
N
440000 mE
439000 mE
16
5
4
2
3
1
200 M

Figure 7

General geology of the Big Fish River and Boundary Creek areas. Dashed wiggly lines delineate faults; solid lines delineate contacts between formations; dashed lines delineate uncertain contacts.

K_{bc} = Boundary Creek Formation

K_{if} = phosphatic iron formation

K_{usd} = Upper Siltstone Division

JK = Lower Cretaceous and older

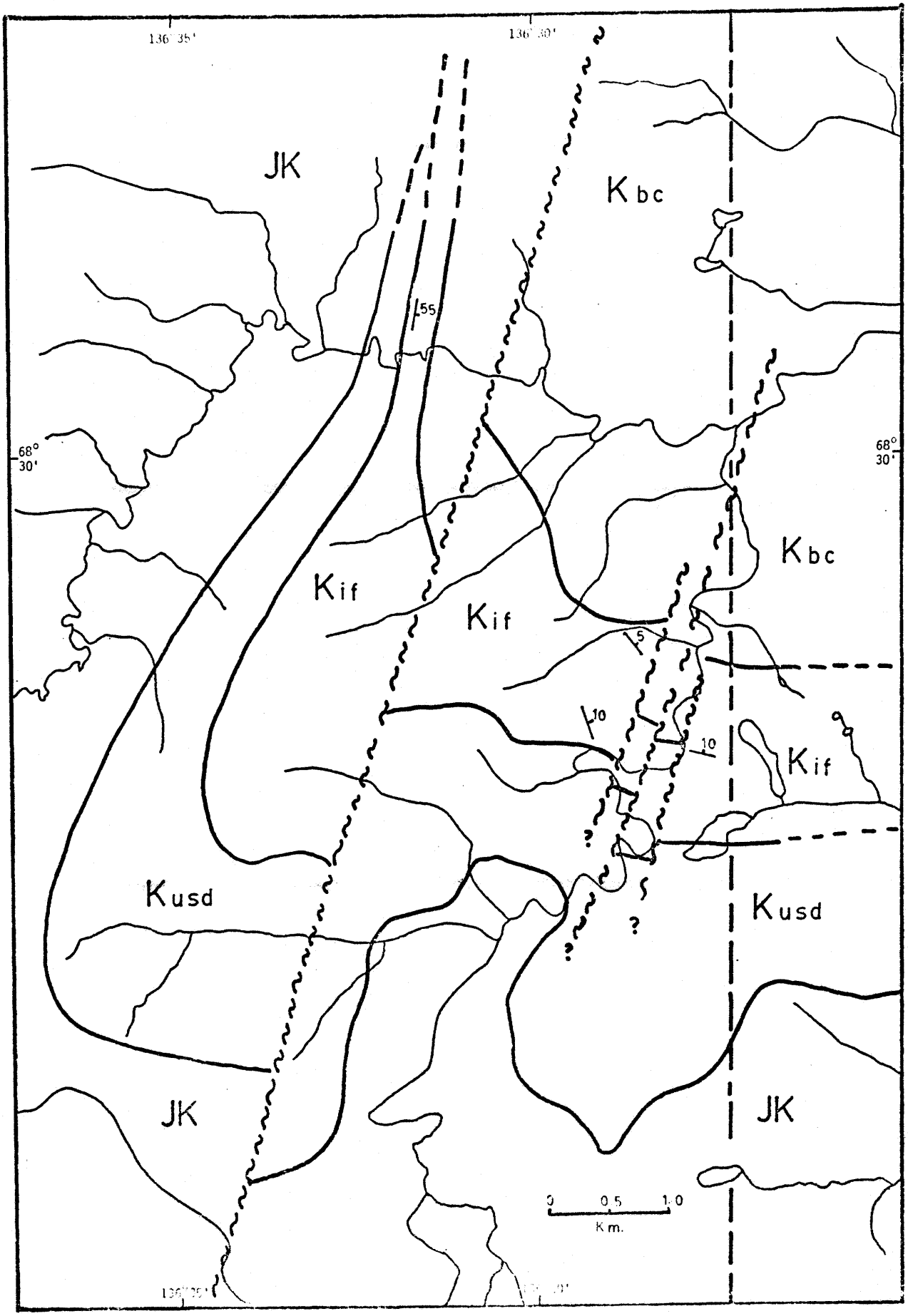
136° 35'
136° 30'
JK
Kbc
55
68° 30'
Kif
Kif
5
10
10
Kbc
Kif
Kusd
Kusd
JK
JK
0 0.5 1.0
Km.

from a distance in the north wall of the "Big Bend", where strata of the Upper Siltstone Division, dipping at an angle of less than five degrees to the unconformity, are overstepped to the east by the iron formation.

At Big Fish River, the iron formation consists of three ironstone units of interbedded mudstone and ferruginous splintery shale and pelletal phosphate shale separated by two units of soft and recessive grey shale (Figure 8). The grey shales both are about 20 meters thick, whereas the ironstone units are 78, 8, and 35 meters, respectively, from bottom to top.

The lower half of the lower ironstone contains phosphate and pyrite nodules. Several of these nodules are definitely recrystallized replacements of ammonites and pelecypods, while many bear only a vague resemblance to ammonites and some bear no resemblance to either ammonites or pelecypods (for more detail see pp. 124-135). One ammonite impression and a perfectly preserved fish scale were found at the top of the lower ironstone. Disoriented coalified plant remains (stems ?) were found at the top of the upper ironstone.

The grey shales are almost identical to those of the overlying Boundary Creek Formation described by Young (1975). However, selenite was not observed in them and they contain interbeds of ironstone only near contacts with one of the ironstone units. This transitional type of contact between grey shale and ironstone was not observed at the base of the lower

Figure 8

Big Fish River section.

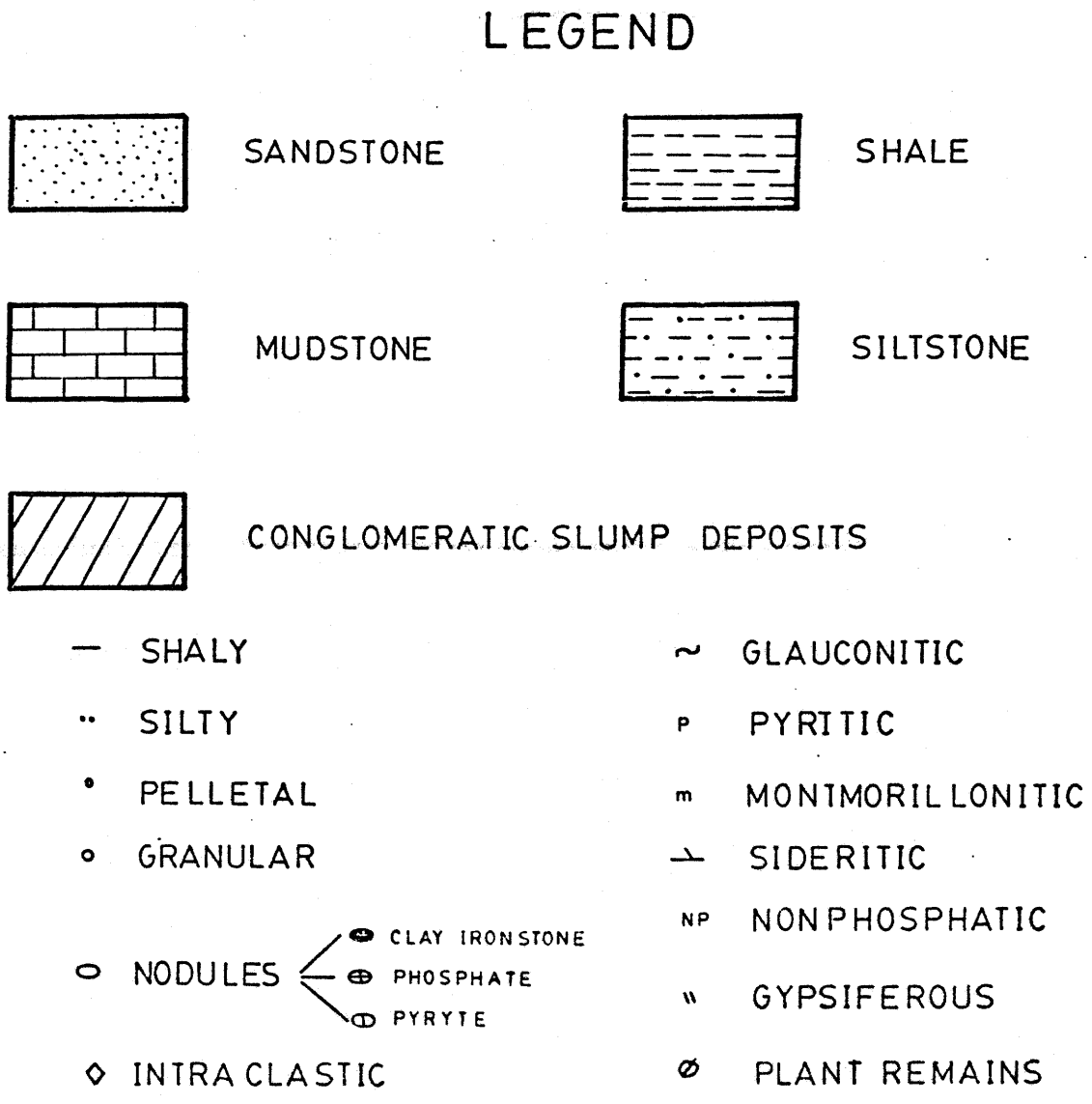

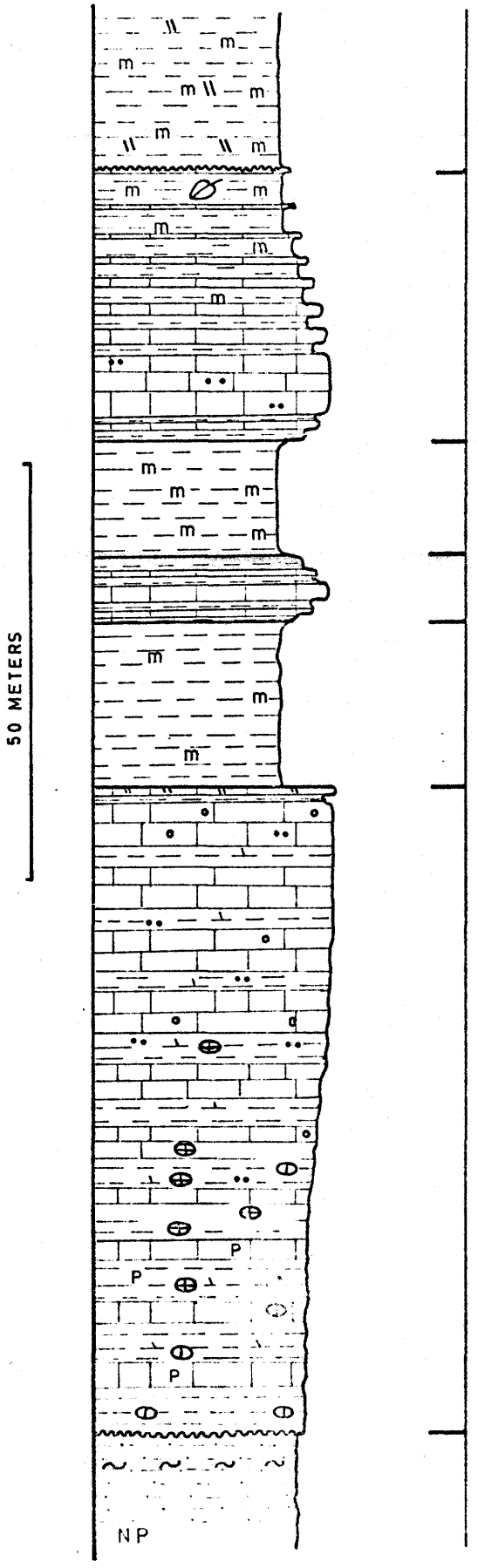

BOUNDARY CREEK FORMATION

UPPER IRONSTONE

UPPER GREY SHALE UNIT

MIDDLE IRONSTONE

LOWER GREY SHALE UNIT

LOWER IRONSTONE

UPPER SILTSTONE DIVISION

grey shale unit. There, the upper beds of the ironstone are fractured and partially filled with a thick iron stain and a drusy coating of gypsum which may represent either a break in deposition of even a period of subareal exposure between these units.

The ironstones consist of alternations of mudstone and shale beds (Plate 1a). Both rock types may contain minor laminations of siltstone. These couplets can be up to two meters thick but are generally less than forty centimeters thick. The mudstone beds are up to one meter thick, have sharp basal contacts with scours in places and grade up into shale. There is no readily observable regularity in couplet thickness distribution within small portions of the section. There is some regularity, however, in the section overall. In the lower third of the lower ironstone, couplets are dominated by shale. In the upper third of this unit, as well as the whole of the middle and upper ironstone units, couplets are dominated by mudstone beds. In the middle of the lower ironstone, shale beds are about two-thirds as thick as mudstone beds.

In the thicker mudstone beds, there is a layering superimposed on the bed that shows up as alternating heavily and lightly iron-stained layers (Plate 1a). Thin sections of adjacent layers give no indication as to the origin of the alternating stain but, presumably, it must be related to the iron (siderite) content of the mudstones.

PLATE 1

A. Mudstone - shale couplets in the Big Fish River area. Dr. Coleman, who is approximately 186 cm tall, is standing at a point 43 m from the base of the measured section at Big Fish River. Note the gradational upward transition from mudstone (competent rock) to shale (incompetent rock) and the relatively sharp basal contacts in mudstone beds. The alternating light and dark layers within the mudstones are heavily and lightly iron-stained layers, respectively.

B. A portion of the section measured on the third ridge from the west in the Cross-cut Creek valley. 'b' and 'd' denote the contact between Units 4 and 5 and Units 5 and 6, respectively. The contacts between the coarsening-upward sequences and conglomeratic slump deposits in Units 4 and 5 are denoted by 'a' and 'c', respectively. The stratigraphic thickness in this photograph is approximately 45 m. In the center of the photograph in the lower part of the conglomeratic slump deposit in Unit 4, are large (2 x 4 m) blocks of interbedded pelletal phosphate sandstone and mudstone which are tilted relative to the underlying coarsening-upward sequence.

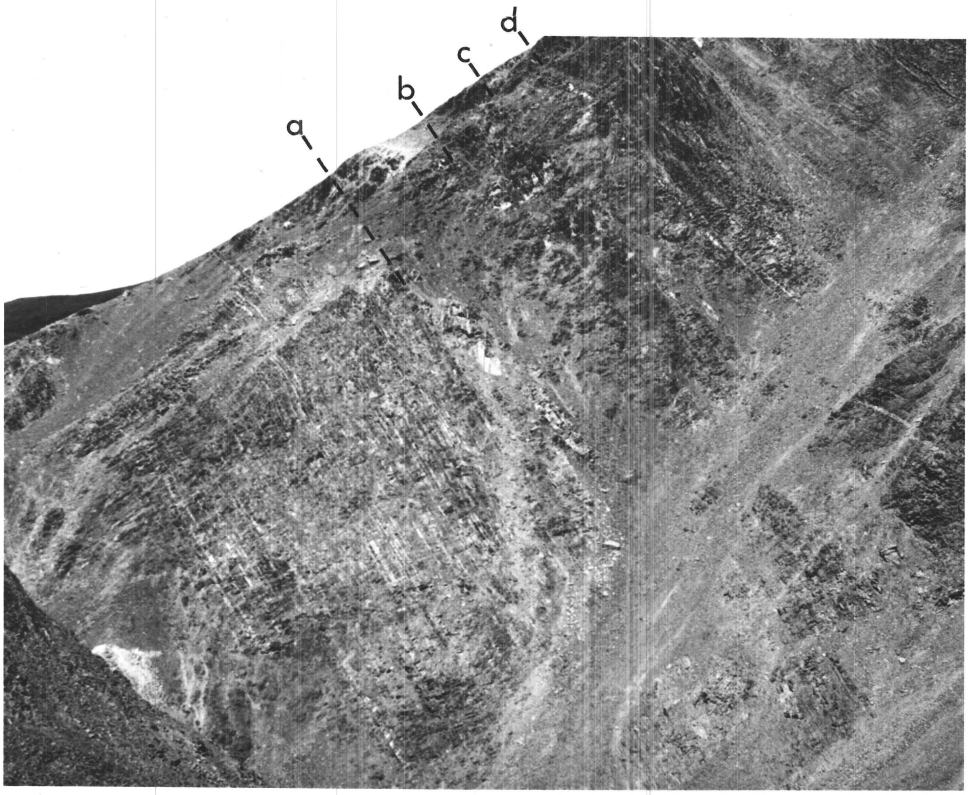
a
b
c
d

Cross-cut Creek

At Cross-cut Creek (Figures 9 and 10), the phosphatic iron formation is folded and forms a large syncline which plunges approximately 15^{o} due north. The entire section is exposed in a cut through the west limb of the syncline along Cross-cut Creek. From the Concretionary Shale Member of the Upper Sandstone Division to the Boundary Creek Formation, the section is 380 meters thick. The lower contact is gradational and arbitrarily picked at the uppermost clay ironstone concretion. The upper contact is transitional, as it is in the Big Fish River area, and picked at the top of the uppermost ironstone bed.

The area is dissected by a number of faults, most of which have unknown displacements. Several small conjugate kink folds and compressed (fault-thickened) beds occur on the west limb of the syncline. In many places, surficial creep has rotated bedding by as much as 120^{o}.

The section along Cross-cut Creek is divided into nine units based on bedding characteristics and abundances of various rock types (Figures 11 a and b).

Units 1 to 5:

At Cross-cut Creek, the lower 60 m of the section is characterized by five units, each of which consists of a coarsening-upward sequence capped by a conglomeratic slump

Figure 9

General geology of the Rapid Creek area.

K_{bc} = Boundary Creek Formation

K_{if} = phosphatic iron formation

K_{usd} = Upper Siltstone and Upper Sandstone Divisions

JK = Lower Cretaceous and older

The rectangular area is enlarged in Figure 10.

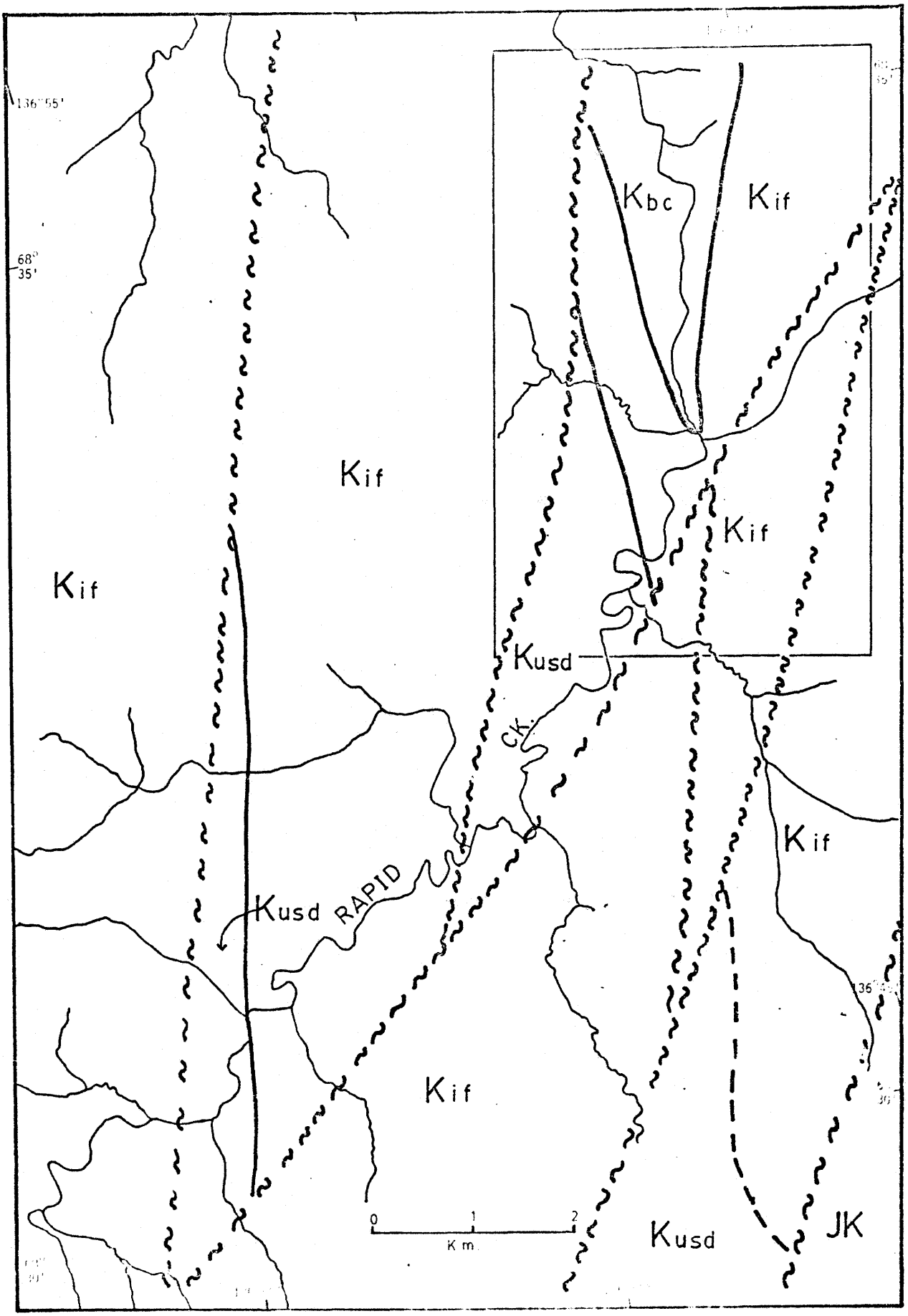
136° 55'
68° 35'
Kbc
Kif
Kif
Kif
Kif
Kusd
CK.
Kusd
RAPID
Kif
Kif
Kusd
JK
0
1
2
Km.

Figure 10

Detailed geology of the Cross-cut Creek area.

K_{bc} = Boundary Creek Formation

K_{if} = phosphatic iron formation

K_{usd} = Upper Siltstone and Upper Sandstone Divisions

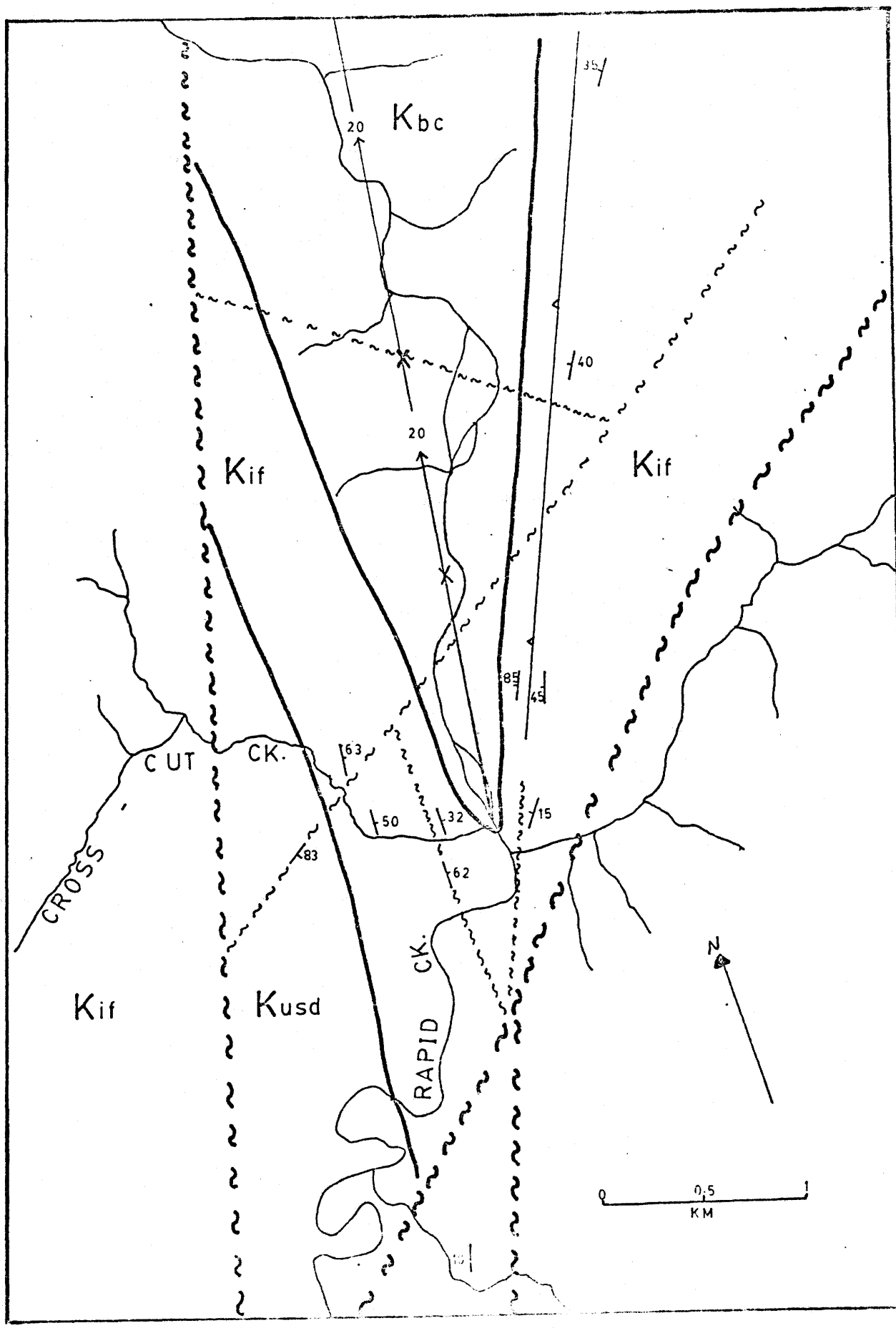
Kbc
Kif
Kif
Kif
Kusd
CUT CK.
CROSS
RAPID CK.
20
20
35
40
85
45
63
50
32
15
83
62
N
0
0,5
1
KM

Figure 11a

Cross-cut Creek section.

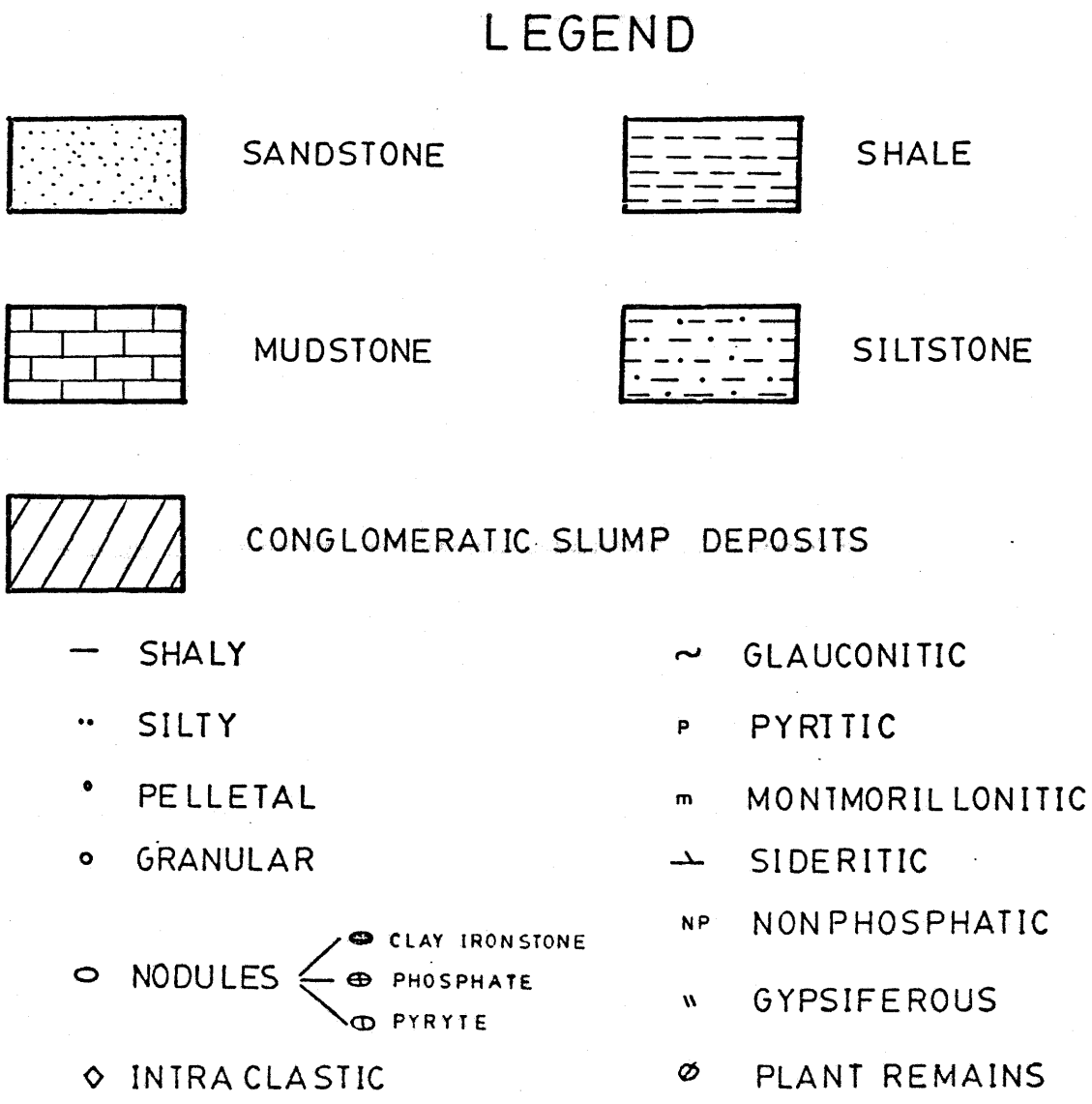

(CONTINUED
ON NEXT PAGE)

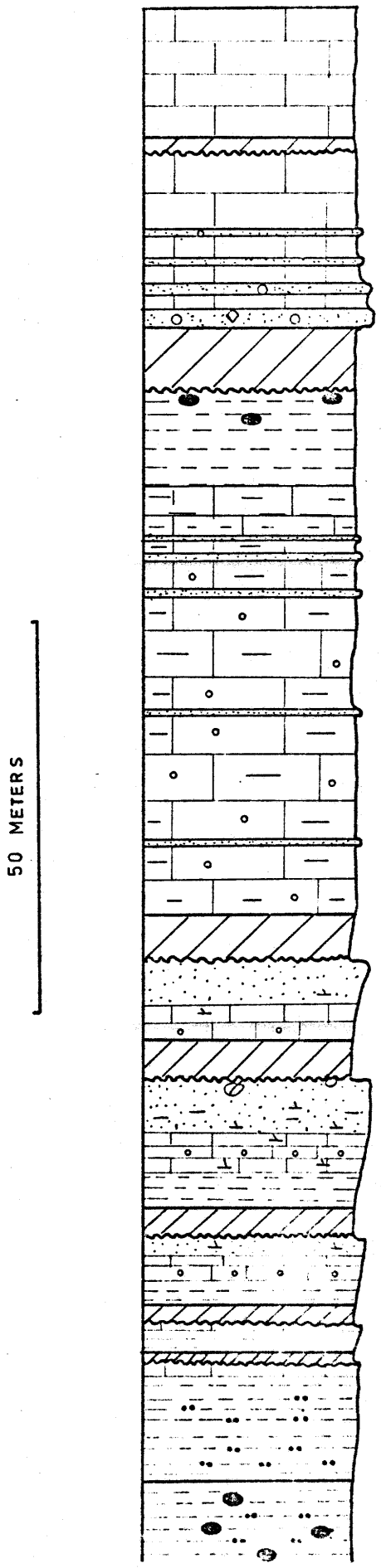

50 METERS

UNIT 8

UNIT 7

MINERALIZED ZONE 2

UNIT 6

UNIT 5

MINERALIZED ZONE 1

UNIT 4

UNIT 3

UNIT 2

UNIT 1

UPPERSANDSTONE DIVISION

Figure 11b

Cross-cut Creek section.

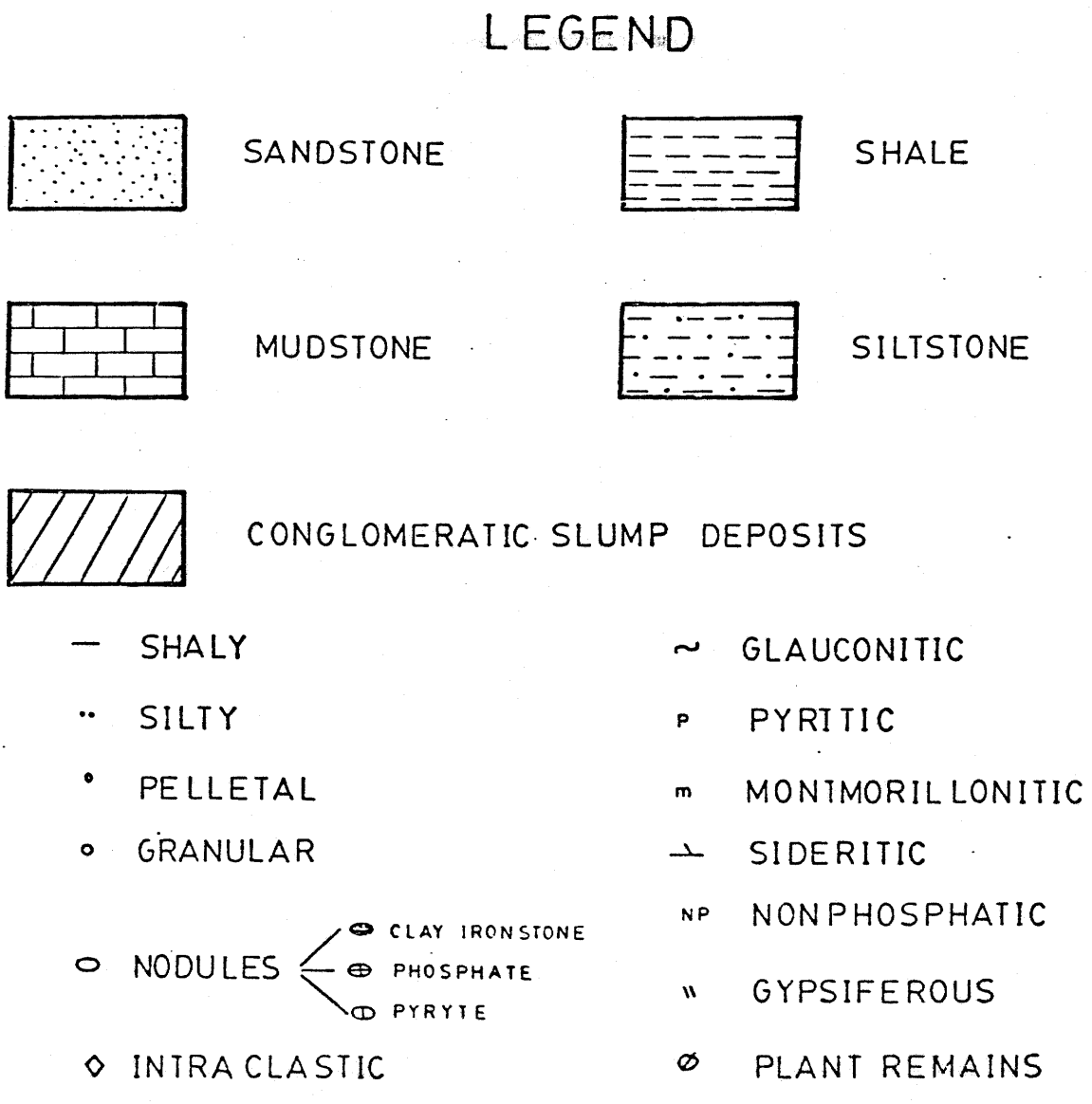

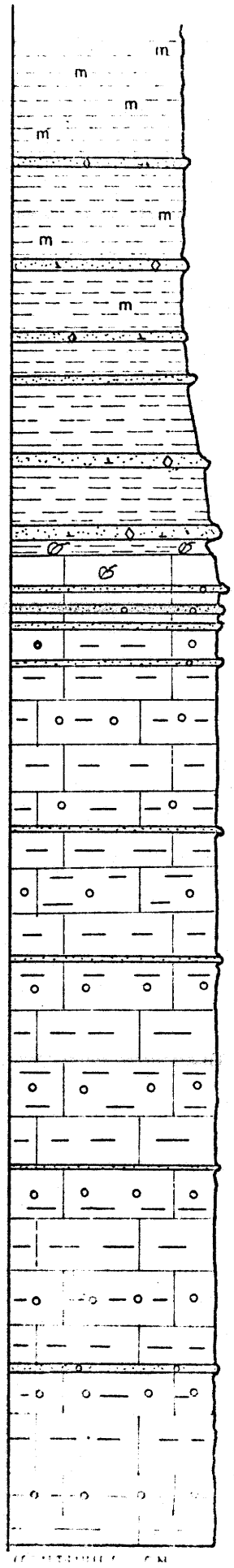

50 METERS

BOUNDARY CREEK FORMATION

UNIT 9

MINERALIZED ZONE 3

UNIT 8

deposit (Plate 1b). In general, the thick slump deposits occur at the top of the thicker coarsening-upward sequences.

The conglomeratic slump deposits are one to five meters thick with the thickest occurring between 45 and 50 m above the base of the section. There is usually a noticeable unconformity at the base of the deposit and there may be as much as 10^{o} difference in apparent dip between adjacent coarsening-upward sequences. In most places, a single continuous bed marks the base of the succeeding strata. The contacts between conglomeratic slump deposits and overlying strata are marked by a gradual change from blocky to well-bedded mudstone and in several outcrops they coincide with a sharp increase in phosphate stains.

The slump deposits pinch and swell so that a single deposit varies in thickness by more than a factor of 3 along its length.

The matrix of the slumps consists of platy to massive, non-phosphatic shale, and blocky to massive non-phosphatic mudstone. Lamination or bedding is well developed near the base and is generally parallel to the basal unconformity. In larger slump deposits in Spain, this feature has been interpreted as a series of decollements (Rupke, 1971). In the middle of the deposits, the laminations and bedding are disorganized and wrapped around clasts or tightly folded in

every direction. At the top of the slump deposits, blocky to weakly bedded mudstone is preponderant.

Clasts are from 5 to 100 cm in diameter and are concentrated in the middle or, to a lesser extent, upper portion of the slump deposits. Most clasts are dark, massive, non-phosphatic mudstone, or, less commonly, non-phosphatic quartz siltstone and pelletal phosphate sandstone. In the thickest slump deposit, large blocks, up to 4 m long and 2 m thick, have been tilted relative to the underlying coarsening-upward sequence (Plate 1b). Where present, clasts make up to a maximum of fifteen percent of the deposit.

The coarsening-upward sequences are at least twice as thick as the overlying slump deposits. They consist of a variety of phosphatic rock types including, in decreasing order of abundance, mudstone, pelletal phosphate sandstone, shale, and siltstone. In outcrop, the pelletal phosphate sandstone beds increase in both thickness and abundance through each sequence. These beds are more resistant to weathering than other rock types and generally stand out because of their lighter weathering colors. There is a tendency for pellet size to increase upward but pellet size is somewhat erratic due to metamorphic recrystallization.

Unit 4 is the thickest and best-developed coarsening-upward sequence and can be divided into three parts. The lower part is dominated by dark grey shale. Interbedded with the dark grey

shale is finely bedded, weakly-phosphatic mudstone and minor amounts of pelletal phosphate shale and phosphatic quartz siltstone. The middle part is dominated by non-pelletal phosphate mudstone interbedded with minor amounts of pelletal phosphate shale, mudstone, and sandstone with minor laminations of phosphatic quartz siltstone. The upper part is dominated by pelletal phosphate sandstone interbedded with platy shale, pelletal and non-pelletal phosphate mudstone and phosphatic quartz siltstone.

The thicknesses of the three parts are roughly 5:5:10 m respectively from base to top in Unit 4. The other four sequences appear to be equivalent to portions of this sequence (Figure 12). Units 1 and 2 are equivalent to the lower part of Unit 4. Unit 3 is equivalent to the lower and middle parts and Unit 5 is equivalent to the upper part of Unit 4. Thus, Unit 4 can be considered the best developed coarsening-upward sequence. There is a general coarsening-upward nature to the five units overall.

In the top meter of the coarsening-upward sequence in Unit 4, at the top of a thick pelletal phosphate sandstone bed, sparse plant remains and a large oblate sideritic concretion occur. The sandstone bed was vaguely divided into blocks 40 cm on a side. The blocks were not apparent in fresh exposure but were only evident on surfaces with a moderate amount of weathering and showed up as regular depressions. This feature

Figure 12

Unit 4 detailed section showing one coarsening-upward sequence and slump deposit. The relationship of rock types within other units (1 to 3 and 5) is also shown. Note the coarsening-upward nature to the five units overall.

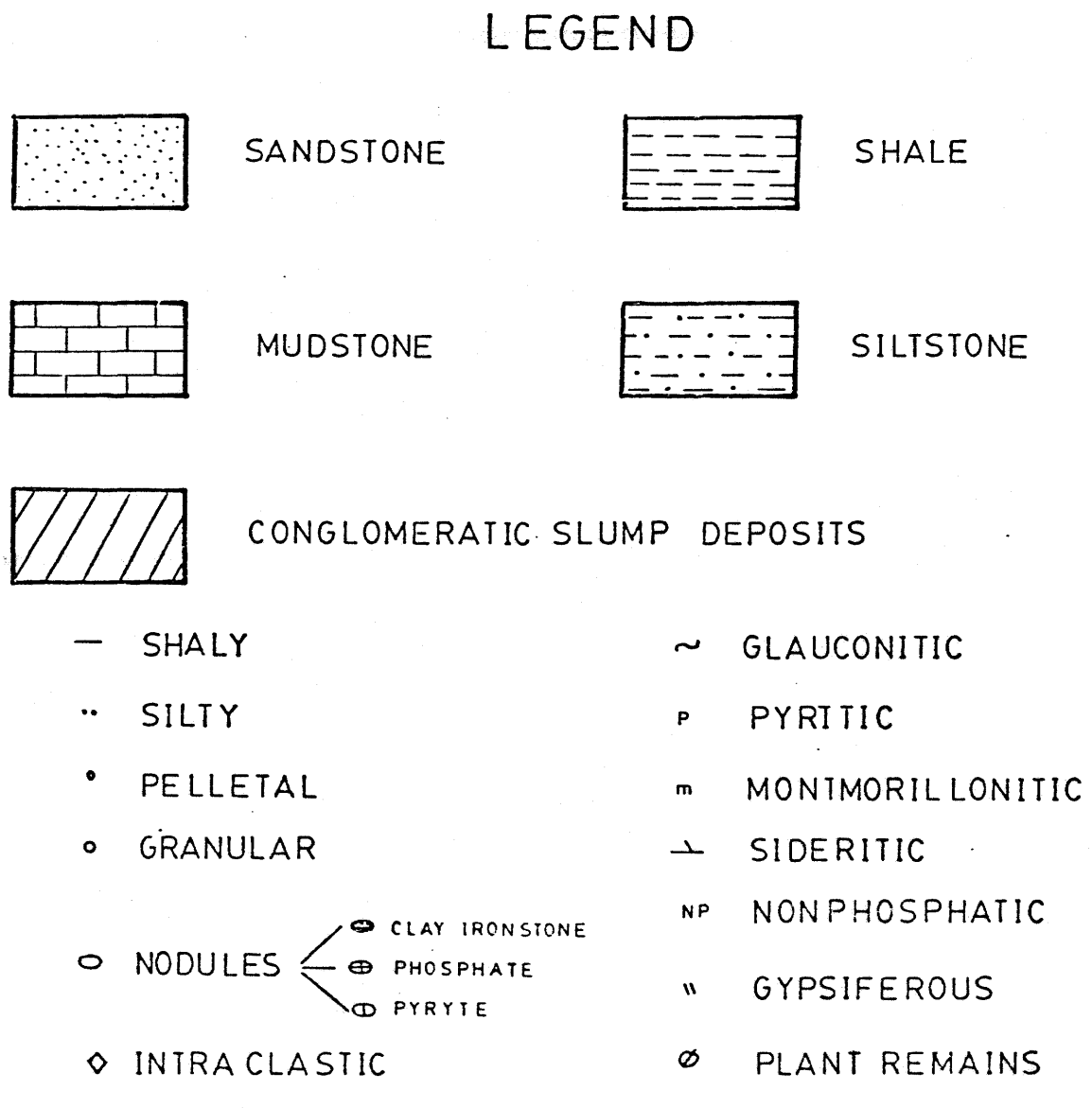

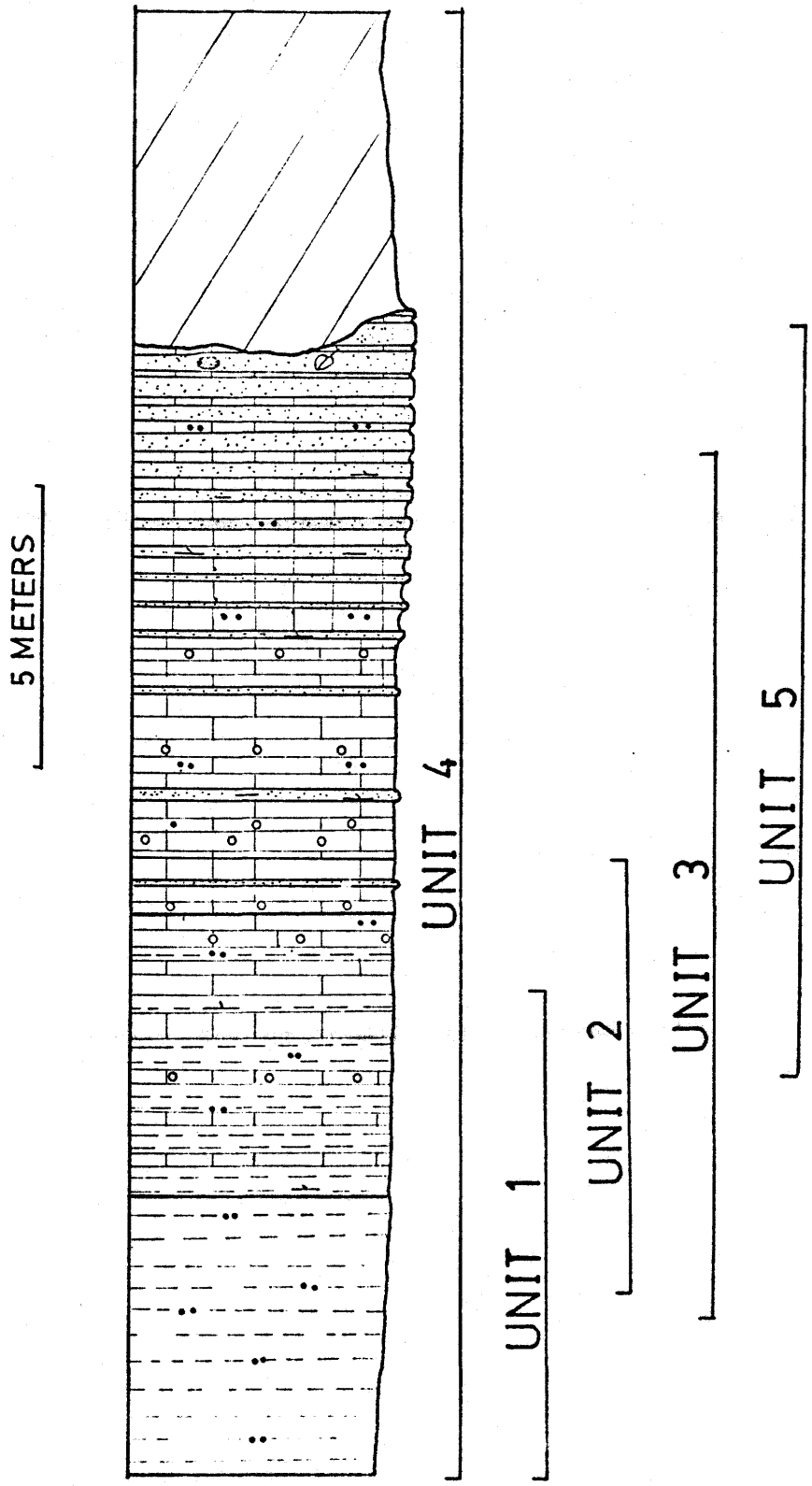
5 METERS
UNIT 4
UNIT 1
UNIT 2
UNIT 3
UNIT 5

has all the appearances of poorly developed spheroidal weathering which has been masked by metamorphism and may represent subareal exposure before slump deposition.

Unit 6:

The interval from 60 to 158 m in the Cross-cut Creek section is characterized by a paucity of sandstone beds. Phosphatic (pelletal and non-pelletal) mudstone dominates this portion of the section with minor amounts of pelletal phosphate shale and phosphatic quartz siltstone interbeds. Sandstone beds are thin (5 to 20 cm). Single beds traced over 200 m usually show an order of magnitude change in thickness with several beds pinching out completely.

At 138 m, the proportion of mudstone declines and dark grey shale becomes dominant to 143 m where it is the only rock type. There are small and irregularly distributed clay ironstones concretions within the dark grey shale from 145 to 153 m. From 153 to 158 m, there is a conglomeratic slump deposit similar to those in previous units but it contains only small non-phosphatic mudstone clasts.

Unit 7:

The interval from 158 to 182 m is similar, for the most part, to the lower portion of Unit 6. It begins with a crudely developed fining-upward sequence where relatively thick granular

phosphate sandstone beds give way rapidly (within 5 m) to thin pelletal phosphate beds. The top of this unit was picked at the top of the uppermost conglomeratic slump deposit.

Unit 8:

The interval from 182 to 325 m is similar to that of the lower portion of Unit 6, except for the upper 15 m, where pelletal phosphate sandstone bed abundance increases upward. This final coarsening-upward sequence is not capped by a slump deposit. Instead, the uppermost sandstone bed is followed by a thin green shale which contains abundant plant remains. This probably represents a disconformity because all of the following beds are essentially non-phosphatic.

One pelletal phosphate sandstone bed within this unit fills a large scour 70 cm deep. The upper surface of the bed displayed a peculiar 'nobby' appearance that was observed on talus samples elsewhere in the section. The origin of the scour is evident, while the origin of the nobby upper surface of the sandstone bed is uncertain but probably due to load casting.

Unit 9:

The interval from the green shale to the uppermost ironstone bed, 325 to 380 m, marks a transition from ironstones to splintery shale. The ironstones are actually pelletal siderite sandstone with variable amounts of mudstone

intraclasts. They decrease in abundance and bed thickness upward. The splintery shale is heavily iron-stained in the lower portion of this unit but becomes progressively lighter in color upward so that, near the top of this unit, it is indistinguishable from the grey shales of the overlying Boundary Creek Formation.

Boundary Creek

At Boundary Creek, the complete phosphatic iron formation is exposed with the strata dipping 60^{o} to the east. Only one very thin grey shale unit was observed. The rest of the strata are lithologically identical to those of the Big Fish River area. The lower contact is an angular unconformity with a channel sand in the Upper Siltstone Division. In the upper part of this sand, plant remains aligned perpendicular to bedding were interpreted as fossil roots. The upper contact with the Boundary Creek Formation is obscured but upper beds in the iron formation are slightly warped into open folds and may be truncated, as in one outcrop in the Big Fish River area. This contact is believed to be an unconformity by Young (1975).

Area 3

Area 3 is located on the east side of Rapid Creek (Figure 5). Only 55 m of secton is exposed here. This section is almost identical with the interval 270 to 325 m in the

Cross-cut Creek section, except that the pelletal phosphate sandstone beds at the top of the coarsening-upward sequence are a little thicker than those along Cross-cut Creek.

Area 7

The strata in area 7 were not measured because faulting has disrupted bedding to a high degree, but the rocks were examined in the field. The area lies along strike with the Cross-cut Creek section but the rocks are almost identical with those in the Big Fish River area. They consist of thin alternating beds of mudstone and shale. Pelletal phosphate sandstone and grey shale were not observed in this area. The abundant white coating of dypingite is common here, as it is in the Big Fish River area.

PETROLOGY

Nomenclature

Many of the rocks encountered in this study could be classified by either iron-rich or phosphate-rich rock classification schemes because several of the major constituent minerals are iron phosphates or because both siderite and calcium phosphate (apatite group minerals) are present in abundance. Therefore, any classification scheme that relies solely on mineralogy (e.g., James, 1954; for iron formations) or chemistry (Cressmand and Swanson, 1964; for phosphorite) could be used for these rocks, but neither is suitable.

Dimroth and Chauvel (1973) have presented a classification scheme for iron-rich rocks based on textures which is analogous to Folk's (1959, 1962) scheme for carbonate rocks. A basic component of their scheme is chert which occurs in the matrix or as cement. In samples from this study, chert was not recognized in proportions significant enough to justify the use of Dimroth and Chauvel's classification.

Riggs (1979a) has presented a detailed classification scheme for phosphate sediments similarly analogous to Folk's scheme for carbonate rocks. He has not, however, made any allowance for phosphorites which have undergone metamorphic changes other than those associated with supergene weathering. The rocks encountered in this study have been regionally and/or

hydrothermally metamorphosed such that phosphate and siderite grains and skeletal fragments have been recrystallized and/or replaced by 'metamorphic' phosphate minerals (e.g., gormanite-souzalite). Therefore, Riggs' classification is also unsuitable for these rocks.

The most striking feature of the rocks encountered in this preliminary study is their clastic appearance, particularly in the field. Thus, general clastic terminology has been adopted to characterize the major divisions of these rocks - shale, mudstone, siltstone and sandstone (Table 1 and Figure 13). Almost all rock types in this study are iron-rich but not all are phosphate-rich, so that major divisions can be subdivided into phosphatic and non-phosphatic rock types. Phosphatic rock varieties are identified by the nature of the phosphate component (e.g., pelletal phosphate mudstone). Where siderite can be easily recognized, it is similarly identified.

The terms used here are defined as follows:

Ironstone: A bed or group of beds in which the rocks are composed largely of iron-rich minerals. The term is used as a loose reference to mixed or unidentified rock types. (Gray et al., 1973)

Iron formation: Same as for 'ironstone' but in the broader sense, i.e., the deposit as a whole is an iron formation.

Figure 13

Ternary diagram of point counted composition of various rock types (Table 1). Numbers 16 and 17 are non-pelletal phosphate mudstones but are plotted as though the concretionary stars were pellets.

Table 1. Point counting results

Sample	1	2	3	4	5	6	7	8	9	10
Pellets	84	53	36	73	68	77	66	48	70	6
Matrix	11	21	53	22	27	21	30	44	29	11
Quartz	4	22	11	3	4	2	-	8	1	79
Skel. frag.	-	2	-	-	-	-	-	-	-	-
Pyrite	1	2	-	2	1	-	4	-	-	4

Sample	11	12	13	14	15	16	17	18	19	20
Pellets	33	11.5	11	-	57	49.5	39	71	74.5	62
Matrix	46	85.5	87	46	42.5	49.5	57.5	26	23	25
Quartz	21	3	2	52	-	1	3	2	-	3
Skel. frag.	-	-	-	-	.5	-	-	-	-	-
Pyrite	-	-	-	2	-	-	.5	1	2.5	10

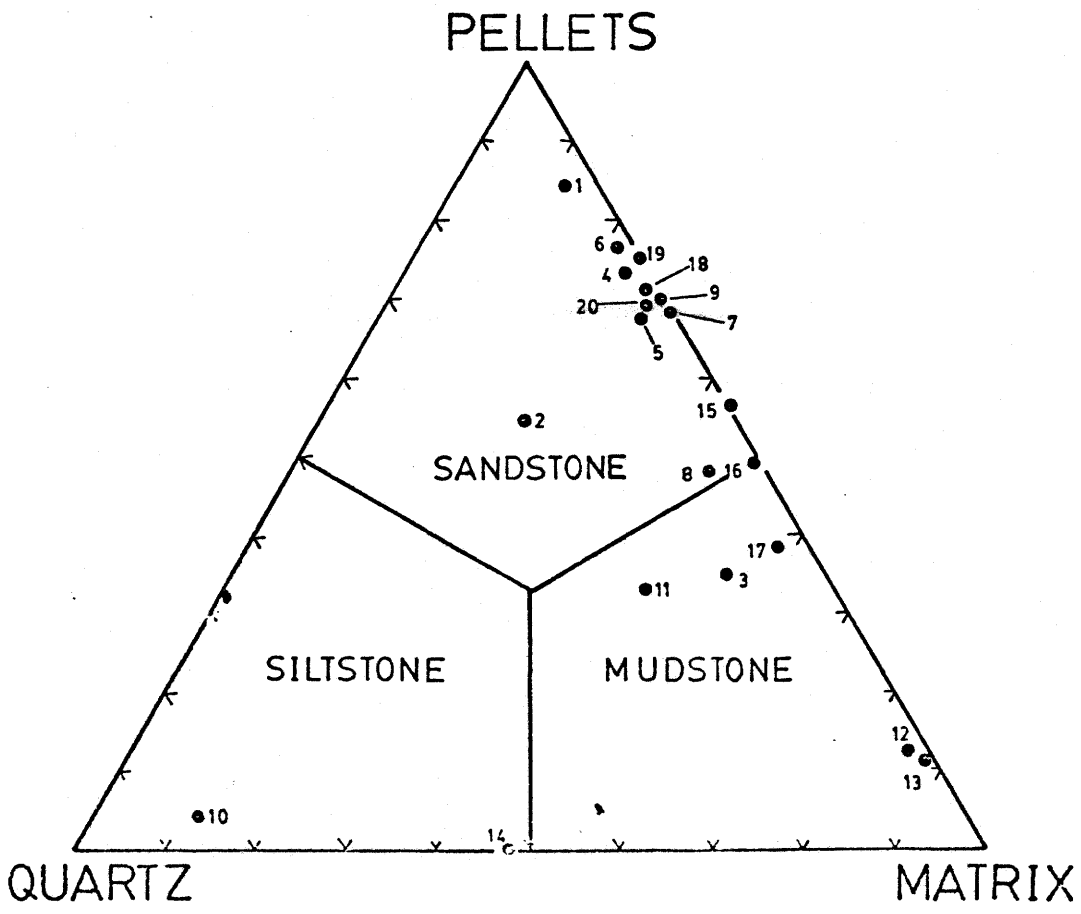

Shale: A laminated or fissile rock with a modal grain size less than 1/100 mm (Pettijohn, 1975, p. 261).

Mudstone: A rock composed predominantly of clay-sized particles (less than 1/256 mm) but lacking distinct lamination or fissility (Pettijohn, 1975, p. 261).

Siltstone: A laminated or nonlaminated rock with more than fifty percent of its grains within the size range 1/16 to 1/256 mm (Pettijohn, 1975, p. 261).

Sandstone: A rock composed largely of sand size (1/16 to 2 mm) particles. (Gray et al., 1973).

Phosphate: A general term used to identify a class of minerals, chemical compounds, particles, grains or nodules, or a mineral deposit (Riggs, 1979a, p. 198).

Phosphatic: A general term used to identify the presence of phosphate minerals in readily recognizable proportions. Riggs (1979a, p. 198) uses 'phosphatic' to indicate from 1 to 10 percent by volume phosphate grains. A one percent lower limit is too low as many normal rocks contain this amount of phosphate grains. Cressman and Swanson (1964, p. 282) use the term for rocks or sediments with between 7.8 and 19.5 weight percent P_2O_5, which can only be determined with chemical analysis. The term is used here in the sense of Riggs (volume % phosphate grains) with limits on the order of Cressman and Swanson (5 to 15 percent).

Pellet (pelletal): A constructional particle 0.062 to 2.0 mm in diameter, having no internal structure. Cressman and Swanson's (1964, p. 282) upper limit for pellet size is 0.2 mm but they did not include a term for such particles in the range 0.2 to 2.0 mm. The term 'pellet' has been extended here to include that size. 'Pellet' also implies an organic or inorganic chemical, rather than terrigenous, origin.

Granule (granular): A constructional particle 2.0 to 4.0 mm in diameter with no internal structure and of the same general origin as pellets.

Intraclast: A fragment of penecontemporaneous sediment that has been transported from within the depositional basin to form part of a new sediment (Riggs, 1979a).

Nodule: A discrete particle larger than 4 mm in diameter and generally rounded. Nodules are not considered part of the rock that encloses them. Instead, they are concretionary or replacement entities.

Mineralogy

The dominant component of the rocks in both Big Fish River and Rapid Creek areas is siderite with only minor amounts of manganese and magnesium substituting for iron. In many samples, goethite or limonite alters from siderite, particularly along cleavage traces or fractures in the rock. Preliminary oxygen

and carbon isotopic data suggest that siderite in rock samples in the Rapid Creek area has re-equilibrated with the hydrothermal solution which was responsible for precipitation epigenetic minerals in fractures.

The only clay mineral reported by Young (1972) was kaolinite. More recent examination (Young, pers. comm.) indicates the presence in variable amounts of chlorite, illite and montmorillonite. Pyrite occurs as finely disseminated anhedra in most samples and, in places, it has recrystallized to form patches of intergrown euhedra or lenses up to 1 cm thick. Quartz generally is detrital, although in several samples it replaces chert.

Carbonate-apatite is the major phosphate phase in mudstone. Relatively broad diffraction peaks indicate poor crystallinity. Whole rock chemical analyses (see p. 81) indicate that the mineral is not pure calcium phosphate but contains other elements substituting for calcium.

Satterlyite (Mandarino et al., 1978) is the dominant phosphate mineral in pelletal and granular phosphate sandstone. It is a major to minor constituent of siderite sandstone and phosphatic mudstone. The whole rock x-ray diffraction of several samples gives satterlyite patterns identical to that reported by Mandarino et al. (1978, p. 412, Table 1). Satterlyite has very low birefringence, is generally not colored, and gives either uniaxial negative or, more commonly,

biaxial negative interference figures. Biaxial figures have a low $2V_x$ generally less than 25^o.

Microprobe analyses (Table 2a and 2b) indicate only minor variation in composition. Wyllieite 175 (see Appendix II) was used as a probe standard. Water content is from Mandarino et al. (1978, p. 412). Fe:Mg ratios range from 3.94:1 to 2.35:1 and Fe:Mn ratios range from 486:1 to 23:1 with variable amounts of Na from 0 to 2.89 weight percent.

Satterlyite is found in association with all other minerals but particularly arrojadite, which appears to be altered directly from it.

Arrojadite is an abundant mineral in the pelletal and granular phosphate sandstones in the upper four units of the Cross-cut Creek section. It is a minor to trace constituent in siderite sandstones and phosphatic mudstones. Arrojadite has not been recognized in rocks from the Big Fish River area.

Arrojadite occurs as patches of laths closely associated with satterlyite. It has low birefringence (about that of quartz), moderate dispersion, is faintly pleochroic in very pale greens, shows a low inclined extinction (maximum 14^o) about one good cleavage and is biaxial negative with a large (close to 85^o) $2V_x$.

Microprobe analyses of arrojadite from three rock samples are listed in Table 3. Arrojadite from Big Fish River was used as a probe standard. Fe:Mg ratios are essentially constant

Table 2a. Satterlyite compositions from rock samples A355 and A352

	A355					A352			
	1	2	3	4	5	1	2	3	4
Na_2O	-	1.63	.65	1.25	1.06	.58	1.15	2.14	.54
MgO	6.95	7.70	7.55	7.96	7.53	9.21	9.84	10.32	9.19
CaO	.03	.08	.06	.08	-	-	-	.05	.12
MnO	2.02	2.17	2.04	1.89	1.92	.92	.91	.93	.91
FeO	48.75	48.18	49.06	47.80	49.16	48.18	47.12	45.92	48.42
Al_2O_3	.23	.35	.33	.36	.38	.35	-	.40	.48
P_2O_5	34.16	34.11	34.89	34.52	33.17	35.05	35.36	34.38	33.95
H_2O	5.2	5.2	5.2	5.2	5.2	5.2	5.2	5.2	5.2
Total	97.79	99.42	99.78	99.06	98.42	99.49	99.58	99.34	98.81
Atomic proportions based on .99 P:									
Na	-	.11	.04	.08	.07	.04	.07	.14	.04
Mg	.35	.39	.38	.40	.40	.46	.48	.52	.47
Ca	-	-	-	-	-	-	-	-	-
Mn	.06	.06	.06	.05	.06	.03	.03	.03	.03
Fe	1.38	1.38	1.37	1.35	1.45	1.34	1.30	1.31	1.39
Al	.01	.01	.01	.01	.02	.01	-	.02	.02
P	.99	.99	.99	.99	.99	.99	.99	.99	.99
Total-P	1.80	1.95	1.86	1.89	1.99	1.88	1.88	2.02	1.95

Table 2b. Satterlyite compositions from rock samples A355 and A352

	A161			A363			
	1	2	3	1	2	3	4
Na_2O	.64	1.71	-	.12	1.46	2.89	2.63
MgO	9.71	11.14	9.67	9.39	10.01	9.26	9.81
CaO	.03	.03	.05	.07	-	.07	.07
MnO	.28	.33	.10	1.69	1.69	1.57	1.50
FeO	49.84	46.78	48.58	47.81	46.49	45.54	45.83
Al_2O_3	.21	.24	.23	.33	.29	.10	.32
P_2O_5	33.82	34.11	34.39	34.89	34.40	34.50	33.99
H_2O	5.2	5.2	5.2	5.2	5.2	5.2	5.2
Total	99.73	99.54	98.22	99.50	99.54	99.13	99.35
Atomic proportions based on .99 P:							
Na	.04	.11	-	.01	.10	.12	.18
Mg	.50	.57	.49	.47	.51	.47	.50
Ca	-	-	-	-	-	-	-
Mn	.01	.01	-	.05	.05	.05	.04
Fe	1.44	1.34	1.38	1.34	1.32	1.29	1.32
Al	.01	.01	.01	.01	.01	-	.01
P	.99	.99	.99	.99	.99	.99	.99
Total-P	2.00	2.04	1.88	1.88	1.99	1.93	2.05

Table 3. Arrojadite compositions from rock samples

	A161			A355	A352		
	1	2	3		1	2	3
Na_2O	7.94	8.40	8.02	6.66	7.10	7.39	5.75
K_2O	1.86	1.99	1.91	1.74	1.76	1.82	1.88
MgO	3.40	3.59	3.52	3.23	3.75	3.45	3.37
CaO	3.09	3.37	3.65	3.04	3.07	2.34	3.56
MnO	.94	.73	1.15	5.65	2.47	3.06	2.51
FeO	39.94	39.29	39.86	36.57	40.26	39.04	39.56
Al_2O_3	2.15	1.76	1.96	1.77	1.81	2.05	2.07
P_2O_5	39.60	39.93	40.13	40.46	39.95	39.62	40.98
Total	98.92	99.06	100.20	99.12	100.17	98.76	99.68
Atomic proportions based on 12.00 P:							
Na	5.51	5.78	5.49	4.52	4.89	5.12	3.85
K	.85	.90	.86	.77	.80	.83	.83
Mg	1.81	1.90	1.85	1.69	1.98	1.83	1.74
Ca	1.19	1.28	1.38	1.14	1.16	.90	1.32
Mn	.29	.22	.34	1.68	.74	.92	.74
Fe	11.96	11.66	11.77	10.71	11.96	11.68	11.45
Al	.96	.74	.82	.73	.76	.87	.84
P	12.00	12.00	12.00	12.00	12.00	12.00	12.00
Total-P	22.52	22.48	22.51	21.24	22.29	22.15	20.77

between samples. Fe:Mn ratios are an order of magnitude lower in arrojadite than in satterlyite from the same rock but are generally related. Rock sample A355 has the lowest Fe:Mn ratio for both arrojadite and satterlyite while sample A161 has the highest for both and sample A352 is intermediate for both.

Gormanite-souzalite is an abundant mineral in pelletal and non-pelletal phosphate mudstones, particularly in the first five units of the Cross-cut Creek section, where it is a replacement of carbonate-apatite. It is a minor to trace constituent of pelletal and granular phosphate sandstone where it is a replacement of satterlyite. Gormanite-souzalite occurs as patches of fibrous needles and is strongly pleochroic in bright greens. One microprobe analysis (Table 4, no. 4) shows that the material is Fe-rich.

Lazulite has a similar occurrence to gormanite-souzalite but is much rarer. Lazulite occurs as coarsely crystalline patches and is strongly pleochroic from blue to colorless, similar to vivianite-baricite, but does not possess cleavage.

Vivianite-baricite occurs as an alteration product of other iron-rich phosphate minerals. It also occurs as a pore filling in phosphate and siderite sandstone. Vivianite-baricite is not a major component in any rock type - a maximum of 3% by volume has been observed. It is colorless to deep blue, depending on the degree of oxidation, and has one micaceous cleavage. When colored, it is also strongly pleochroic.

Table 4. Various minerals

	1	2	3	4	5	6
MgO	1.26	4.15	10.78	7.32	7.89	7.66
CaO	.64	.46	2.55	.10	6.66	6.74
MnO	.39	.53	.26	.30	3.77	3.16
FeO	45.83	42.35	43.00	16.35	11.57	12.72
Al_2O_3	.78	.90	.25	26.54	13.37	13.29
P_2O_5	32.95	33.86	39.15	36.82	36.12	36.06
H_2O	16.77	16.77	-	12.11	21.40	21.40
Total	98.62	99.02	95.99	99.54	100.78	101.03
Atomic proportions based 2, 3 or 4 P:						
Mg	.13	.43	1.45	1.40	1.54	1.50
Ca	.05	.03	.25	.01	.93	.95
Mn	.02	.03	.02	.03	.42	.35
Fe	2.75	2.47	3.26	1.76	1.27	1.31
Al	.07	.07	.03	4.01	2.06	2.05
P	2.00	2.00	3.00	4.00	4.00	4.00
Total-P	3.02	3.03	5.01	7.21	6.22	6.16

1, 2. Ludlamite; rock sample Ac37; Wyllieite 175 standard; average of 2 analyses.

3. Unknown; rock sample A161; Wyllieite 175 standard; average of 3 analyses.

4. Gormanite; rock sample A363; Wyllieite 175 standard; average of 3 analyses.

5, 6. Whiteite; rock sample Ac37; Whiteite 176 standard; both are an average of 2 analyses.

Ludlamite has a similar occurrence to vivianite-baricite but occurs as a rock alteration only in area 3. Microprobe analyses (Table 4, nos. 1 and 2) are similar to those in Table 18 (Appendix II) for vein-filling ludlamite.

Whiteite has a similar occurrence to ludlamite and is also restricted to area 3. Microprobe analyses (Table 4, nos. 5 and 6) are similar to vein-filling whiteite from other areas.

Rock sample A161 contained an unknown (at least unidentified) mineral. It is identical to satterlyite in thin section. Its composition is listed in Table 4, number 3, and probably belongs to the apatite group of minerals, having the formula $(Fe_{3.26}Mg_{1.45}Ca_{.25}Al_{.03}Mn_{.02})_{5.01}(PO_4)_{3.00}(OH\ ?)$.

Rock Types

There are basically four rock types in the study area: shale, mudstone, siltstone, and sandstone. All except sandstone have phosphatic and non-phosphatic varieties. Nonphosphatic rock types weather in shades of brown and yellow or grey to black, due to iron oxides and hydroxides, while phosphatic varieties weather in a variety of shades; gun-metal blue, due to vivianite-baricite, yellow to brown, due to goethite or completely altered vivianite-baricite, or in shades of green, due to metavivianite.

The metamorphic grade of these rocks has not been established, but the effect of metamorphism is prominent. Primary minerals, such as carbonate-apatite and siderite, have altered to or been replaced in places by satterlyite, arrojadite, gormanite-souzalite, vivianite-baricite, ludlamite, and whiteite. Original textures, such as grain size, have also been affected by repeated recrystallization. Original structures, such as cross-bedding, were not observed. Their absence may also be due to metamorphism.

Shale:

There are five different types of shale. Only one of these (e) is phosphatic.

a) Grey shale: These soft shales are identical with those of the Boundary Creek Formation described by Young (1975). Outcrops with bulbous mounds of grey clay indicate a high montmorillonite content.

b) Splintery shale: These shales are medium grey to black, moderately hard, and weather gun-metal blue and maroon to black. They occur in beds up to two meters thick with little or no interbedded material.

c) Dark grey shale: These are similar to splintery shale but generally weather in darker colors (dark grey to black) and display a rubbly appearance in outcrop. Bedding is prominent, being defined by 1 to 5 cm thick lenticular layers that tend to

pinch and swell across the outcrop.

d) Platy shale: Platy shale is usually interbedded with phosphate and siderite sandstone and commonly contains fine laminations of quartz silt. These shales are medium grey to black and weather dark grey to black or gun-metal blue.

e) Pelletal phosphate shale: This is the only shale that was studied in thin section. It is dark grey, relatively hard, and platy. Weathering colors are very variable from yellow and orange-brown to gun-metal blue to black. The matrix consists of clay minerals and microcrystalline siderite. Lamination is well developed and wraps around the pellets.

Pellets make up to 30 percent or less of the rock. They are from 0.1 to 2.0 mm in diameter and rounded to irregular in outline. Pellets are composed of a fine-grained mixture of siderite and carbonate-apatite. Most pellets are dominated by carbonate-apatite but contain up to 50 percent siderite and up to 5 percent pyrite. Rarely, satterlyite, arrojadite and/or gromanite-souzalite replace portions of pellets. This replacement, where present, is commonly concentrated in the rims of the pellets.

Mudstone:

Mudstone is the most abundant rock type in the Rapid Creek area and a substantial component in the Big Fish River area. The varieties described below can be distinguished positively

only in thin section. All contain weak wavy laminations which are similar to those shown by Dimroth and Chauvel (1973, p. 122, Figure 7E) and interpreted as stylolites by them.

a) Non-phosphatic mudstone: These mudstones are dense, hard, dark grey, and massive. They consist of microcrystalline siderite, clay minerals, and fine silt-sized detrital quartz with minor amounts of pyrite. The only alteration observed was weathering of siderite to form goethite. These rocks occur as clasts and matrix in the conglomeratic slump deposits.

b) Pelletal phosphate mudstone: These mudstones are similar to the pelletal phosphate shales except that lamination is poorly developed due to a lower clay mineral content. Pellets are variable in size and composition, poorly sorted, and make up to 50 percent of the rock (Plate 2a).

Phosphate pellets occur in layers or stringers which are 1 to 2 mm thick with pellets ranging in size from 0.1 to 2.0 mm. They consist mainly of microcrystalline siderite and carbonate-apatite, which is partly altered to or replaced by satterlyite, arrojadite, and gormanite-souzalite. These pellets are irregular in outline, elongate to spherical, and occasionally merge into one another.

Shale and mudstone intraclasts are subrounded, less than 0.1 mm in diameter, iron-stained, and very common. Chert pellets are relatively common, up to 1.5 mm and generally elongate with regular and rounded outlines. In some of these

PLATE 2

A. Pelletal phosphate mudstone. The majority of the mixed siderite - carbonate-apatite pellets are concentrated in thin (less than 1 mm) laminations but they also occur randomly scattered throughout the rock. The small veinlets, filled with siderite, quartz, and apatite, are common in the Rapid Creek area. (field of view is 5.4 x 4.1 mm)

B. Non-pelletal phosphate mudstone. The star-shaped bodies are concretionary and composed of carbonate-apatite and siderite. A series of stylolites crosses the sample from lower left to mid-upper right. (field of view is 4.2 x 3.3 mm)

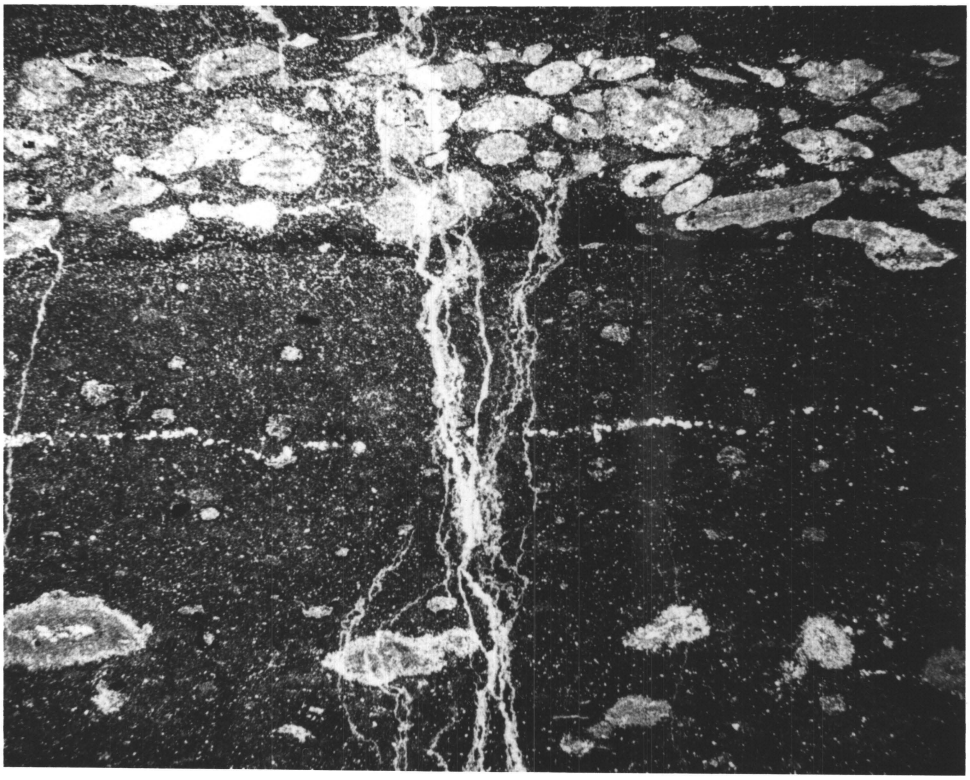

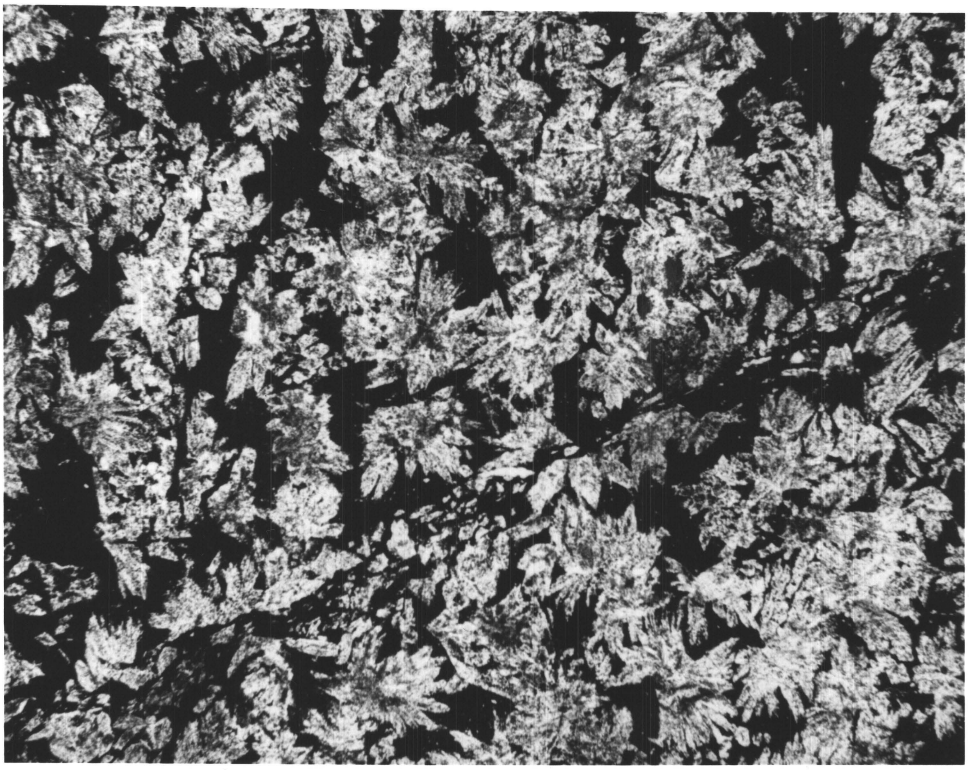

pellets, up to 40 percent of the chert has recrystallized and is concentrated in the center of the pellet. Quartz-rimmed pellets are very rare, less than 0.3 mm, spherical, and consist of a dark siderite center with a silt-sized quartz outer margin.

A variety of pelletal mudstone found in the Big Fish River area has 40 percent siderite pellets which are 0.5 mm in diameter, very well sorted, ovoid, and oriented parallel to bedding.

c) Non-pelletal phosphate mudstone: This rock type has been observed mainly in the lower portion of the Cross-cut Creek section where it occurs in beds up to 20 cm thick. In hand specimen, it is identical to pelletal phosphate mudstone. In thin section, the most striking features are small, 0.5 to 1.0 mm, star-shaped bodies (Plate 2b), which make up to 70 percent of the rock. The stars are composed of carbonate-apatite or siderite or a combination of both components. Individual stars may be partially or completely altered to or replaced by gormanite-souzalite and, less commonly, satterlyite. Pyrite and secondary quartz (recrystallized chert) make up less than 3 percent of individual stars. In places, arms of the stars cut through fine silt laminations and weak wavy laminated clay rich layers indicating that they are post-lithification.

Siltstone:

Siltstones are relatively uncommon in all areas studied and usually occur as 1 to 2 mm thick laminations in other rock types.

a) Non-phosphatic quartz siltstone: These siltstones consist of angular to subangular, 0.01 to 0.1 mm, detrital quartz grains in a matrix of either siderite or chert. Completely non-phosphatic quartz siltstones were observed only as clasts in conglomeratic slump deposits.

b) Phosphatic quartz siltstone: These siltstones are identical to the non-phosphatic variety except that the matrix is completely replaced by gormanite-souzalite.

Sandstone:

The phosphate and siderite sandstones, in thin section, are the most variable rocks in the Rapid Creek area, yet in hand specimen they are virtually identical to each other. They are easily distinguished from other rock types by their resistance to erosion. Most have either a brownish or greenish surface alteration due to the weathering of siderite and iron phosphate minerals. On fresh surface they are light green to grey.

There is a complete spectrum in composition from phosphate to siderite sandstone and in grain size from pelletal (about 0.1 mm) to granular (up to 4 mm). Siderite end-members of this

spectrum are relatively rare whereas almost pure phosphate sandstones are common.

These sandstones (Plate 3a) are composed of siderite and phosphate pellets and granules, detrital quartz grains, skeletal fragments, intraclasts of various rock types, and matrix. Figure 13 demonstrates the gradation between almost pure pelletal sandstone, up to 88 percent pellets, and pelletal phosphate mudstone, with up to 89 percent matrix. This gradation was also observed by Cressman and Swanson (1964, p. 314) in the Permian Phosphoria Formation.

The matrix consists of clay minerals, microcrystalline siderite and pyrite. Pyrite usually is finely disseminated but is commonly recrystallized, forming patches of euhedral crystals.

Skeletal fragments are uncommon in these rocks and, where present, make up less than two percent of the total. They are easily recognized in thin section as they are generally larger than all other particles (up to 1 cm), have sharp, concave outlines, and are completely replaced by gormanite-souzalite.

Quartz grains are predominantly detrital, although recrystallized chert grains can occasionally be recognized. Detrital grains range from 0.01 to 1.0 mm and make up to 33 percent of the rock. The larger the quartz grains are, the more rounded and spherical they tend to be. Overall, there is a weak correlation between detrital quartz grain size, pellet size, and

PLATE 3

A. Pelletal phosphate sandstone. The majority of pellets are rounded and composed predominantly of satterlyite. Dark rounded grains are mudstone intraclasts. Angular clear grains, such as the one in the center of the photomicrograph, are detrital quartz grains. (field of view is 4.2 x 3.3 mm)

B. Pelletal phosphate sandstone. This photomicrograph illustrates a gradation from relatively fresh phosphate sandstone, on the left, to completely recrystallized sandstone, on the right. The thin, parallel dark lines in the lower right define the boundaries between continuous blades of satterlyite that can occur up to 1 cm long and represent a complete loss of the pelletal texture. (field of view is 5.4 x 4.1 mm)

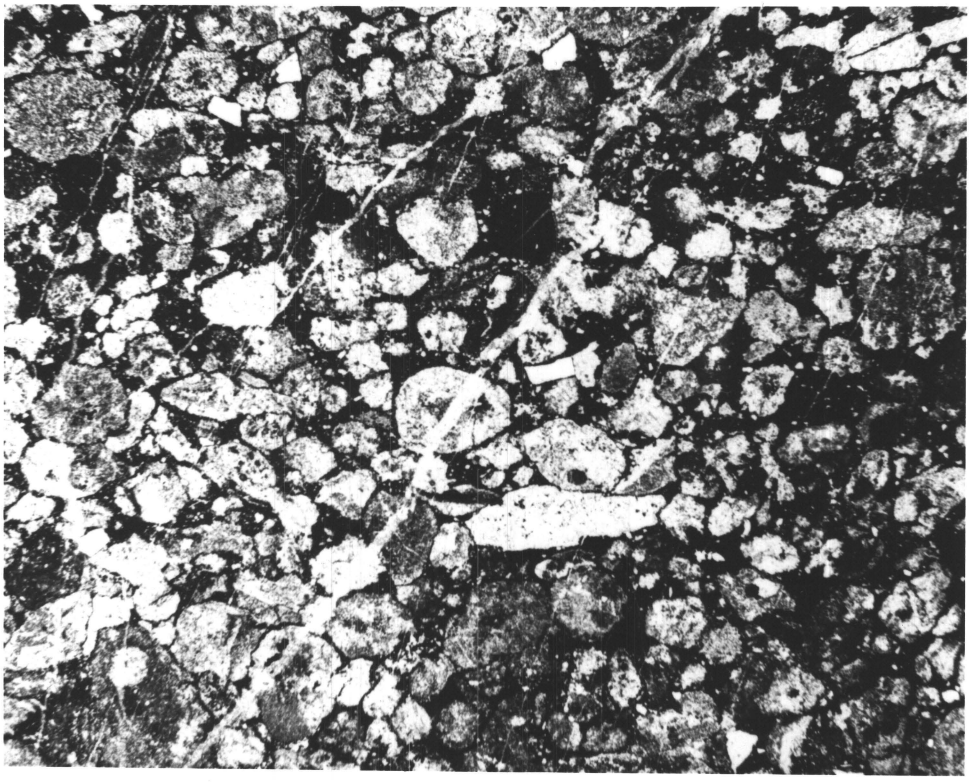

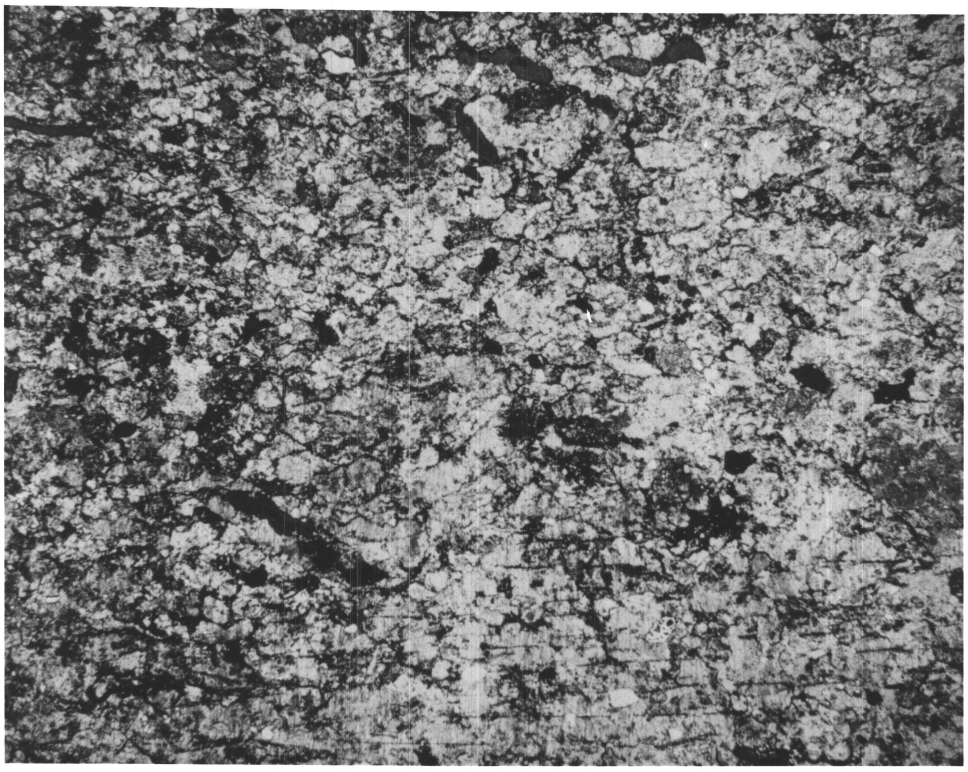

the percentage of matrix. As the percentage of matrix decreases, the quartz grain size increases with an associated increase in pellet size. Care must be taken when determining pellet size because it has been altered during metamorphism (Plate 3b). Recrystallization of microcrystalline phosphate material in the pellets may also have incorporated phosphate material from the matrix.

Pellets and granules are rounded to subrounded and structureless. They consist of satterlyite, siderite, pyrite, quartz, clay minerals, and their alteration products. Pyrite and clay minerals never make up more than a few percent of the pellets. Quartz in the pellets is either recrystallized patches of chert or included detrital grains. Although quartz is a relatively uncommon constituent of pellets, several samples have up to 15 percent recrystallized chert.

Satterlyite is recrystallized from a fine grained aggregate into crystallographically continuous pellets. There is some evidence that this process was repeated several times and that the fine-grained aggregate is itself a recrystallization (or replacement) of a microcrystalline or amorphous material. One sample has several pellets with coarse patches of satterlyite displaying goethite-stained rhombohedral cleavage traces. Satterlyite does not possess cleavage, so this must be a replacement of siderite.

Satterlyite is replaced, in whole or in part, by arrojadite in almost all samples. The arrojadite occurs as bundles of well defined laths which commonly are confined to the more central portions of individual sandstone beds. Arrojadite is definitely a post-lithification feature as laths of the mineral commonly cut across pellet boundaries. Replacement of satterlyite by gormanite-souzalite also is very common, in many places, with arrojadite replacement. Only two samples have shown partial replacement of pellets by lazulite. Other alteration products in pellets are not common but include whiteite, ludlamite and vivianite-baricite. These may be even later than arrojadite replacement because vivianite-baricite appears to fill pore spaces between arrojadite laths. Whiteite and ludlamite replacement is confined to area 3.

The distinction between pelletal and granular sandstone is not clear cut. The boundary was arbitrarily chosen at a grain size of 2 mm but complete gradation from 0.1 to 4.0 mm was observed, with many samples containing both pellets and granules. Most granules appear to be large pellets, though generally somewhat higher in satterlyite content.

Several thin sections have indicated that satterlyite recrystallization is extensive (Plate 3b). Large areas, up to 2 cm in diameter are texturally similar to normal pelletal and granular phosphate sandstone but in which all the satterlyite pellets and granules have the same crystallographic orientation.

Shale and mudstone intraclasts in pelletal phosphate and siderite sandstones are generally rounded and not very common. As pellet size increases towards the upper limit of granule size, there is a tendency for intraclast size, angularity and abundance to also increase. Mudstone intraclasts up to 2 cm in greatest dimension have been observed, but are usually less than 5 mm.

GEOCHEMISTRY

Compositions of various rocks types are given in Table 5. Unfortunately, CO_2 values were not available at the time of this writing. A case can be made, however, for the assumption that L.O.I. is roughly equivalent to CO_2. Samples A215.2 and A380 contain about 65 and 60 percent siderite respectively, which would convert to 19.4 and 17.9 weight percent CO_2. These values are very close to the L.O.I. (18.73 and 18.32 percent, respectively) reported for these samples. An estimation of siderite contents of other samples in Table 5, particularly the mudstones, would be advantageous to confirm the above statement, but these rocks are too fine-grained to make a meaningful determination of siderite content.

The relationship betweeen CaO and P_2O_5 is illustrated in Figure 14a. CaO shows a poor positive correlation with P_2O_5, with a slope of 0.70. The close to zero intercept for both best fit and maximum slope lines suggests that CaO is contained solely in phosphate phases. The maximum slope (1.06) is closer to the slope of Price and Calvert (1978) which is representative of normal phosphate deposits. The data in Figure 14a suggest that either the single primary phosphate phase is variable in composition with other elements substituting for Ca or there is more than one primary phosphate phase or other calcic phases. The only abundant phosphate minerals identified in these rocks are satterlyite, arrojadite and a member of the apatite group (carbonate-apatite) which are Fe-,

Table 5

Chemical composition of rocks from the Big Fish River and Rapid Creek areas (major-element oxides in weight percent, minor elements in ppm, Fe is reported as total Fe_2O_3)

Aa-21	=	Siltstone clast from a conglomeratic slump deposit in Unit 4
A 81	=	Non-pelletal phosphate mudstone from the lower part of Unit 4
A 87	=	Pelletal phosphate sandstone from the middle part of Unit 4
A 215.2	=	Pelletal siderite sandstone from the middle of Unit 8
A 380	=	Granular siderite sandstone from the top of Unit 9
B-1	=	Mudstone from a couplet in the Big Fish River section
B-2	=	Shale from a couplet in the Big Fish River section
A 1-10	=	Average of nine analyses reported in Table 9

	Aa-21	A 81	A 87	A 215.2	A 380	B-1	B-2	A 1-10
SiO_2	75.2	25.8	28.8	15.9	20.4	21.0	48.5	19.5
TiO_2	.52	.25	.24	.04	.09	.26	.65	.23
Al_2O_3	6.61	4.10	4.92	1.14	1.06	5.12	12.27	3.40
Fe_2O_3	7.75	19.1	25.4	37.0	30.5	35.6	22.1	23.2
MgO	.61	2.22	3.89	3.02	3.46	2.67	2.47	3.27
MnO	.15	.31	.27	3.36	3.88	5.14	.20	.31
CaO	1.1	18.5	5.8	7.5	10.2	5.0	.4	15.1
K_2O	.91	.58	.32	.21	.04	.44	1.87	.29
Na_2O	1.65	.58	1.10	.83	.08	.33	.33	.98
P_2O_5	1.1	17.5	16.5	10.6	9.9	6.6	.9	22.0
H_2O	.50	.10	.24	.24	.10	1.00	.79	.22
L.O.I.	2.61	9.12	11.70	18.73	18.32	15.59	9.31	10.70
Total	98.71	98.16	99.18	98.57	98.03	98.75	99.79	99.03
Ba	1112	2107	1108	1194	1058	636	1158	1658
Sr	276	580	530	1276	1164	357	172	870
Zn	63	94	130	92	80	145	232	88
Cu	22	26	32	100	14	40	86	118
V	44	102	138	44	71	202	387	119
Y	25	16	26	7	28	70	60	25
Rb	50	30	15	10	10	25	125	18

Figure 14

The relationship between:

A. CaO and P_2O_5

B. Fe_2O_3 and L.O.I.

C. MgO and L.O.I.

D. Sr and L.O.I.

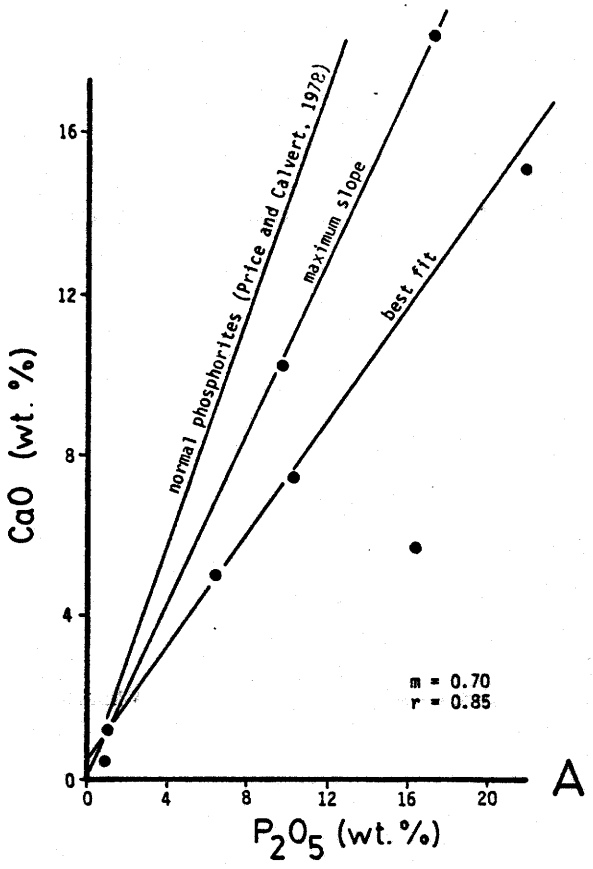
normal phosphorites (Price and Calvert, 1978)
maximum slope
best fit
m = 0.70
r = 0.85
CaO (wt. %)
P_2O_5 (wt. %)
A

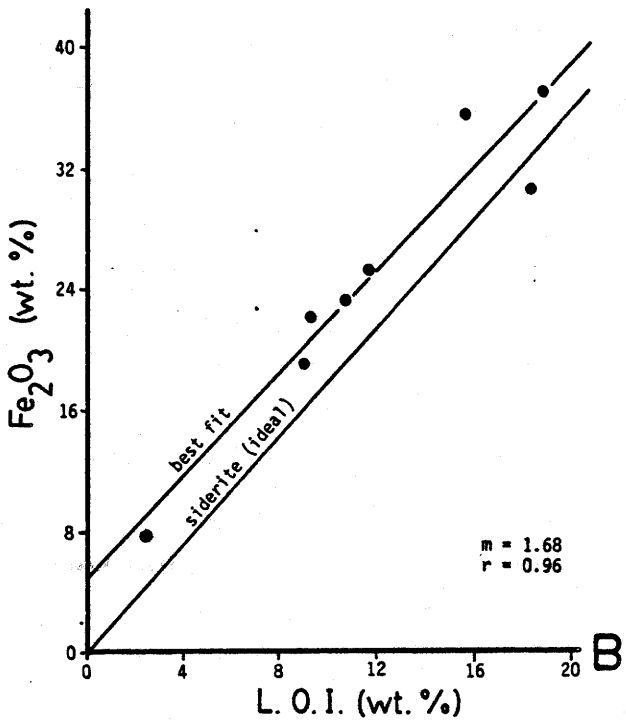
best fit
siderite (ideal)
m = 1.68
r = 0.96
Fe_2O_3 (wt. %)
L. O. I. (wt. %)
B

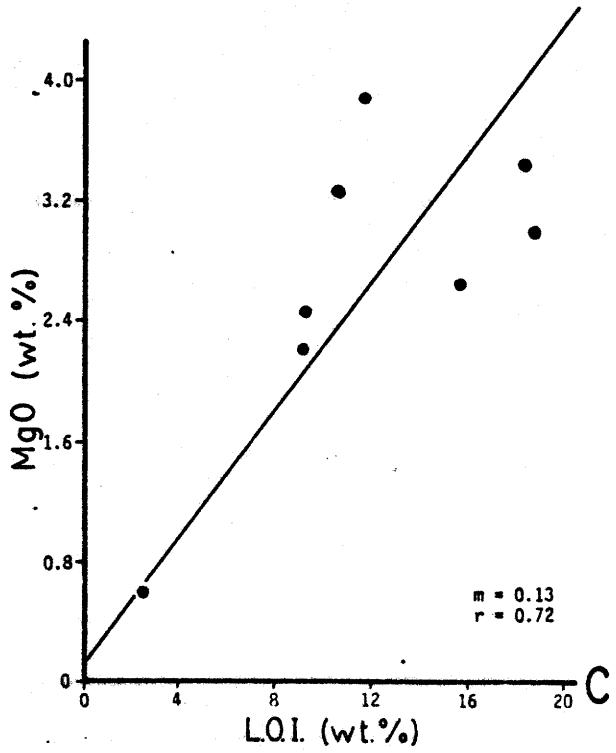
m = 0.13
r = 0.72
MgO (wt. %)
L.O.I. (wt. %)
C

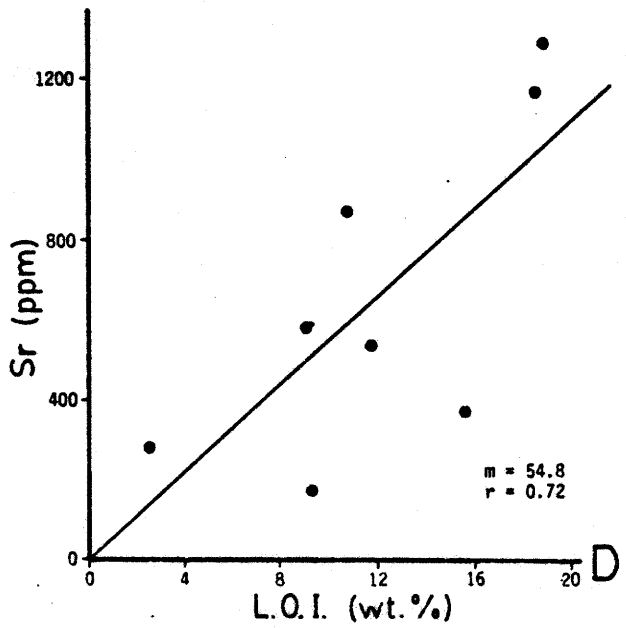
m = 54.8
r = 0.72
Sr (ppm)
L.O.I. (wt. %)
D

Na-Fe-, and Ca- phosphates respectively. Arrojadite is an alteration of satterlyite which itself is not a primary mineral. Thus the primary phosphate mineral in these rocks must be a mixed Ca-Fe (or Ca-Mg) apatite-like mineral with a highly variable composition. Efforts to positively identify this phase proved fruitless, but the unknown mineral listed in Table 4 (no. 3) may represent the Fe-rich end-member of a series with apatite.

There is a strong positive correlation between Fe_2O_3 and L.O.I. (Figure 14b) with a slope of 1.68. The intercept value of about 5 percent Fe_2O_3 suggests that some Fe is contained in another, minor phase (probably pyrite or a phosphate or an oxide) but that most of the Fe is contained in a carbonate phase (siderite). Samples 5 and 6 both plot close to the siderite ideal slope but can be seen in thin section to contain a high proportion of satterlyite and lesser arrojadite. This indicates that siderite was a primary mineral but, through alteration, has produced Fe-phosphates at the expense of siderite. Since the L.O.I. ($=CO_2$) values still plot as siderite, CO_2 has not been lost during the alteration. This suggests a metasomatic event in which siderite and the mixed Ca-Fe apatite-like mineral exchanged cations (Fe and Ca respectively) to produce a secondary Fe-phosphate (satterlyite) and Ca-rich siderite.

The poor positive correlation between MgO and L.O.I. (Figure 14c) suggests that some Mg substitutes for Fe in siderite, but that Mg is contained in other phases as well.

Strontium likewise shows a poor positive correlation with L.O.I. (Figure 14d). In other phosphate deposits (Gulbrandsen, 1966; Price and Calvert, 1978), Sr is associated with apatite. Strontium in this deposit is probably incorporated in both carbonate and phosphate phases and this accounts for its poor correlation with either L.O.I. or P_2O_5. The poor correlation may also be due to mobilization of Sr during alteration. Using data solely from Table 9 for nine analyses of one bed of mudstone, a good positive correlation (Figure 15a) between Sr and P_2O_5 is produced. This suggests that in this sample Sr is contained in the phosphate phase.

K_2O, TiO_2, V, Zn and Rb all show good to reasonable correlation with Al_2O_3 (Figures 15b, c, d and 16a, b) and show that these elements are associated with clay minerals. Sample Aa-21 is a transported clast from a conglomeratic slump deposit. If it is deleted from the plots, correlation factors are all greater than 0.95.

Correlation for SiO_2, MnO, Na_2O, Ba, Cu, and Y could not be found. SiO_2 in the rocks is contained largely in terrigenous detrital quartz and should not be expected to correlate with any other element. Na_2O, Ba, and Y might be expected to correlate with CaO or P_2O_5 because these elements are known to substitute in the apatite structure (McConnell, 1973). Obviously, some other phase(s) also contains these elements. Using data solely from Table 9 for nine analyses of one mudstone bed, a fair correlation

Figure 15

The relationship between:

A. Sr and P_2O_5 (data from Table 9)

B. K_2O and Al_2O_3

C. TiO_2 and Al_2O_3

D. V and Al_2O_3

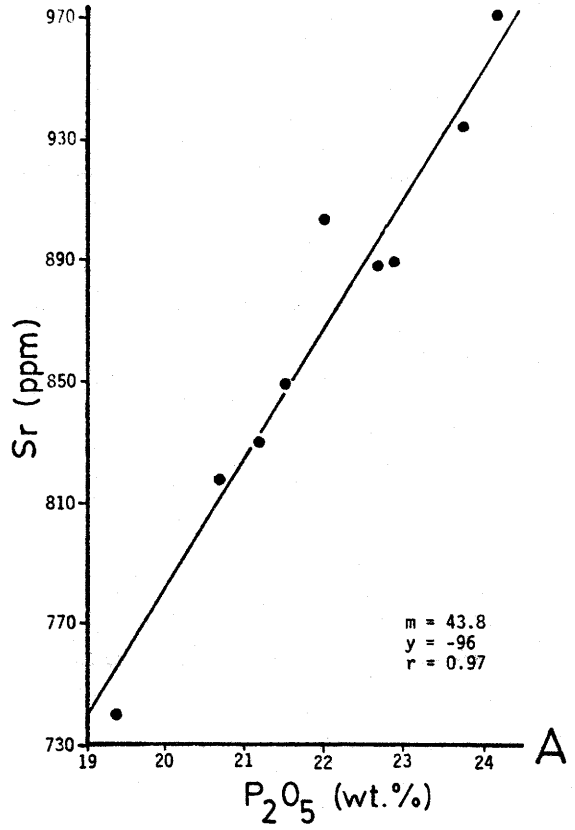
970
930
890
850
810
770
730
Sr (ppm)
19
20
21
22
23
24
P_2O_5 (wt.%)
m = 43.8
y = -96
r = 0.97
A

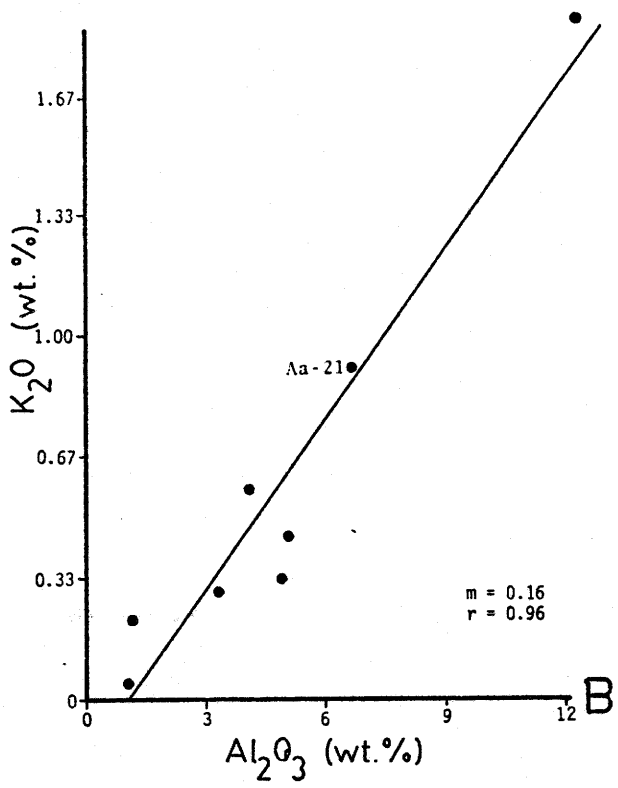
1.67
1.33
1.00
0.67
0.33
0
K_2O (wt.%)
Aa-21
0
3
6
9
12
Al_2O_3 (wt.%)
m = 0.16
r = 0.96
B

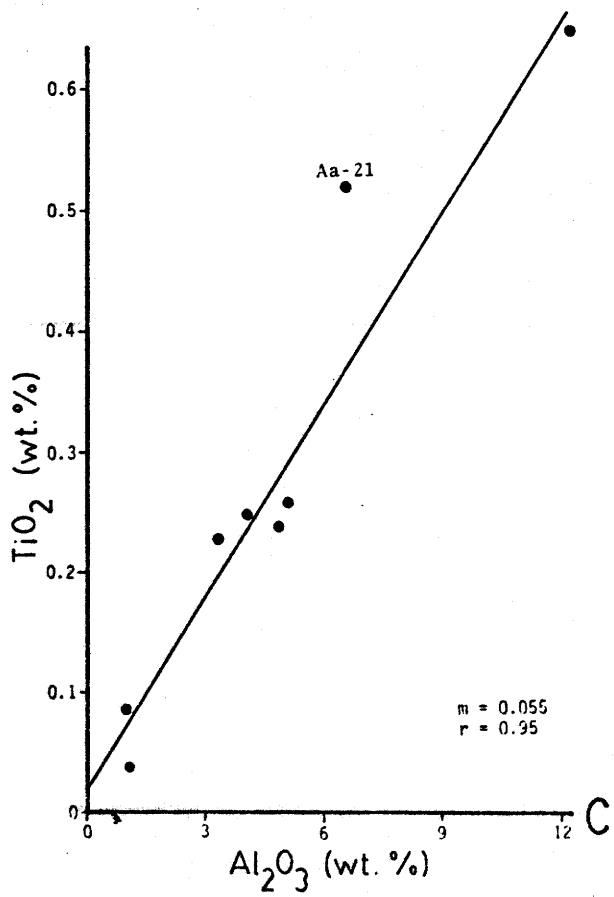
0.6
0.5
0.4
0.3
0.2
0.1
0
TiO_2 (wt.%)
Aa-21
0
3
6
9
12
Al_2O_3 (wt.%)
m = 0.055
r = 0.95
C

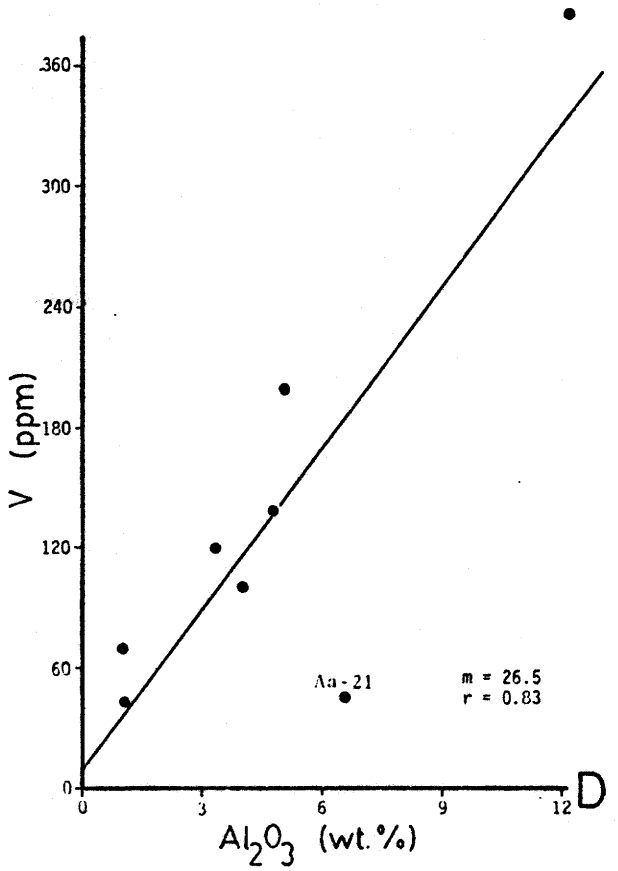
360
300
240
180
120
60
0
V (ppm)
Aa-21
0
3
6
9
12
Al_2O_3 (wt.%)
m = 26.5
r = 0.83
D

Figure 16

The relationship between:

A. Zn and Al_2O_3

B. Rb and Al_2O_3

C. Na_2O and P_2O_5 (data from Table 9)

D. Ba and P_2O_5 (data from Table 9)

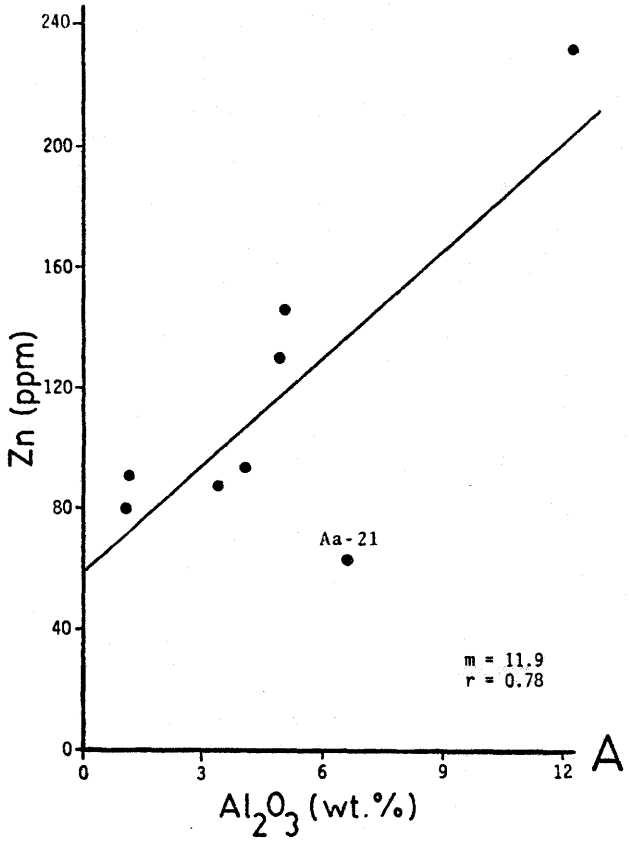
Zn (ppm)
240
200
160
120
80
40
0
Aa-21
m = 11.9
r = 0.78
0
3
6
9
12
Al_2O_3 (wt.%)
A

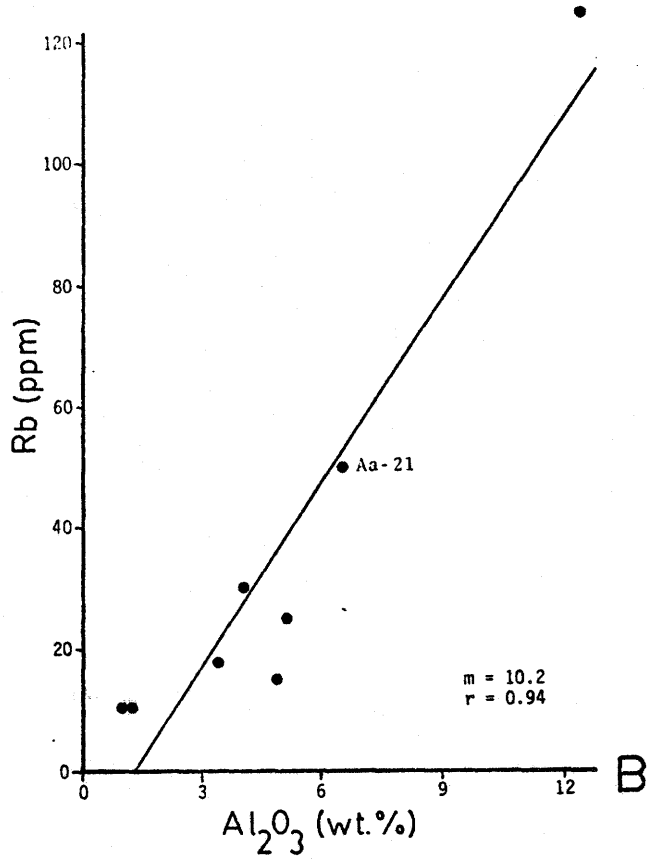
Rb (ppm)
120
100
80
60
40
20
0
Aa-21
m = 10.2
r = 0.94
0
3
6
9
12
Al_2O_3 (wt.%)
B

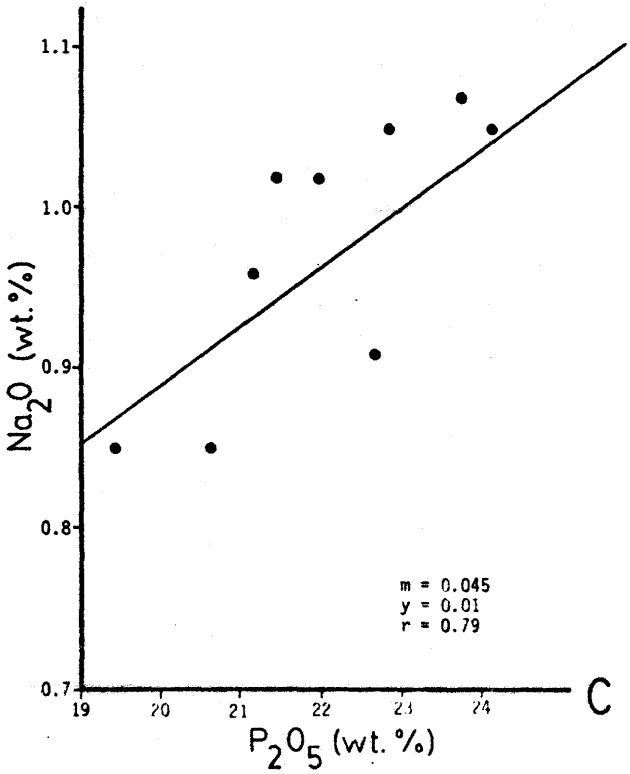
Na_2O (wt.%)
1.1
1.0
0.9
0.8
0.7
m = 0.045
y = 0.01
r = 0.79
19
20
21
22
23
24
P_2O_5 (wt.%)
C

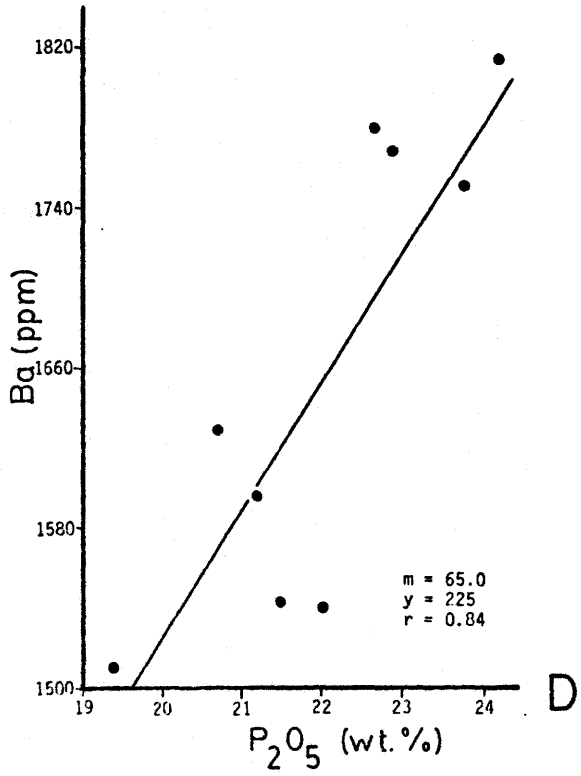
Ba (ppm)
1820
1740
1660
1580
1500
m = 65.0
y = 225
r = 0.84
19
20
21
22
23
24
P_2O_5 (wt.%)
D

between Ba and P_2O_5 (Figure 16c) and Na_2O and P_2O_5 (Figure 16d) was observed. Cu is probably contained in pyrite, but sulphur was not analyzed in this study. Mn is also probably contained in a sulphide (or oxide) phase.

Samples B-1 and B-2 (Table 5) are interbedded shale and mudstone, respectively, from a couplet in the Big Fish River section. By subtracting the shale composition from the mudstone, some insight into the composition of the 'extra' phases in the mudstone can be gained.

In Table 6 the composition of the shale has been recalculated such that Al_2O_3 mudstone - Al_2O_3 shale = 0. The subtraction of the shale from the mudstone results in a composition which represents one or more minerals which are contained in the mudstone and not in the shale or are at least more abundant in the mudstone. Hydroxyl has been subtracted from L.O.I. because it is contained in the phosphate mineral and the remainder is assumed to be CO_2. This assumption is not truly valid because some SO_4 (from pyrite) must contribute to L.O.I., but the assumption is the best approximation that can be made with the present data. Also, even if there are large quantities of sulphur in these samples the composition of the extra phases would not be significantly different after the calculation in Table 6, but the proportion of phases (carbonate to sulphide, etc.) might.

The extra minerals in the mudstone, then, are a mixed Ca-Mg-Fe phosphate (with minor Na), siderite, and Fe and Mn oxides. If

Table 6
Mudstone composition minus shale composition.

	A	B	C	D	E	F	G
SiO_2	20.2	.8	.37	1.3			
TiO_2	.27	-					
Al_2O_3	5.12	0					
Fe_2O_3	9.2	26.4	18.46	33.1	33.1	31.7	6.2
MgO	1.03	1.64	.99	4.1	4.1		
MnO	.08	5.06	3.92	7.1	7.1	7.1	7.1
CaO	.2	4.8	3.43	8.6	8.6		
K_2O	.78	-					
Na_2O	.14	.19	.14	.6	.6		
P_2O_5	.4	6.2	2.71	8.8	8.8		
(OH)		(.49)	.029	2.9	2.9		
L.O.I.	3.88	11.71					
(CO_2)		(11.22)	3.06	25.5	25.5	25.5	

A = B-2 recalculated such that $Al_2O_3 = 5.12$
B = B-1 minus B-2
C = metal weights
D = atomic proportions
E = take out all SiO_2 as quartz
F = take out all Ca, Mg, Na and some Fe as a hydrated phosphate of the apatite formula ($X_5(PO_4)_3(OH)$): $(Ca_{8.6}Mg_{4.1}Fe_{1.4}Na_{.6})_{14.7}(OH)_{2.9}$ or $(Ca_{2.9}Mg_{1.4}Fe_{.5}Na_{.2})_5(PO_4)_3(OH)$
G = take out some Fe as siderite ($FeCO_3$)

phosphate is extracted in the formula type $X_2PO_4(OH)$, instead of the apatite-type formula, the results are almost the same; a mixed Ca-Fe-Mg phosphate (with minor Na), siderite, and Fe and Mn oxides in the remainder.

In Table 7 the shale composition has again been subtracted from the mudstone composition, but this time has not been recalculated. The results are similar to those in Table 6; a mixed Ca-Fe-Mg phosphate and siderite, with minor Mn substitution for Fe, and the remainder is Mn oxide. If the phosphate is extracted in the formula type $X_2PO_4(OH)$, the results are the same; a mixed Ca-Fe-Mg phosphate and Mn-bearing siderite with Mn oxide in the remainder.

These calculations demonstrate and confirm earlier statements that the primary autochtonous minerals in this deposit are siderite and a mixed Ca-Fe-Mg phosphate.

Table 7
Mudstone composition minus shale composition.

	A	B	C	D	E
SiO_2	-				
TiO_2	-				
Al_2O_3	-				
Fe_2O_3	13.5	9.4	16.83	12.08	
MgO	.20	.12	.49		
MnO	4.94	3.82	6.95	6.95	5.79
CaO	4.6	3.29	8.21		
K_2O	-				
Na_2O	-				
P_2O_5	5.7	2.5	8.07		
(OH)	(.46)	.27	2.69		
L.O.I.	6.28				
(CO_2)	(5.82)	1.59	13.24	13.24	

A = B-1 minus B-2, but B-2 is not recalculated, i.e., raw data
B = metal weights
C = atomic proportions
D = take out Ca, Mg and some Fe as a hydrated phosphate of the formula type $X_5(PO_4)_3(OH)$:
$(Ca_{8.21}Fe_{4.75}Mg_{.49})_{13.45}(PO_4)_{8.07}(OH)_{2.69}$ or $(Ca_{3.05}Fe_{1.77}Mg_{.18})_5(PO_4)_3(OH)$
E = take out all Fe and some Mn as carbonate: $(Fe_{12.08}Mn_{1.16})_{13.24}(CO_3)_{13.24}$ or $(Fe_{.91}Mn_{.09})CO_3$

DISCUSSION

The primary (or early diagenetic) non-detrital minerals in the Big Fish River - Rapid Creek phosphatic iron formation are pyrite, siderite, and a mixed Ca-Fe-Mg mineral which probably belongs to the apatite group. The intimate association of abundant iron and phosphate minerals is not a common phenomenon, but certainly is not unique. While some writers (Bushinski, 1964) believe that iron-rich and phosphorus-rich sediments are antagonistic, others (Cook and McElhinny, 1979; Nriagu, 1972) believe that conditions of formation of both sediments have several factors in common. Although high iron contents in phosphorites are rare, high phosphorus contents in ironstones are not, with phanerozoic ironstones averaging 1.43 weight percent P_2O_5 (McKelvey, 1973). Birch (1979) describes mixed glauconite-, goethite-, and collophane-rich rocks and sediments from the western margin of South Africa. Parker (1975) reports an average Fe_2O_3 content of 6.71 weight percent for several phosphorite samples from the Agulhus Bank.

Cook and McElhinny (1979) have dealt with the association of iron and phosphorus in some detail. The following discussion is intended to draw on information from other workers to develop some understanding of the environment of deposition and origin of various rock types in the Big Fish River - Rapid Creek phosphatic iron formation.

Source and transportation of phosphorus and iron

River runoff supplies the oceans with phosphorus derived from continental weathering. Inorganic phosphorus in seawater is contained and transported as phosphoric acid (H_3PO_4) or its dissociation products ($H_2PO_4^-$, HPO_4^{2-} , and PO_4^{3-}) or complexes containing these ions (e.g., Na_2HPO_4) (Gulbrandsen and Roberson, 1973). Most of the phosphorus in sea water, however, is contained in organisms (Gulbrandsen, 1969).

Continental weathering also releases iron which is supplied to the oceans by runoff. Iron can be transported as $Fe(HCO_3)_2$ (Borchert, 1960), goethite (FeOOH) and iron hydroxide ($Fe(OH)_3$) (Pearson, 1979), in and absorbed by clay mineral platelets (Carroll, 1958), or as ferric oxide hydrosol in and absorbed by organic colloids (Moore and Maynard, 1929; Krauskopf, 1967) (Pettijohn, 1975).

Deposition of phophorus and iron

Although there are only small amounts of phosphorus and iron in sea water, they can become concentrated in sediments if conditions are suitable. The mechanism, however, is not known precisely. Some writers (Cook, 1976; Birch, 1979; Ames, 1959; D'Anglejan, 1968) believe that it is by the inorganic replacement of carbonates, particularly calcite, and other materials. Others (Bushinski, 1964; Cressman and Swanson, 1964)

believe that phosphate is inorganically directly precipitated in the sediment. Price and Calvert (1978) and Gulbrandsen (1969) believe that phosphorus is derived from the breakdown of planktonic organic material and then diagenetically precipitated in the sediment. Fuller (1979) has found evidence of all three mechanisms in phosphorites on the western and southern coastal areas of southern Africa with the latter being the dominant mechanism.

Apatite has been shown to replace $CaCO_3$ in experiments in which pH was greater than or equal to 7.0 and PO_4^{3-} concentrations were 0.1 ppm or more (Ames, 1959). Calcite and aragonite have not been documented in the rocks of this deposit but a similar mechanism with siderite is certainly possible.

The precipitation of apatite, as well as calcite, is mainly controlled by pH. Apatite is precipitated in the range pH = 7.1 to 8.5 (Gulbrandsen, 1969) but at pH = 7.8 or more calcite is precipitated and will overwhelm apatite because of its greater abundance in sea water.

The suggestion that Eh is a critical factor in the deposition of marine apatite (Berge, 1972) has not been substantiated. Nriagu (1976) has shown that the precipitation of calcium and aluminum phosphates is independent of Eh.

The mechanisms for siderite and pyrite deposition are similar to those for carbonate-apatite. Ferric compounds are the only iron minerals that can exist in equilibrium with

depositional (oxidizing) waters. Siderite and pyrite are in equilibrium with the sediment pore water and are, thus, diagenetic (Curtis and Spears, 1968). Pyrite is formed by bacterial sulphate reduction (Berner, 1970) and is linked directly with organic matter in the sediment. Siderite is formed at near neutral to slightly basic pH, low Eh, where there is a high iron to calcium ratio, high dissolved carbonate, and where dissolved sulphide concentration is low (Pearson, 1979; Curtis and Spears, 1968). Pyrite formation will proceed until sulphide activity is low enough to allow siderite formation.

The lower redox potential of fine grained sediment, as opposed to the oxygen-enriched sea water, is maintained by the decomposition of mechanically included organic matter and will tend to produce ferrous compounds as long as iron and other constituents are available. Pearson (1979) has shown that iron in the form of pyrite at the abundance found in many sedimentary rocks (a few percent) probably has its source in clay minerals and detrital iron phases, but that iron in the form of large amounts of siderite (e.g., clay ironstone concretions and sideritic mudstones) must have an 'external' source. James (1954) believes that such fine grained, low Eh sediments are isolated from the depositional sea water. Clearly, if these sediments are isolated from sea water, then they could not produce high concentrations of siderite. There must be an exchange mechanism that allows the sediment to retain its low

redox potential but is open enough to permit diffusion of materials across the sediment/water interface.

The deposition of a primary diagenetic iron- or mixed iron and calcium phosphate is a distinct possibility for the Big Fish River - Rapid Creek phosphatic iron formation. Nriagu (1972) has presented theoretical evidence for vivianite formation in a variety of sedimentary environments but states that it is unlikely to be preserved over long periods of time. Vivianite has been documented in recent fresh water (lake) sediments by Nriagu and Dell (1974) and Rosenquist (1970) but is unkown in marine sediments.

Murray et al. (1978) and Emerson (1976) have shown that remineralization of organic matter in iron-dominated sediments will tend to produce iron-carbonate and -phosphate phases. Crystalline siderite, Mn-sulphide and a mixed Mn-carbonate and non-crystalline Fe-sulphide, Mn-phosphate, and a mixed Fe-Ca phosphate have been identified as diagenetic products of microbial decomposition of organic matter in recent sediments from the Landsort Deep in the Baltic Sea (Suess, 1979).

Environment of deposition

A depositional environment is a function of several complexly interrelating factors; tectonic, physical, chemical, and biological conditions at the site of deposition.

Tectonic conditions at the time of formation of this

deposit are not well known because stratigraphic and structural investigation of the northern Yukon region as a whole is rudimentary. High terrigenous input in the western side of the Blow Trough indicates strong uplift. The Cache Creek High, however, received little terrigenous material, but this does not necessarily mean that it was tectonically stable.

Physical factors in depositional environments include submarine topography, water depth, current patterns, and climate. A close spatial relationship between phosphorites and evaporites has been documented for many ancient deposits and indicates a warm, arid climate (Cook and McElhinny, 1979). Climatic indicators have not been documented for this deposit.

Although rivers are the main supplier of phosphorus and iron, the environment of deposition need not be estuarine, as suggested by Bushinski (1964), Pevear (1966), and Parker (1975). Most marine phosphorite investigators agree that these deposits are associated with areas of upwelling ocean water. The solubility of phosphate decreases as temperature and pH increase, so that the ocean water becomes supersaturated with phosphate when it rises close to the surface (McKelvey, 1967; Roberson, 1966). Also, the nutrient-rich water will sustain an abundance of life, leading to organic-rich sediments. McKelvey notes four situations of ocean current systems in which upwelling might occur. Two of these are possible situations for the Big Fish River-Rapid Creek deposit; "where two currents meet

to produce turbulence... [and] in upper latitudes where highly saline water from the tropics tends to sink as a result of winter cooling (convection)". (McKelvey, 1967, p. D5).

If the northward current in the Western Canada Seaway was stronger than the southward one and if the northward current reached as far as the Rapid Creek area, then it would have converged with any current (eastward or westward) along the arctic coastline.

Most phosphorites were deposited at low latitudes with the maximum known being 65^{o} away from the paleoequator (Cook and McElhinny, 1979). From the paleolatitude map of Seyfert and Sirkin (1979, p. 372) and Firstbrook et al. (1979), the Big Fish River-Rapid Creek rocks were deposited at approximately 75^{o} or 70^{o}N, respectively. Clearly, if northbound warm waters reached this latitude, then convection due to winter cooling is quite possible.

Holland (1973) has shown that upwelling sea water is also the likely situation for major iron deposits.

Several writers have used phosphorites as evidence of shallow water deposition. Indeed, most modern phosphorites are deposited between 50 and 150 m depth (Christie, 1978). Independent evidence of shallow water is lacking in both Rapid Creek and Big Fish River areas. Megafauna in the Rapid Creek area are non-existant. The Big Fish River area, however, offers several lines of evidence indicating a shallow water environment

which is opposite to Kimberley's (1978) classification of this deposit as a deep water iron formation.

The association of large flat, thin shelled inocerami with ammonites and a lack of heavy shelled (very shallow water) pelecypods suggests a low energy, normal salinity environment (Jeletzky, pers. comm.). The Pholadomya sp. indet. is a deeply burrowing organism that prefers a mid- to outer neritic environment.

In the Big Fish River area, the phosphatic iron formation is bounded by unconformities. The lower unconformity is angular, indicating a period prior to the ironstone deposition in which the Cache Creek High was emergent. Although an angular relationship between the Boundary Creek Formation and ironstone was observed in only one locality, the similarity of the transitional contact in both Big Fish River and Rapid Creek areas suggests a disconformity which may be locally angular. The hiatus in the upper contact, then, is probably less than the hiatus of the lower contact, with only local and minor emergence, if any. The sharp contact between the lower ironstone and the lower grey shale unit may indicate an unconformity within the ironstone sequence. This is supported by an apparent thinning of the lower grey shale unit on the east side of Big Fish River and its complete absence in the Boundary Creek area, and by the open fracture, weathered-looking nature of the top of the lower ironstone.

Fossil twigs, several centimeters to one half meter long, have been noted in several parts (mainly upper) of both Cross-cut Creek and Big Fish River sections. Although these twigs may have floated in from other areas, e.g., across the Blow Trough from the Keele-Old Crow Landmass, the fragile nature of some of the twigs indicates short transport. It is more likely that these twigs originated from some emergent part of the Cache Creek High.

Many of the spherulitic nodules in the Big Fish River area are replaced ammonites and pelecypods. This indicates a rich pelagic (nektonic) biota immediately above the site of deposition of the phosphatic iron formation similar to shelf regions in the present environment (e.g., the Grand Banks). The lack of current related structures, such as ripple marks, and the fine-grained nature of the sediment indicate an environment protected from currents, such as an embayment, or deposition below wave base. However, the coarsening-upward nature of the lower five units of the Cross-cut Creek section indicates shallowing.

Physio-chemical factors in depositional environments include temperature, salinity, pH, and Eh. Efforts to determine the temperature of formation through oxygen isotopic investigation of siderite is in progress. Preliminary results indicate that the siderite has re-equilibrated with a higher temperature hydrothermal solution during metamorphism (or

metasomatism). Meagre fossil evidence (above) indicates normal salinity and well oxygenated waters. Estimated values of acidity and redox potential, from primary (or early diagenetic) minerals, are pH = 7 to 8 and Eh = -.02 to 0.0 volts, but these probably represent conditions in the sediment rather than conditions of the depositional water.

Biological factors are the most difficult to assess because they are largely dependant on preservation. Numerous ammonite-like spherulitic nodules suggest a rich pelagic fauna. The well-developed and continuous lamination in shales and mudstones suggests few burrowing organisms. The almost complete lack of microfauna may indicate conditions of very poor preservation rather than original scarcity.

Origin of pellets

Shaly laminations wrapping around pellets in the pelletal phosphate shales and mudstones indicate that either the pellets formed on the sediment surface and were progressively covered up or they formed within unconsolidated sediment and later acted as semi-rigid bodies during compaction. The pellets in most mudstones and shales do not appear to have been transported. Although most are roughly spherical to elliptical in outline, the boundaries of the poorly sorted pellets are generally irregular or undulatory. Cressman and Swanson (1964, p. 375),

discussing similar rocks of the Phosphoria Formation, state that such pellets do not appear to be a replacement of a carbonate precursor and, in fact, they know of no calcareous sediment even remotely similar in texture to these phosphatic mudstones.

A suggestion popular in the earlier part of this century was that most, if not all, phosphate pellets were faecal pellets which may or may not have been completely phosphatized. Cressman and Swanson (1964) believe that most faecal pellets are those of burrowing benthonic organisms, because the pellets of planktonic organisms are friable and rarely preserved. Because lamination in the phosphatic shales and mudstones is continuous and apparently undisturbed, they believe that the apatite pellets of the Phosphoria Formation are not faecal pellets. Fossil evidence indicates that bottom dwelling organisms were not common in this as in most phosphorites, thus reinforcing the conclusion that phosphate pellets formed either by direct precipitation from sea water or by organic or indirectly by organic accretion within unconsolidated sediment.

Pellets in sandstones differ markedly from those in phosphatic mudstones and shales. These pellets grade in size to granules and are generally more rounded with smooth, sharp boundaries and show a higher degree of sorting, which is generally accompanied by a higher phosphate mineral content. Sandstone pellets are also highly recrystallized and replaced by

satterlyite which is probably due, in part, to the greater permeability of sandstone.

Origin of rock types

Many writers (Cheney et al., 1979; Fuller, 1979; Cook, 1967; Christie, 1978; and others) have stressed the importance of winnowing and, in some cases, transportation as a vital factor in the upgrading of phosphorites. Direct evidence of currents in the Big Fish River and Rapid-Creek areas is lacking. Cross-bedding was observed in only a few of the quartz siltstone samples. If it was present in the sandstones, subsequent metamorphism (recrystallization, replacement, and alteration) and recent surficial weathering have completely obliterated it. In the Rapid Creek area, several sandstone beds have basal contacts that cut across shale laminations. Indeed, one bed fills a partially exposed scour approximately 70 cm deep. The pellets in the sandstones appear to have been transported in that they are rounded with smooth grain boundaries and are in tangential contact with one another. Also, with a higher degree of sorting there is generally a decrease in the proportion of matrix material. Fuller (1979) and Cook (1967) believe that the parent material of similar phosphate sands was phosphatic mudstone in which the lighter, non-phosphatic particles had been winnowed out. Winnowing alone cannot explain sorted pelletal and granular phosphate and siderite sandstone beds up to 60 cm

thick. Cheney et al. (1979, p. 259) used the evidence above to prove the action of currents and a transportation origin for pelletal phosphorites elsewhere. Fuller (1979, p. 230) believes that pelletal phosphorites originate "from storm-wave disrupted inorganically precipitated semi-lithified collophane muds on the floors of shallow lagoons, [which are] subsequently redistributed into other regions on the shelf." The storm-wave generated beds (pelletal sandstones) in the Rapid Creek area thin slightly to the west, indicating that the source area is somewhere to the east.

Phosphatic shale, mudstone and siltstone have different origins. Pelletal phosphate shale and mudstone are the precursor to pelletal phosphate sandstone in which the fines have not been or are only partially winnowed out.

Phosphatic quartz siltstone occasionally contains a few pellets, but most of the phosphate material occurs as a replacement of the matrix between quartz grains.

Non-pelletal phosphate mudstones have the highest P_2O_5 content of all the rock types in this deposit. Most of the phosphate occurs in star-shaped concretionary bodies. There is no indication that these bodies are recrystallized pellets because true pellets can also be found. The original crystals which made up the stars' arms are not preserved. The stars were probably not originally phosphatic as they now contain some

amorphous collophane, carbonate-apatite, siderite and other minerals which occur as a replacement.

Besides the phosphatic varieties, there are non- or weakly phosphatic rock types. These are distinct from the former in that there does not appear to be a gradation between 'normal' rock and its phosphatic equivalent. Whereas other writers (Cressman and Swanson, 1964; Birch, 1979) refer to terrigenous clastic material as a dilutent in phosphorites, the present writer prefers the opposite point of view. Phosphatic material appears to be the dilutent superimposed on an otherwise normal sequence of iron-bearing beds. This is displayed particularly well in the conglomeratic slump deposits in which a thick accummulation of iron-rich sediment was deposited too quickly to be phosphatized.

Non-phosphatic shales generally form thick beds. Apparently, the locus of deposition or, more likely, the chemical condition of the sea water is different for non-phosphatic and phosphatic shales, despite the different genesis between the phosphatic rock types.

Facies analysis of the varied lithologies in the Big Fish River-Rapid Creek phosphatic iron formation is not possible with the present limited data.

P A R T I I

MINERAL OCCURRENCE

The rocks of the area are characteristically fine grained and their mineral constituents, therefore, are not macroscopically identifiable. However, phosphates not only occur in them as integral parts of these rocks, which thus are not macroscopically recognizable, but also occur in more coarsely crystalline segregations in which they and associated minerals are readily identifiable. These segregations are most commonly epigenetic fracture fillings (veins) and also include vugs, concentrations along bedding-plane partings, fillings in fault breccias, and isolated nodules. The last type of occurrence is restricted to the Big Fish River and boundary Creek areas and is described separately.

Quartz and siderite are ubiquitous and occur in association with almost all phosphates. Aragonite is associated solely with gorceixite and gypsum is not associated with any other mineral. The various phosphate minerals that have been observed in the area are outlined in Table 8, with their compositions and characteristic chemical associations.

Phosphate minerals:

Apatite occurs as well formed stout prismatic crystals in association with lazulite. Crystals are less than 5 mm long and white. Several samples are tinged pink due to a trace amount of manganese.

Table 8
Minerals, compositions, and characteristic associations.

Mineral	Composition	Characteristic Associations
Apatite	$Ca_5(PO_4)_3(OH,F,Cl)$	Ca
Arrojadite	$K(Na,Ca)_5(Fe,Mn,Mg)_{14}Al(PO_4)_{12}(OH)$	Fe-Mg, N
Augelite	$Al_2PO_4(OH)_3$	U
Brazilianite	$NaAl_3(PO_4)_2(OH)_4$	Na, Ba
Carbonate-apatite	$Ca_5(PO_4,CO_3)_3(OH,F)$	N, U
Childrenite	$(Fe,Mn)AlPO_4(OH)\cdot H_2O$	U, Ca, Fe-Mg
Collinsite-messelite	$Ca_2(Mg,Fe,Mn)(PO_4)_2\cdot 2H_2O$	Ca, Fe-Mg
Destinezite	$Fe^{3+}{}_2PO_4SO_4(OH)\cdot 5H_2O$	U
Gorceixite	$BaAl_3(PO_4)_2(OH)_5\cdot H_2O$ (?)	Ba
Gordonite	$MgAl_2(PO_4)_2(OH)_2\cdot 8H_2O$	U
Gormanite-souzalite	$(Fe,Mg)_3(Al,Fe^{3+})_4(PO_4)_4(OH)_6\cdot 2H_2O$	Fe-Mg, U
Kryzhanovskite	$(Fe,Mg,Mn)Fe^{3+}{}_2(PO_4)_2(OH)_2\cdot H_2O$	Fe-Mg
Kulanite-penikisite	$Ba(Fe,Mg,Mn,Ca)_2(Al,Fe)_2(PO_4)_3(OH)_3$	Ba
Lazulite	$(Mg,Fe)Al_2(PO_4)_2(OH)_2$	Na, Ca. Ba, Fe-Mg
Ludlamite	$(Fe,Mg,Mn)_3(PO_4)_2\cdot 4H_2O$	Fe-Mg, U

Marićite	$NaFePO_4$	N
Metavivianite	$Fe_3(PO_4)_2 \cdot 8H_2O$	U, Na, Fe-Mg, N
Nahpoite	Na_2HPO_4	N
Satterlyite	$(Fe,Mg,Fe^{3+},H,Na,Mn)_2PO_4(OH)$	N
Varulite	$(Na,Ca)(Mn,Fe)_2(PO_4)_2$	N
Vivianite-baricite	$(Fe,Mg)_3(PO_4)_2 \cdot 8H_2O$	U, N, Na, Fe-Mg, Ca
Wardite	$NaAl_3(PO_4)_2(OH)_4 \cdot 2H_2O$	U, Na, Ba
Whiteite	$Ca(Fe,Mn)Mg_2Al_2(PO_4)_4(OH)_2 \cdot 8H_2O$	Ca
Wolfeite	$(Fe,Mn,Mg)_2PO_4(OH)$	N

N = nodules
U = alone
Na = Sodium-bearing association
Ca = Calcium-rich association
Ba = Barium-rich association
Fe-Mg = Iron-magnesium-rich association

Arrojadite occurs as subparallel aggregates of or as individual well developed diamond-shaped blades, up to 1 cm across. It is generally associated with other iron-rich phosphates, such as ludlamite and vivianite-baricite, and is characteristically green in the Big Fish River area but commonly orange-brown in the Rapid Creek area.

Augelite occurs as well developed, pseudorhombohedral crystals that are not associated with other phosphates. It varies from colorless to white to green but is most commonly faintly green and transparent. Large crystals, up to 3 cm across, are found associated with faults.

Brazilianite occurs with quartz and lazulite or with kulanite-penikisite. Its crystals are either stout or elongate pseudorhombohedral prisms, up to 1 cm across. It is usually white to colorless but commonly displays a light blue tint.

Carbonate-apatite occurs alone as a finely crystalline botryoidal crust and is always colorless.

Childrenite occurs as coarse radial or stellate fibrous groups of transparent yellow to red-brown or translucent cream colored acicular crystals. It is commonly associated with vivianite--baricite, and other iron phosphates, or else occurs alone in veins. Crystals up to 1.5 cm long have been observed but most are much smaller.

Collinsite-messelite occurs as fine-grained mammillary radial groups up to 1 cm across or coarse radial groups of laths up to 2.5 cm long. Collinsite-messelite is associated with many other

phosphates, particularly whiteite, gormanite-souzalite, and kryzhanovskite. It is typically white or cream to colorless.

Destinezite occurs as equant microcrystalline lumps. The only specimen observed by the writer was 1 cm across and cream colored. Its characteristic association is not known.

Gorceixite occurs as flattened hexagonal plates up to 8 mm across and is not associated with any other phosphate minerals. It is cream to white in color.

Gordonite occurs as tiny (less than 2 mm across) radial groups of white acicular crystals and is associated with wardite in only one area.

Gormanite-souzalite occurs as massive or radial groups of bright to dark green acicular crystals up to 3 cm across. It occurs either alone or with iron-rich phosphates.

Kryzhanovskite occurs as deep red-brown to black cleavable masses up to 5 cm across or as poorly developed prismatic crystals up to 1 cm long. It is generally associated with arrojadite, ludlamite, vivianite-baricite, gormanite-souzalite, and collinsite-messelite.

Kulanite-penikisite occurs as well developed platy crystals, up to 2 cm across, associated with brazilianite, wardite, and lazulite and is deep green in color. In several places, the platelets are arranged in rosettes.

Lazulite occurs as well formed, acute equant to platy crystals in association with most other phosphates. Individual

crystals range from microscopic to as much as 1.5 cm across. The azure-blue color is characteristic but some lazulites are bluish green.

Ludlamite occurs as large cleavable masses or in groups of parallel fibers. It either occurs alone or with other iron phosphates and is always bright green in color.

Maricite occurs as radial prismatic crystals up to 15 cm long in spherulitic nodules. It is commonly associated with satterlyite, wolfeite, arrojadite and varulite and is brownish green to grey in color.

Metavivianite occurs as green micaceous masses either with other phosphates or alone. Masses up to 15 cm across have been found but are usually much smaller.

Nahpoite occurs as a white encrustation along fractures directly associated with maricite.

Satterlyite occurs as radial prismatic crystals up to 20 cm long in spherulitic nodules either alone or is associated with maricite, wolfeite, arrojadite and varulite. It is yellow in color.

Varulite occurs as deep green masses in spherulitic nodules. It is associated with maricite, satterlyite, arrojadite and wolfeite.

Vivianite-baricite occurs as colorless to deep blue, cleavable to micaceous masses associated with most of the other phosphates. It is commonly light blue when first uncovered and

deepens in color with prolonged exposure. Prismatic crystals are rare in the Rapid Creek area but are relatively common in veins in the Big Fish River area. It is a common constituent of phosphate nodules.

Wardite occurs as colorless or white to yellowish, horizontally striated dipyramidal crystals ranging from microscopic to as much as 4 cm across. Crystals that are macroscopically readily visible usually occur alone or with lazulite, and rarely with kulanite-penikisite.

Whiteite occurs as cream to white colored platy to tabular or stout prismatic crystals associated with lazulite, vivianite-baricite, and quartz. It also commonly occurs alone.

Wolfeite occurs as deep red, radial prismatic crystals up to 20 cm long in spherulitic nodules either alone or is associated with satterlyite, maricite, varulitė and arrojadite.

Associations:

Epigenetic fracture fillings contain either one, two, or many phosphates. Simple veins, containing only one or two phosphates, are relatively small (less than 2 m long and 5 cm wide) and are found either associated only with one rock type or else occur in any rock type present in the area. They generally have no preferred orientation relative to bedding. Most veins having more complex mineralogy are perpendicular to bedding, are vertical and strike 100^{o}. It, therefore, appears that they

are related to the same vein-forming event. These veins are up to 40 cm wide and 10 m long and generally transect more than one bed and rock type; thus they have no specific association. However, they usually occur in parts of the section which are dominated by a single rock type, thus accounting for the four chemical associations: Ca-rich (occurring with phosphatic mudstone), Na-bearing (with phosphate sandstone), Fe-Mg-rich (with siderite sandstone-dominated portions of the section), and Ba-rich (with conglomeratic slump deposits).

Simple associations:

Almost all bedding planes between phosphatic beds have some vivianite-baricite and/or metavivianite mineralization along them. In many places, this mineralization is up to 3 mm thick and laterally continuous, up to 5 m. Where vivianite-baricite is present, it is usually highly altered to a yellow, friable mass while metavivianite retains its deep green color even when intensely altered. This mineralization accounts for most of the color on outcrop surfaces.

Only two samples containing carbonate-apatite have been observed by the writer and in them it is the sole macroscopically visible mineral present. It occurs as a botryoidal crust lining cavities in a solution breccia and, since both samples were found in talus, its association with rock type is not known.

Gypsum is relatively uncommon in the area and occurs as a late stage mineral in fractures that were probably generated by near-surface weathering. These veins have been found cutting all rock types but are generally more abundant in non-phosphatic shale and mudstone.

Augelite-bearing veins are found associated with faults either lining the walls of solution cavities or fault breccias or superimposed on other veins which have been transected by faults. Its crystals generally decrease in size away from the fault zones indicating its genetic relationship.

Childrenite, wardite and gormanite-souzalite are the most common minerals in simple veins. Childrenite veins are smaller than the other two, being less than 1 mm wide. Wardite veins are usually more than 3 mm wide and gormanite-souzalite veins are intermediate.

In the Big Fish River area, asbestiform ludlamite occurs along bedding plane partings in a manner similar to the occurrence of vivianite-baricite and metavivianite in the Rapid Creek area. Occasionally, fibers of ludlamite are curved into an 'S' form, indicating slippage along the bedding plane during mineralization.

Arrojadite associated with vivianite-baricite and quartz also occurs in the Big Fish River area. Either of the three components can dominate the vein or occur by itself, but vivianite-baricite is generally scarce and arrojadite is more

common than quartz. All three minerals occur as well developed crystals. The quartz crystals in these veins are characteristically terminated by a single pyramid rather than the more usual pair.

Mineral association in the more complex veins is characterized by the dominance of one or two elements which tend to be represented by one or more minerals. Minerals in the following descriptions are listed in what is considered to be an approximate paragentic sequence as based on observations of cross-cutting relationships. In many places, siderite is replaced by goethite or limonite but siderite was undoubtably the original phase. Also, all of the following associations can be found with a coating of dypingite or nesquehonite, products of weathering, and so these two minerals are excluded from the mineral lists.

Calcium-rich association:

Two associations that are calcium-rich have been recognized.

1. Quartz + siderite + lazulite + apatite
2. Quartz + siderite + lazulite + whiteite + collinsite-messelite + childrenite + vivianite-baricite

Of these two, the first is by far the most common association. It is commonly found totally enclosed in phosphatic (either pelletal or non-pelletal) mudstone which is

thus both the source and the host rock. The abundance of these rocks in the Rapid Creek area makes this a very common assemblage. In these veins any of the four minerals can exist alone or dominate over the other three. However, most contain equal proportions of quartz and siderite, slightly larger quantities of lazulite and very little apatite.

The second association, which is not as common, is also related to phosphatic mudstone, has a more complex mineralogy, and does not appear to be represented by any one typical mineral assemblage. Instead, all combinations of those minerals listed above are found and examples have been noted in the field where several veins occurring side by side and of the same general size contain radically different assemblages. One may contain whiteite and lazulite, a second whiteite and vivianite-baricite, while another only whiteite. The only generalization concerning these veins is that collinsite-messelite is a very minor component, being well developed in only one place, and that childrenite is even rarer. The childrenite that occurs in this association is distinct from that found in the simple veins in that it is always cream colored (although microprobe analysis indicates similar compositions to other childrenite samples).

Sodium-bearing association:

The sodium-bearing association is the second commonest and is characterized by:

Quartz + brazilianite + lazulite + siderite + apatite + wardite + metavivianite

Whereas assemblages of the calcium-rich association commonly contain a high proportion of the calcium-rich mineral phase (whiteite, apatite, or collinsite-messelite), this association rarely has more than a scattering of crystals of the sodium-rich phase (either brazilianite or wardite).

Quartz and lazulite usually dominate these veins with apatite and metavivianite occurring only rarely in patches.

Calcium-rich associations occur most commonly in pelletal phosphate sandstone dominated sections of strata. However, because the length of the vein is generally greater than the thickness of a single bed, there must be some contribution from other rock types.

Iron-magnesium-rich association:

The iron-magnesium-rich association is the most variable of all. This is partly due to its complex mineralogy:

Quartz + siderite + arrojadite + lazulite + kryzhanovskite + gormanite-souzlaite + collinsite-messelite + ludlamite + vivianite-baricite + metavivianite + childrenite

In this association, lazulite and collinsite-messelite are very rare constituents and gormanite-souzalite is not common but, where present, is abundant relative to the other minerals.

As in the calcium-rich association, no typical assemblage was observed by the writer. However, in general one of either arrojadite, kryzhanovskite, or ludlamite dominates over all other minerals in a vein and veins containing only arrojadite are quite common.

This association is found only in strata dominated by siderite-rich phosphate and siderite sandstone in the upper portion of the section measured at Cross-cut Creek and in stratagraphically equivalent rocks on the east side of Rapid Creek.

Barium-rich association:

The barium-rich association is relatively rare in the area studied and is of two types on the basis of which barium-containing mineral is present.

1. Quartz + siderite + lazulite + gorceixite + aragonite
2. Quartz + apatite + siderite + lazulite + kulanite-penikisite + brazilianite + wardite

Only two occurrences of the first association were observed, one in the conglomeratic slump deposit at the top of unit 4 in the measured section at Cross-cut Creek and the other within a brecciated fault zone in area 1 where only siderite and rare gorceixite crystals were observed. In the first, any of the first four minerals can dominate portions of the vein and aragonite occurs in small spherulite atop quartz crystals. A

similar association has been observed by H. G. Ansell (pers. comm.) in the upper reaches of Rapid Creek (near area 7); in it occurs goyazite, a strontium aluminum phosphate related to gorceixite.

The second barium-rich association is also uncommon but generally occurs in conglomeratic slump deposits. In it, lazulite and apatite are usually not major constituents; brazilianite and wardite are also relatively scarce and mutually exclusive. Wardite associated with kulanite-penikisite was observed only in area 7. One occurrence of this association has been observed in pelletal phosphate sandstone beds immediately below a slump deposit. In it, lazulite is relatively abundant.

Nodule occurrence:

The occurrence of phosphates in nodular segregations is restricted to the Big Fish River and Boundary Creek areas. In these areas, only the lower ironstone unit contains significant quantities of macroscopic phosphates, occurring mainly in spherulitic nodules. There are three distinct types of such nodules; ones that resemble ammonites or pelecypods in outline and show remnant ribs or costae; ones that resemble ammonites in outline only; and ones that bear no resemblance to ammonites or pelecypods. All types, when found in situ, show laminations of shale or mudstone draped over the edges of the nodules.

The first type of nodule is very rare. Sixteen of this type were submitted to J. A. Jeletzky for identification and were confirmed as recrystallized replacements of ammonites and, more rarely, pelecypods. The second type is most abundant in the Big Fish River area and is illustrated in figure 17. These nodules have a peculiar raised three-armed stellate structure on one or, more commonly, both sides. On several, found in situ, the stellate pattern was observed on the basal side only. The third type of nodule which is most abundant in the Boundary Creek area has three subtypes which are distinguished by their cross-sectional shape; either plano-convex, convex-convex, or plano-plano (Figures 18-20).

A fourth type of nodule occurs only in the basal five meters of the Big Fish River measured section. Nodules of this type are irregular, lumpy and composed wholly of micro-crystalline pyrite.

Many nodules are monomineralic, but some contain a variety of minerals. The dominant minerals in these nodules are pyrite, wolfeite, satterlyite, maricite, vivianite-baricite, and varulite, which are in part altered to ludlamite, metavivianite, carbonate-apatite, secondary pyrite and secondary vivianite-baricite. Quartz is a rare constituent of these nodules. Nahpoite, a new mineral, was found as a fine, white encrustation in fractures in maricite and is presumably an

Figure 17

Two phosphate nodules from the Big Fish River area. Note the similarity of the outline to ammonite and the three-armed stellate structure in A.

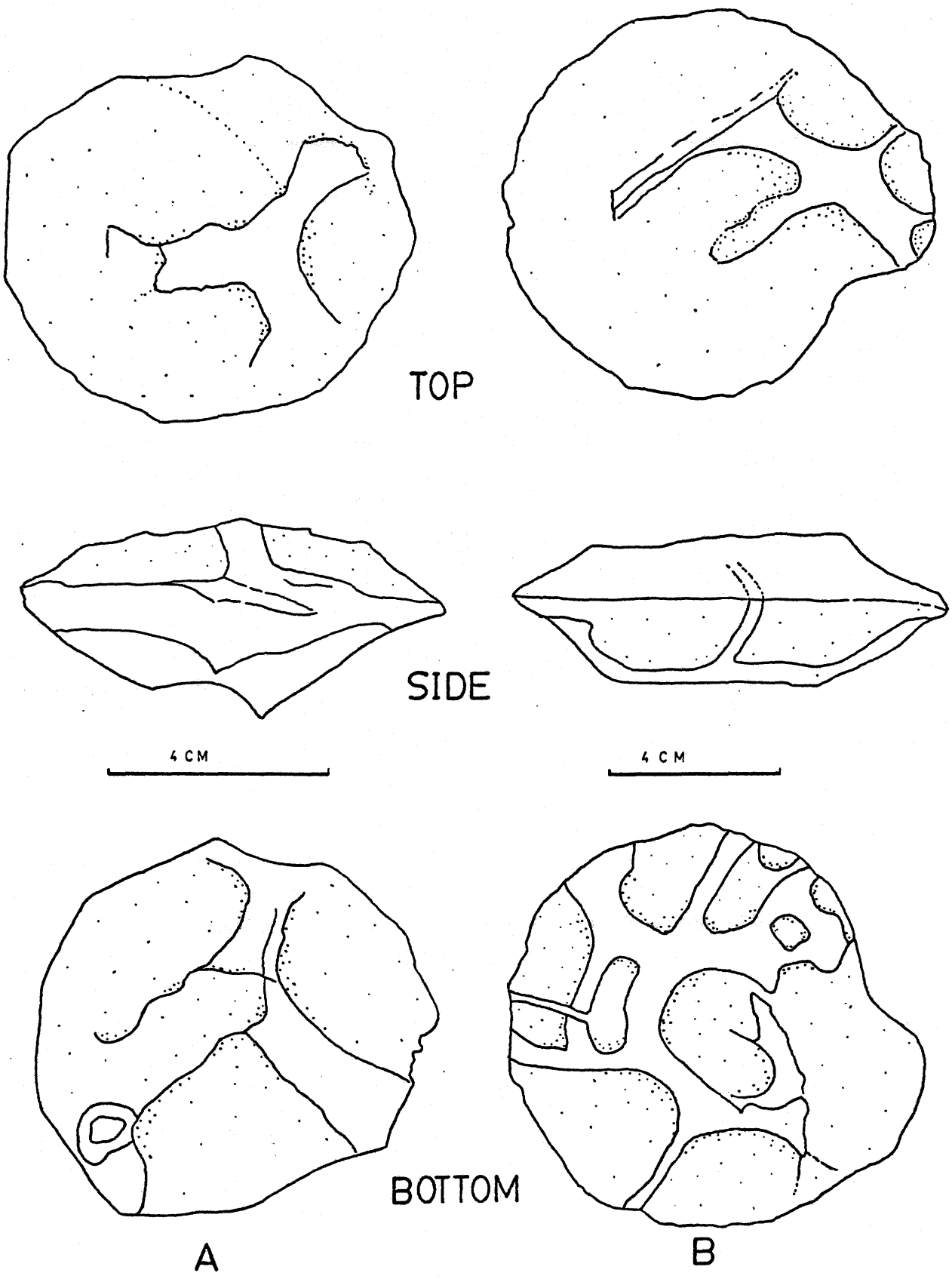
TOP
SIDE
4 CM
4 CM
BOTTOM
A
B

Figure 18

Two plano-convex nodules from the Boundary Creek area.

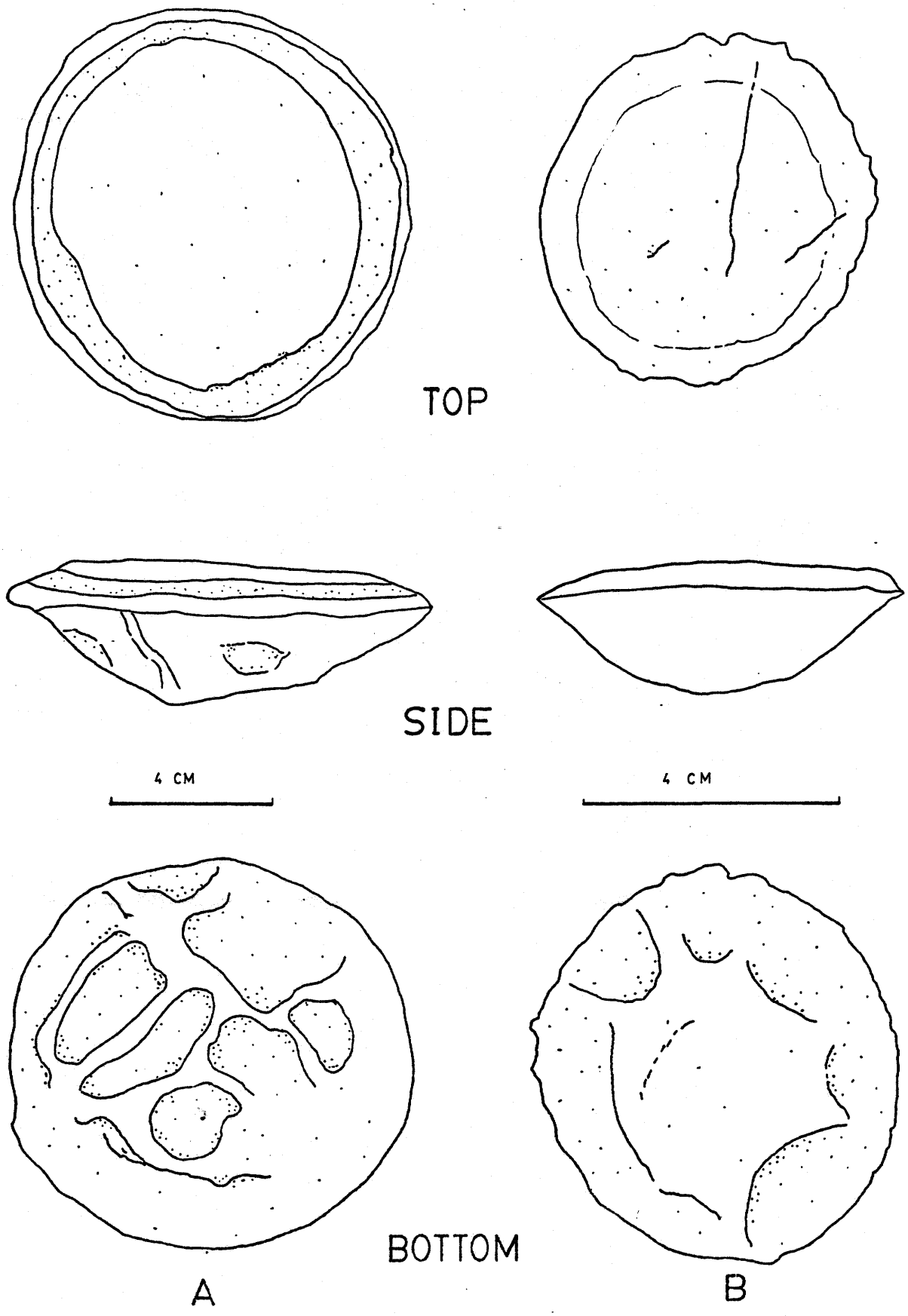
TOP
SIDE
4 CM
4 CM
BOTTOM
A
B

Figure 19

Two plano-plano phosphate nodules from the Boundary Creek area.

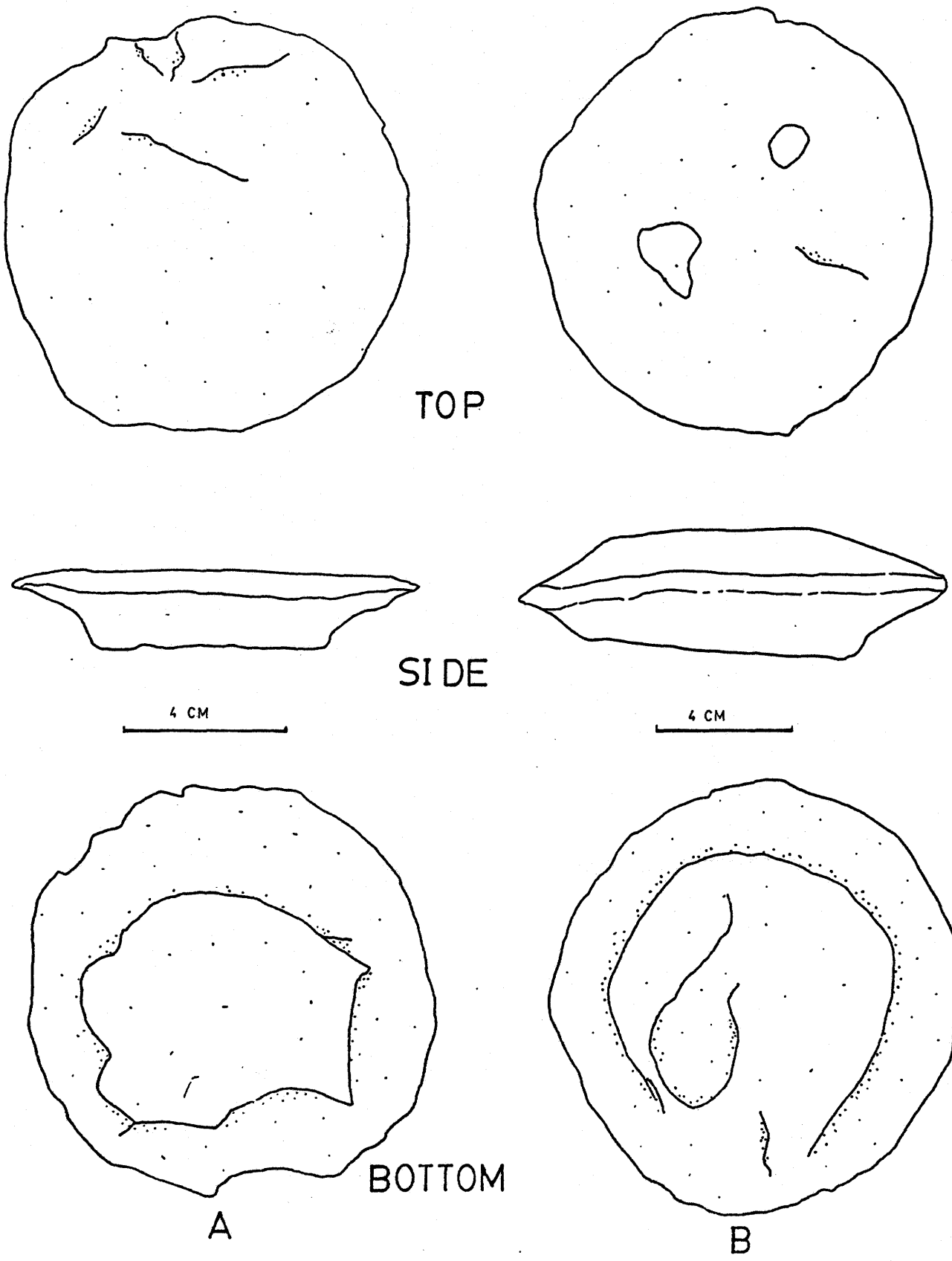
TOP
SIDE
4 CM
4 CM
BOTTOM
A
B

Figure 20

A. A large composite nodule from the Boundary Creek area.

B. A convex-convex phosphate nodule.

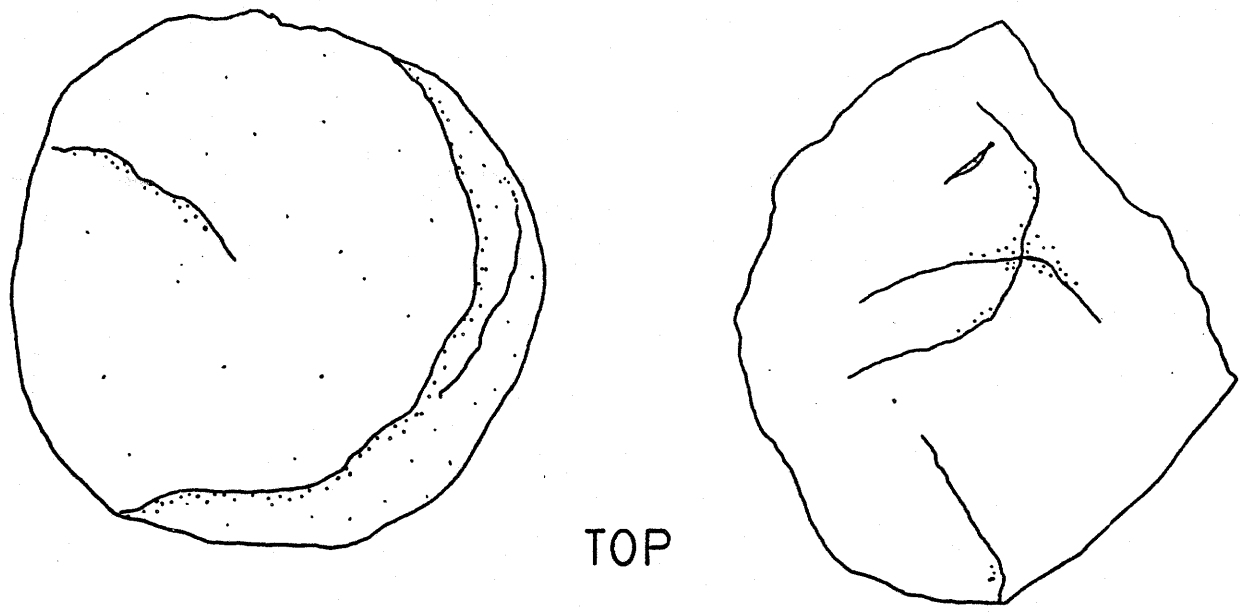
TOP

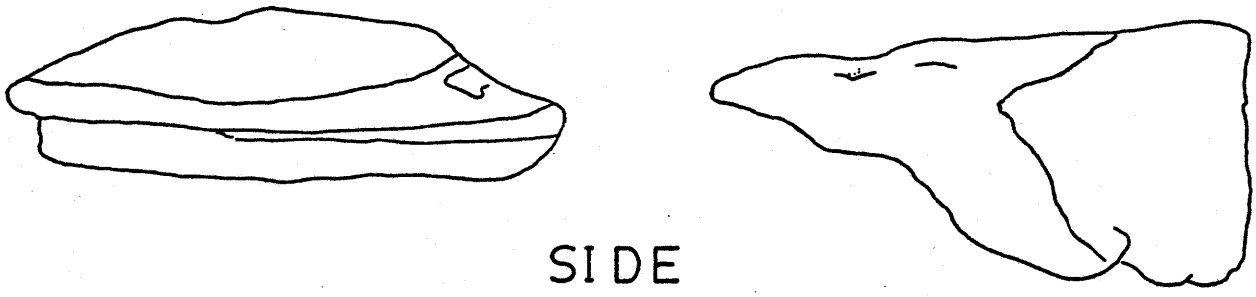
SIDE

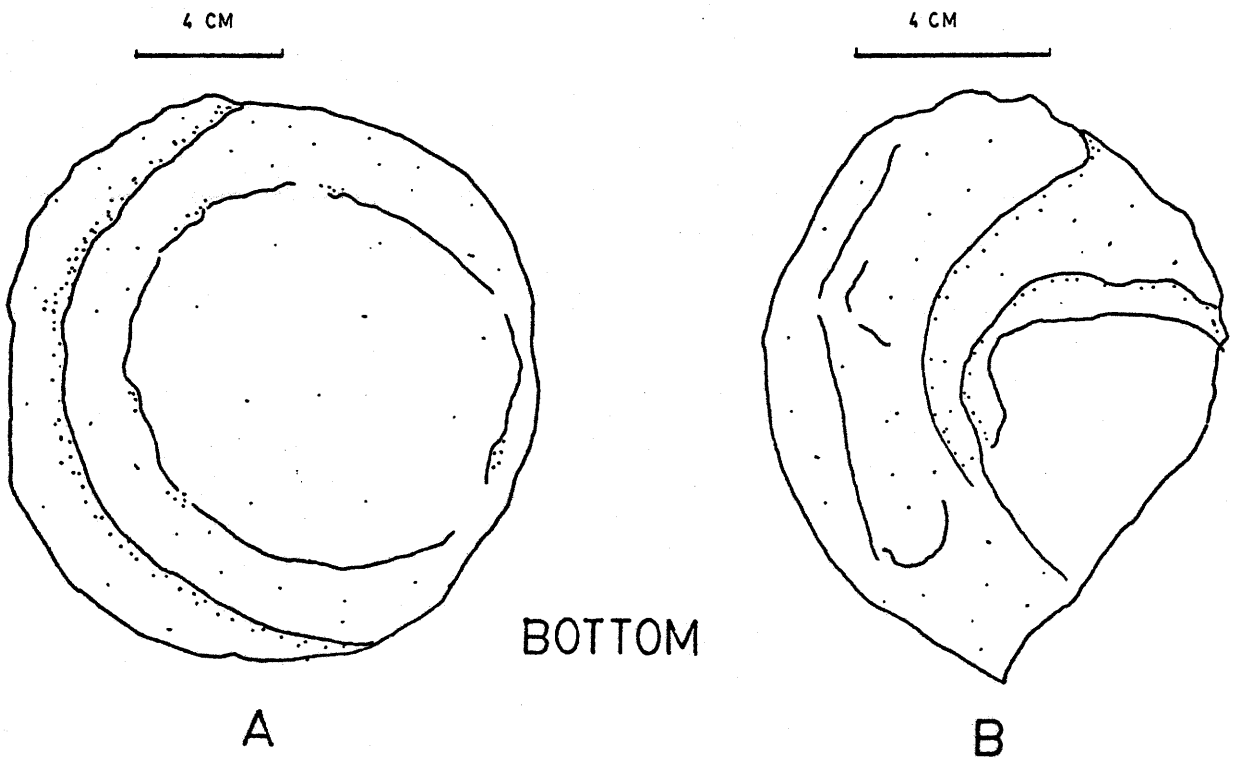
4 CM
4 CM
BOTTOM
A
B

alteration of that mineral. A 4 cm thick mudstone bed, 73 m above the base of the lower ironstone, contains small (5-10 mm) structureless nodules composed of carbonate-apatite.

A brief study of the distribution of nodules was carried out to discover if there existed any regularity in their mineralogy within single beds or from bed to bed. Unfortunately, many of the nodules were too altered on their surfaces to make a positive mineral identification. In the Big Fish River area, many of them have been plucked from the outcrop surface by previous collectors. For these reasons, the results of this study are not too definite.

The procedure followed was to count the number of nodules of each mineral present along a single bed, usually 0.5 to 1 m thick, as far as it could be traced or reached and then to move 2 to 3 m up the section and repeat the procedure.

The results indicate that there is no significant difference in mineral compositions of nodules in shale and in mudstone. The overall abundance is about the same in both types of rock and varies almost randomly in the section as a whole. Pyrite nodules dominate the lowermost portion of the section but give way to phosphate nodules as one goes up the section to about 50 m from its base where the nodules become less and less abundant until they are nonexistant 20 m further up. In the portion of the Big Fish River section studied in detail,

wolfeite occurs in 1:1 to 2:1 ratios with pyrite, 20:1 with satterlyite and 30:1 with maricite. Vivianite-baricite nodules were not observed in situ.

At Boundary Creek, nodules consisting mostly of wolfeite made up 90 percent of the total. Pyrite nodules were fairly rare (1 in 20) and satterlyite nodules were almost as rare (1 in 10). Maricite and vivianite-baricite nodules were not observed in situ in this area.

Variations:

The most varied mineralization in the Rapid Creek area is found in the valley of Cross-cut Creek. Within the section that was measured there, the mineralization is confined to three horizons (mineralized zones 1, 2, and 3, Figures 11a and 11b). Other parts of that section contain only trace or very minor amounts of visible phosphate mineralization.

Mineralized Zone 1:

Mineralized zone 1, which is most varied in character, contains three coarsening-upward sequences with associated slump deposits (Units 3 to 5) between 20 to 60 m in the measured section. This zone is exposed along eight ridges (denoted 1 to 8 from west to east) in the upper reaches of the valley. The lower coarsening-upward sequence contains mineralization only in

ridge 8 where rare whiteite crystals associated with quartz were found.

The middle coarsening-upward sequence (from 30 to 47 m in the measured section) contains the greatest amount of mineralization and is dominated by the Ca-rich association. In ridge 1, veins are scarce and contained only quartz, siderite and lazulite except near the top where apatite is also common. This assemblage was noted in ridge 2, but was less abundant. Ridge 3 contained quartz, siderite, lazulite, and apatite in the lower and upper parts of the sequence with lazulite commonly dominating these veins. In the middle of the sequence, veins are not common but contain rare metavivianite patches with quartz and lazulite. The slump deposit immediately above this sequence in ridge 3 contains two veins of the Ba-rich association; one with gorceixite and the other with exceptionally well developed kulanite-penikisite crystals. This is the type locality for kulanite. Augelite occurs on the southwestern side of this ridge in association with a small fault that separates ridges 3 and 4. Ridge 4 contains only augelite in association with this fault.

The presence of large trenches paralleling veins indicates that many of the lazulite specimens for which this area is noted have been obtained from ridge 5 where that mineral dominates most of the veins. In one vein, messelite was found along a half meter interval as were rare whiteite crystals. Quartz,

siderite and apatite are not as abundant in these veins as in those on other ridges.

Ridge 6 contains veins with whiteite, lazulite, vivianite-baricite and quartz. One sample of vivianite-baricite also contains a large cream colored crystal of childrenite. This ridge is the type locality for baricite.

Ridge 7 is dominated by exceptional whiteite with quartz, lazulite and vivianite-baricite. The middle coarsening-upward sequence is not exposed in ridge 8.

Mineralized Zone 2:

Zone 2 is contained within the upper portion of the slump deposit at the top of Unit 6 and the lower beds of the following fining upward sequence. In the slump deposit, small rosettes of kulanite-penikisite (this is the type locality for the latter) occur on siderite with minor amounts of quartz, apatite and, more rarely, brazilianite crystals. In the overlying beds, separate veins contain gormanite-souzalite, childrenite and wardite.

Mineralized Zone 3:

Veins in zone 3 are generally small but contain a variety of minerals including quartz, lazulite, vivianite-baricite, ludlamite, siderite, wardite and brazilianite and, less commonly, arrojadite, childrenite and apatite. The lowermost

veins contain the Ca-rich association and are commonly dominated by lazulite. The middle veins contain the Fe-Mg-rich association and are commonly dominated by arrojodite and ludlamite. Simple wardite veins dominate the uppermost part of the zone. Childrenite, apatite and vivianite-baricite occur randomly in patches in the lower and middle veins and brazilianite occurs in veins of the Na-bearing association throughout the zone.

In all but one of the seven other areas examined in this study (apart from Boundary Creek and Big Fish River areas), the observed associations are similar to those in mineralized zone 3, i.e., the Fe-Mg-rich association is dominant, simple wardite veins are common and Na-bearing and Ca-rich associations are present but scarce. The exception is in area 1 where the Ca-rich association is abundant.

Elemental migration study:

In order to determine which and to what extent elements have been leached from host rocks and deposited in veins, a 29 cm long portion of a bed of non-pelletal phosphate mudstone between two veins of the calcium-rich association was cut into ten slabs parallel to the veins. Nine of these slabs were analyzed for major, minor and for several trace elements. The results are listed in Table 9 and plotted in Figures 21 and 22.

The variation of element abundance confirms correlations

Table 9

Chemical composition of nine slabs of a non-pelletal phosphate mudstone (major-element oxides in weight percent, minor elements in ppm)

	A-1	A-2	A-3	A-4	A-6	A-7	A-8	A-9	A-10
SiO_2	18.8	18.7	14.8	17.8	17.4	21.4	19.8	22.1	21.7
TiO_2	.22	.23	.23	.23	.22	.23	.21	.24	.22
Al_2O_3	3.39	4.00	3.50	3.11	3.55	3.16	3.25	3.31	3.30
Fe_2O_3	22.9	22.5	23.8	20.8	24.4	24.6	25.7	22.6	22.2
MgO	3.29	3.27	3.42	3.45	3.34	3.58	3.26	3.58	3.39
MnO	.32	.31	.29	.30	.34	.34	.32	.31	.30
CaO	15.6	15.9	17.3	18.1	15.3	12.5	13.8	13.4	14.4
K_2O	.38	.32	.31	.31	.29	.26	.24	.27	.27
Na_2O	1.02	1.02	1.07	1.05	.96	.85	.85	.91	1.05
P_2O_5	21.5	22.0	23.8	24.2	21.2	20.7	19.4	22.7	22.9
H_2O	.23	.20	.40	.05	.13	.20	.20	.20	.36
L.O.I.	10.65	10.11	10.08	9.99	11.17	12.11	11.56	10.89	9.74
Total	98.30	98.56	99.00	99.39	98.40	99.93	98.59	100.51	99.83
Ba	1544	1540	1750	1814	1596	1628	1511	1779	1764
Sr	849	904	934	972	830	818	740	889	890
Zn	71	79	91	86	79	106	80	94	102
Cu	49	57	692	81	65	29	17	24	46
V	112	113	122	124	128	118	112	123	120
Y	26	25	26	31	31	18	19	24	22
Rb	15	25	20	20	20	20	15	15	15

Figure 21

Plot of the relationship of P_2O_5, Fe_2O_3, SiO_2, CaO, L.O.I., MgO, Al_2O_3, and Na_2O, in weight percent, across a bed of non-pelletal phosphate mudstone. Single numbers listed horizontally refer to sample numbers in Table 9.

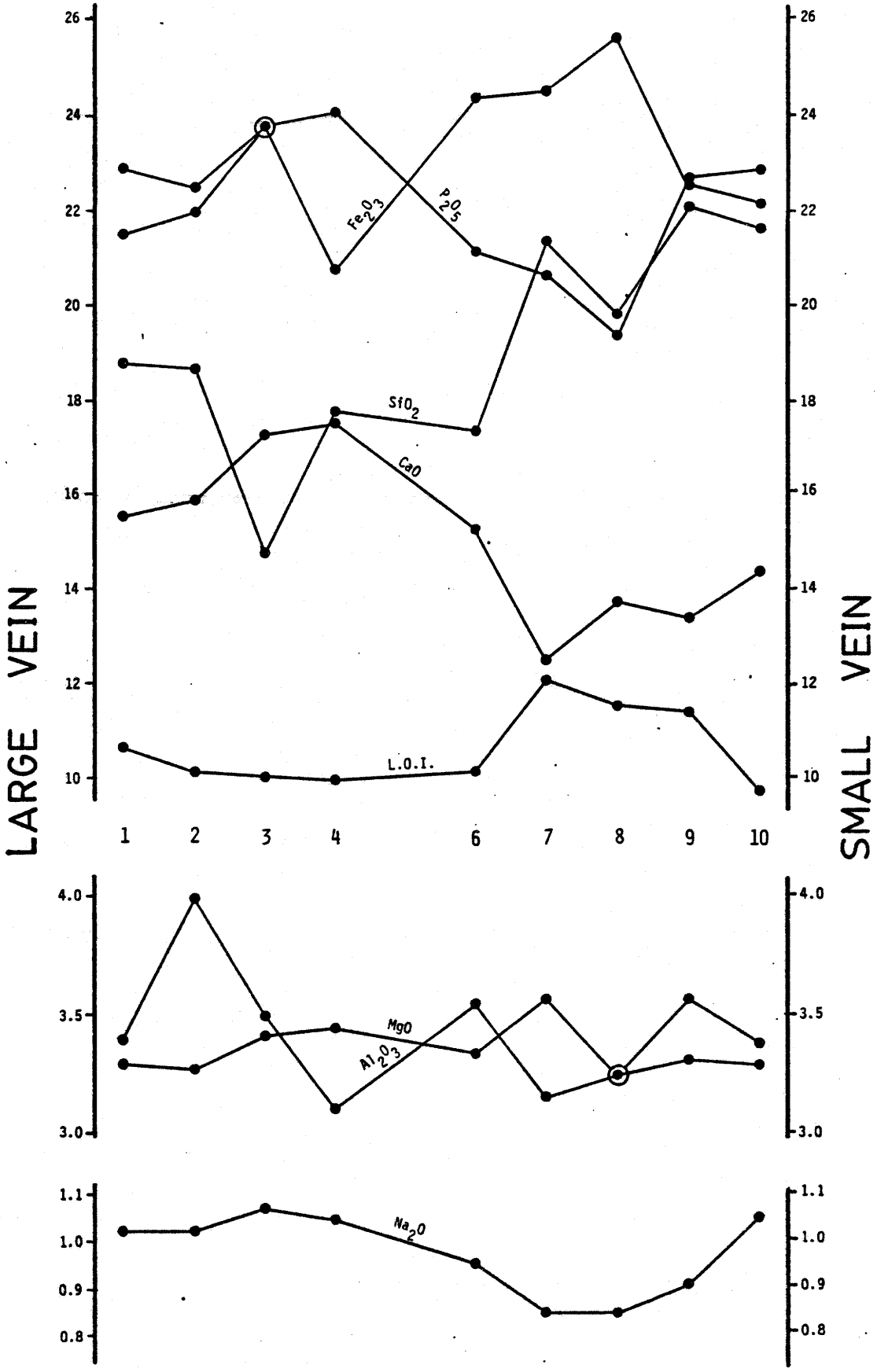
LARGE VEIN
SMALL VEIN
Fe_2O_3
P_2O_5
SiO_2
CaO
L.O.I.
MgO
Al_2O_3
Na_2O
26
24
22
20
18
16
14
12
10
1
2
3
4
6
7
8
9
10
4.0
3.5
3.0
1.1
1.0
0.9
0.8

Figure 22

Plot of the relationship of MnO, K_2O, TiO_2, H_2O, Ba, V, Zn, Sr, Cu, Y, and Rb across a bed of non-pelletal phosphate mudstone. Single numbers listed horizontally refer to sample numbers in Table 9. Ba and Sr values are divided by 10. (element oxides in weight percent, minor elements in ppm)

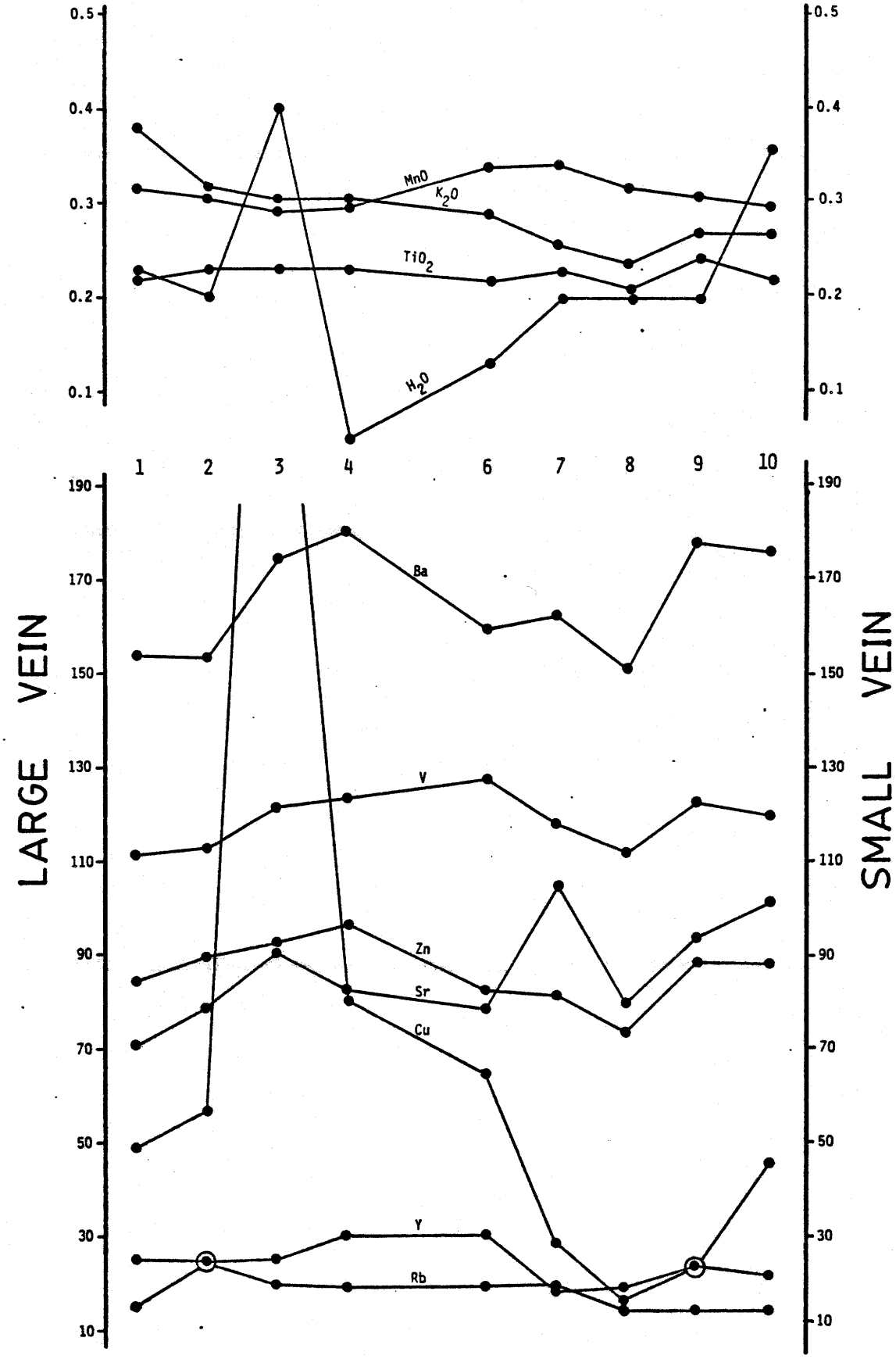
0.5
0.4
0.3
0.2
0.1
MnO
K_2O
TiO_2
H_2O
1
2
3
4
6
7
8
9
10
190
170
150
130
110
90
70
50
30
10
Ba
V
Zn
Sr
Cu
Y
Rb
LARGE VEIN
SMALL VEIN

(Fe_2O_3 vs. L.O.I., CaO vs. P_2O_5, etc.) in the previous section on geochemistry. Unfortunately, the lateral variation from vein to vein is almost random. Although a progressive decrease in P, Ca, Ba, V, Zn, and Sr towards the large vein (samples 4 to 1) is apparent, the magnitude of this variation is less than the variation in the middle of the bed (samples 4 to 8). This suggests that the primary lateral variation in composition of the bed is greater than any change induced by preferential leaching of elements used in forming the vein minerals. The results of this study, then, are inconclusive.

DISCUSSION

Microscopic examination of thin sections of phosphate nodules shows that the paragenetic sequence, determined by cross-cutting relationships, between constituent minerals is complex. Simply, the sequence of mineral formation is as follows: satterlyite + wolfeite + maricite + varulite + arrojadite + ludlamite + vivianite-baricite + metavivianite + goethite. Any of the steps in this sequence can be skipped and examples of wolfeite altering directly to goethite or satterlyite to vivianite-baricite have been noted. The position of carbonate-apatite in this series could not be determined.

Phosphate minerals are replaced by quartz, pyrite, and siderite, paragenetically in that order. Quartz often contains tiny euhedral apatite crystals and usually occurs near the center of nodules. This type of replacement, along with siderite replacement, is uncommon. Many nodules contain large euhedral pyrite crystals. Nodules, other than those at the base of the Big Fish River section, composed wholly of pyrite are believed to be completely replaced phosphate nodules as several still contain rare grains of satterlyite or vivianite-baricite.

A rough paragenetic sequence, based on cross-cutting relationships, was developed for all associations for both the Rapid Creek and Big Fish River areas (Figure 23). Almost all mineralization occurs as undisrupted open space fillings. This

Figure 23

Paragenetic sequence. Arrows indicate zoning and letters in parentheses indicate degree (s = strong zonation, w = weak zonation).

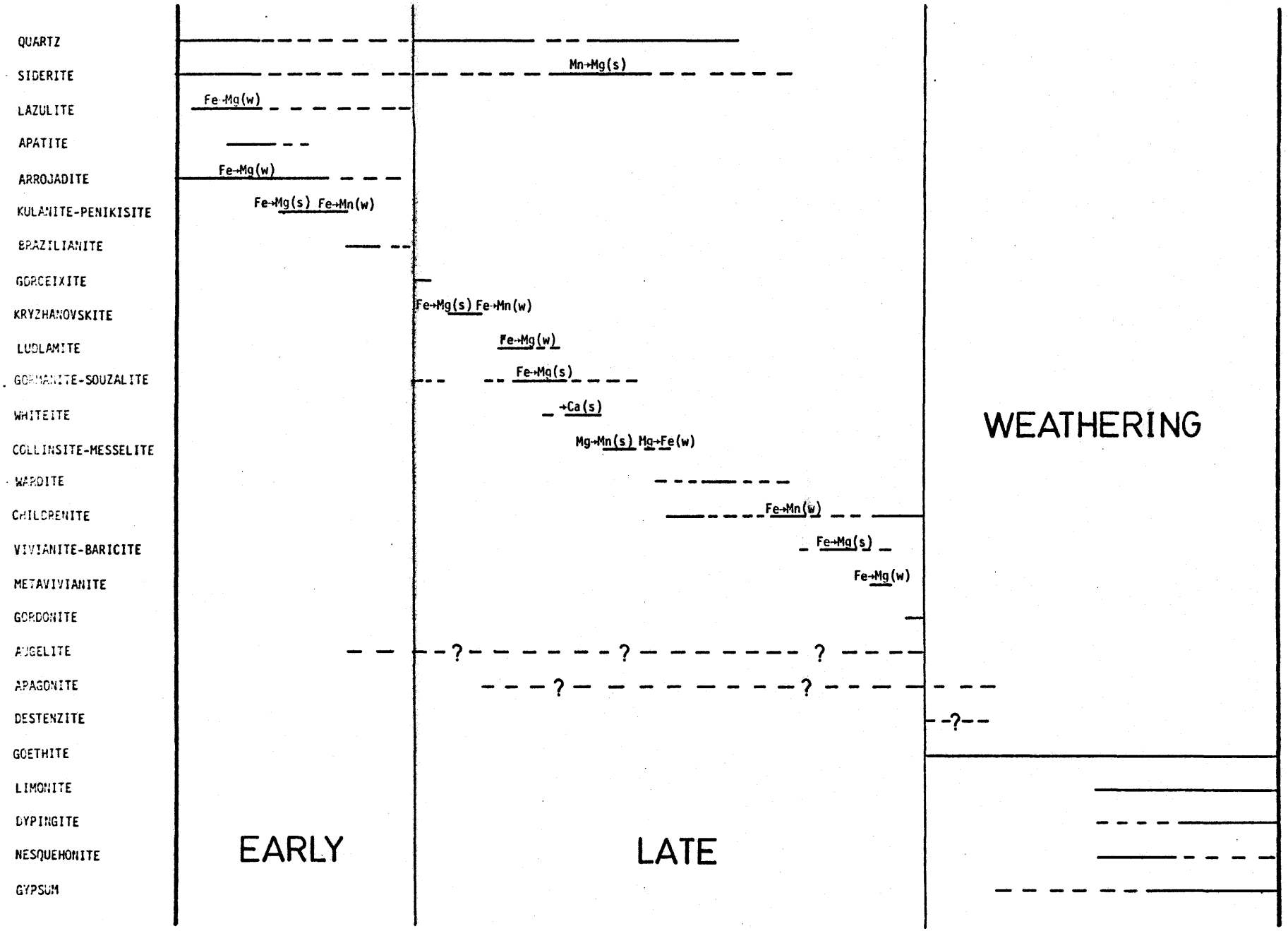
QUARTZ
SIDERITE
LAZULITE
APATITE
ARROJADITE
KULANITE-PENIKISITE
BRAZILIANITE
GORCEIXITE
KRYZHANOVSKITE
LUDLAMITE
GORMANITE-SOUZALITE
WHITEITE
COLLINSITE-MESSELITE
WARDITE
CHILDRENITE
VIVIANITE-BARICITE
METAVIVIANITE
GORDONITE
AUGELITE
APAGONITE
DESTENZITE
GOETHITE
LIMONITE
DYPINGITE
NESQUEHONITE
GYPSUM
Mn→Mg(s)
Fe→Mg(w)
Fe→Mg(s) Fe→Mn(w)
Fe→Mg(s) Fe→Mn(w)
Fe→Mg(w)
Fe→Mg(s)
→Ca(s)
Mg→Mn(s) Mg→Fe(w)
Fe→Mn(w)
Fe→Mg(s)
Fe→Mg(w)
EARLY
LATE
WEATHERING

indicates that the mineralization is epigenetic and formed after the formation of the open fractures. Inverse spherulitic bundles in area 7 indicate that these veins may have been widened during or after initiation of mineral precipitation. The high proportion of void space in many veins indicated that the mineralizing solutions were exhausted before the veins were completely filled.

Most of the minerals in the veins are compositionally zoned to some degree. Figure 23 demonstrates the dominant Fe to Mg zoning. Mn appears to act independently, being either enriched or depleted outwards in different minerals, and is probably related to local variation in that element's abundance. Whiteite shows strong Ca-enrichment outwards. Despite the overall Fe to Mg zoning, mineral series show no Fe-rich to Mg-rich sequence. This is displayed particularly well by the kryzhanovskite-ludlamite-vivianite-metavivianite series, in which the minerals are Mg-rich, Fe-rich, Mg-rich, and Fe-rich, respectively.

The paragenetic sequence of vein minerals in this deposit is similar to the sequence for pegmatite phosphates developed by Moore (1973). Most of the minerals in Moore's sequence formed at above 200°C and several above 500°C. There is no direct evidence of a high temperature origin for the mineralization in the Big Fish River - Rapid Creek phosphatic iron formation.

Indeed, most evidence indicates a very low temperature (less than 100°C) of formation.

The association of montmorillonite-rich clays immediately above the iron formation (in the Boundary Creek Formation) suggests relatively shallow burial. Montmorillonite is transformed to a mixed-layer illite-montmorillonite at temperatures between 70 and 95°C and breaks down completely at about 150°C (De Segonzac, 1970). Kaolinite, which does occur within the iron formation (Young, 1972), would also be destroyed during burial, usually at temperatures between 80 and 180°C (De Segonzac, 1970).

Using Young's (1979) values for thicknesses of Upper Cretaceous and Tertiary strata, a maximum value of about 2300 m can be considered a realistic total for the thickness of strata overlying the iron formation. This would produce a temperature of 96°C with a geothermal gradient of 33°/km and a surface temperature of 20°C.

Preliminary results from an investigation of the oxygen isotopes of vein siderite and quartz indicate that the formation temperature was about 50°C. This suggests that the phosphate minerals of the Big Fish River - Rapid Creek phosphatic iron formation, although more commonly found in higher temperature circumstances, may also originate at quite low temperatures.

The occurrence of definite mineral associations with specific host rock types strongly suggests that the host rocks are also the source for the vein mineralization. The exact nature of this relationship is masked by the fact that most veins intersect more than one rock type.

The calcium-rich association occurs with pelletal and nonpelletal phosphate mudstones. The phosphate phase in these rocks is dominantly carbonate-apatite which can contribute both Ca and P to the veins. Other elements could be supplied by solution of quartz, siderite and clay minerals.

The sodium-bearing association occurs with phosphate sandstones. The amount of Na_2O in these rocks is not significantly different from other rock types. However, the phosphate sandstones are completely altered to satterlyite. If the alteration of a Na-rich apatite group mineral, precursor to saterlyite, was concomitant with vein formation, the Na released in the formation of satterlyite could be either transported to a nearby vein or used to crystallize a more Na-rich alteration mineral, such as arrojadite, which is an abundant mineral in some phosphate sandstones. Other elements were probably derived from interbedded mudstone.

The iron-magnesium-rich association occurs with siderite-rich phosphate and siderite sandstones. Clearly the abundance of siderite in the rocks accounts for the abundance of Fe-rich

minerals in the veins. Sodium is probably supplied to the veins in the same manner as in the sodium-bearing association but here combines with Fe to form arrojadite rather than the Na-Al phosphates, brazilianite and wardite. Other elements were probably derived from interbedded mudstone.

The reason for barium-rich associations to occur within conglomeratic slump deposits is a mystery. The amount of Ba in a siltstone clast, which hosts the barium-rich association vein in Ridge 3 along Cross-cut Creek, is about average and, in fact, much lower than some other samples. Whether gorceixite or kulanite-penikisite forms is probably a function of the amount of CO_2 in the mineralizing solution. In the latter veins, CO_2 would be used up in the formation of siderite but Fe would be left over to form Ba-Fe phosphates. In gorceixite veins, Fe would be used up in the formation of siderite and CO_2 would be left over to form aragonite after the precipitation of an Fe-free Ba phosphate.

The simple association veins probably represent isolated late stage formation where mineralogy is largely dependent on selective leaching of host rocks or on local accummulations of only a few elements.

The dominance of ferrous iron in the veins indicates reducing conditions during mineralization. Abundant ferric iron is present in only one mineral (kryzhanovskite). Although this mineral usually forms via the oxidation of phosphoferrite

(Moore, 1973 and 1971), Sturman (pers. comm.) believes that it is primary in this deposit. It indicates a period of oxidation during mineralization.

The occurrence of hydrated magnesium carbonates, dypingite and nesquehonite, is unusual. They are normally found in caves (Langmuir, 1965) or as weathering products of serpentinites (Raade, 1970). Their occurrence in this deposit is probably related to the simultaneous weathering of siderite and vivianite-baricite. Siderite altering to goethite or limonite releases CO_2. Weathering of Mg-rich vivianite-baricite results in an Fe-rich yellowish compound (kertschenite), a process which would release Mg. Thus the progressive evaporation of the weathering solutions on an outcrop would produce nesquehonite and dypingite.

CONCLUSION

The Albian phosphatic iron formation in the Big Fish River and Rapid Creek areas is far more complex than was realized prior to this investigation. With its diversity of new and rare minerals, unusual rock types, and complex stratigraphic relationships, this deposit provides great scope for further study. New information concerning the phosphatic iron formation which was derived from this investigation is diverse and covers aspects of stratigraphy, paleontology, petrography, mineralogy, and geochemistry. The principal conclusions are:

1. These rocks have a basal Albian age (approximately 107 m.y.a.), on the basis of ammonite fauna.
2. While most ancient phosphate deposits formed at low to middle latitudes, the paleolatitude of this deposit is 70^{o} to 75^{o}N and is the highest reported thus far.
3. Although the Big Fish River and Cross-cut Creek sections are only 15 km apart, they could not be correlated in detail showing that facies relationships are complex and variable over short distances.
4. At Big Fish River, the iron formation consists of three ironstone units separated by two units of soft and recessive montmorillonitic shale. The ironstones consist of gradational mudstone to shale couplets, with the former containing more phosphate, carbonate, and oxide phases than

the latter and, thus, being more resistant to mechanical weathering.

5. At Cross-cut Creek, a tributary to Rapid Creek, the iron formation consists of interbedded mudstone, sandstone, and shale, but the exact chemical differences among these rock types is not known. The lower part of the section in this area is characterized by coarsening-upward sequences capped by conglomeratic slump deposits. The slump deposits may be a proximal facies in some kind of fan deposit. I favor the interpretation that they are earthquake generated and represent tectonic instability during deposition. The rest of the section is dominated by phosphatic mudstone.
6. The iron formation unconformably overlies the Upper Siltstone Division in both the Big Fish River and Boundary Creek areas and gradationally overlies the Concretionary Shale Member of the Upper Sandstone Division in the Rapid Creek area. Its upper contact is transitional into but locally unconformable with the Boundary Creek Formation.
7. The primary phosphate phase was not pure carbonate-apatite, as in other phosphate deposits, but rather a mixed Ca-Fe-Mg phosphate of uncertain identity or two coexisting phases (francolite + ?). The mechanism of deposition (primary precipitation, diagenetic precipitation, or replacement) is also not known.
8. The rocks are composed of four basic components; matrix,

pellets (or granules), detrital quartz grains, and skeletal fragments. Mixed phosphate-siderite pellets (and granules) and matrix constitute a spectrum from sandstone to mudstone and comprise the bulk of the phosphatic iron formation.

9. Preliminary oxygen and carbon isotopic data suggest that the siderite in the Rapid Creek rocks was either recrystallized during metamorphism or else is metasomatic.

10. Metamorphism of non-pelletal phosphate mudstone has produced star-shaped concretionary bodies which were subsequently replaced by carbonate-apatite and siderite with minor satterlyite, arrojadite, and gormanite-souzalite. These may be pseudomorphs after gypsum. Dimroth and Chauvel (1973, Fig. 7H) have found similar pseudomorphs in the Sokoman Iron Formation in Quebec. Such pseudomorphism would be consistent with Kimberley's (1979) model for diagenetic iron formation and with the supposed arid climate for phosphate formation.

11. Metamorphism in coarse-grained rocks has produced satterlyite which is in turn altered to arrojadite or, more rarely, gormanite-souzalite. The precise nature of these alterations and replacements is not known.

12. Fracture-fillings constitute most of the epigenetic mineralization in the Rapid Creek area. Some of the more simple mineral associations (three minerals or less) are related to particular rock types whereas others occur in

any rock type. There are four more complex associations which are categorized by the persistent occurrence or dominance of one or two elements in one or more minerals. These associations are related to particular rock types: Na-bearing association with phosphate sandstone, Ca-rich with phosphate mudstone, Fe-Mg-rich with siderite sandstone, and Ba-rich with conglomeratic slump deposits.

13. The temperature of formation of this mineralization was relatively low, probably less than 100°C.
14. Crystals of most of the epigenetic vein minerals are zoned with respect to iron and magnesium, having iron-rich cores and progressive magnesium enrichment outwards. However, there is no progressive change in the paragenetic sequence, as a whole, from magnesium-rich minerals to iron-rich ones.
15. There is no systematic geographic trend in cation ratios for any of the minerals in veins. Instead, these ratios appear to be dependent largely on local proportions of elements.
16. Lazulite is the dominant Mg-Fe-Al phosphate in veins while gormanite-souzalite is the dominant Fe-Mg-Al phosphate in rocks.
17. There is a high aluminum content in the veins (most vein minerals contain stoichiometric aluminum) while the rocks are relatively low in aluminum (average about 3 weight

percent oxide). The reason for this is not certain but aluminum may have been supplied by solutions moving along faults. This would explain why the only pure Al-phosphate in this area (augelite) is associated solely with faults.

18. Mineralization in the Big Fish River and Boundary Creek areas is largely confined to spherulitic recrystallized replacements of ammonites and pelecypods and concretionary phosphate nodules.

19. Nahpoite (Na_2HPO_4), a new mineral, occurs as an alteration product of maricite in the Big Fish River area.

REFERENCES CITED

Ames, L.L. (Jr.), 1959: The genesis of carbonate-apatites; Econ. Geol., v. 54, p. 829-841.

Berge, J.W., 1972: Physical and chemical factors in the formation of marine apatite; Econ. Geol., v. 67, p. 824-827.

Berner, R.A., 1970: Sedimentary Yr formation; Amer. Jour. Sci., v. 268, p. 13-23.

Birch, G.F., 1979: Phosphatic rocks on the western margin of South Africa; Jour. Sed. Petrology, v. 49, p. 93-110.

Borchert, H., 1960: Genesis of marine sedimentary iron ores; Bull. Inst. Min. Met., no. 640, p. 261-279.

Buddington, A.F., 1950: Composition and genesis of pyroxene and garnet related to Adirondack anorthosite and anorthosite-marble contact zones; Amer. Min., v. 35, p. 659-670.

Bushinski, G.I., 1964: On shallow water origin of phosphorite sediments; Developments in Sedimentology, v. 1, p. 62-70.

Campbell, F.A., 1962: Lazulite from Yukon, Canada; Amer. Min., v. 47, p. 157-160.

Carroll, D., 1958: Role of clay minerals in the transportation of iron; Geochim. Cosmochim. Acta, v. 14, p. 1-27.

Cheney, T.M., McClellan, G.H., and Montgomery, E.S., 1979: Sechura phosphate deposits, their stratigraphy, origin and composition; Econ. Geol., v. 74, p. 232-259.

Christie, R.L., 1978: Sedimentary phosphate deposits - an interim review; Geol Surv. Canada Paper 78-20, 9 p.

Cook, P.J., 1976: Sedimentary phosphate deposits in K. H. Wolf, ed., Handbook of Strata-bound and Stratiform Ore Deposits; Elsevier, Amsterdam, v. 7, p. 505-535.

_____, and McElhinny, M.W., 1979: A reevaluation of the spatial and temporal distribution of sedimentary phosphate deposits in the light of plate tectonics; Econ. Geol., v. 74, p. 315-330.

Cressman, E.R., and Swanson, R.W., 1964: Stratigraphy and petrology of the Permian rocks of southwestern Montana; United States Geol. Surv. Prof. Paper 313-C, p. 275-569.

Curtis, C.D., and Spears, D.A., 1968: The formation of sedimentary iron minerals; Econ. Geol., v. 63, p. 257-270.

D'Anglejan, B.F., 1968: Phosphate diagenesis of carbonate sediments as a mode of in situ formation of marine phosphorites: Observation in a core from the eastern Pacific; Can. Jour. Earth Sci., v. 5, p. 81-87.

De Segonzac, G.D., 1970: The transformation of clay minerals during diagenesis and low-grade metamorphism: A review; Sedimentology, v. 15, p. 281-346.

Dimroth, E., and Chauvel, J.J., 1973: Petrography of the Sokoman Iron Formation in part of the Central Labrador Trough, Quebec, Canada; Geol. Soc. Amer. Bull, v. 84, p. 111-134.

Emerson, S., 1976: ; Early diagenesis in anaerobic lake sediments: chemical equilibria in interstitial water; Geochim. Cosmochim. Acta., v. 40, p. 925-934.

Firstbrook, P.L., Funnell, B.M., Hurley, A.M., and Smith, A.G., 1979: Paleoceanic reconstrucitons 160-0 Ma; published by the National Science Foundation, 41 p.

Fisher, D.J., and Runner, J.J, 1958: Morinite from the Black Hills; Amer. Min., v. 43, p. 585-594.

Folk, R.L., 1959: Practical petrographical classification of limestones; Amer. Assoc. Petrol. Geol. Bull., v. 43, p. 1-38.

_____, 1962: Spectral subdivision of limestone types in Classification of carbonate rocks; Amer. Assoc. Petrol. Geol. Memoir 1, p. 62-84.

Fuller, A.O., 1979: Phosphate occurrences on the western and southern central areas and continental shelves of southern Africa; Econ. Geol., v. 74, p. 221-231.

Gray, M., McAfee, R. (Jr.), and Wolf, C.L. (eds.), 1973: Glossary of Geology; American Geological Institute, Washington, D.C., 805 p.

Gulbrandsen, R.A., 1966: Chemical composition of phosphorites of the Phosphoria Formation; Geochim. Cosmochim. Acta, v. 30, p. 769-778.

_____, 1969: Physical and chemical factors in the formation of marine apatite; Econ. Geol., v. 64, p. 365-382.

_____, and Roberson, C.E., 1973: Inorganic phosphorus in sea water in E.J. Griffith, et al., eds., Environmental Phosphorus Handbook; Wiley and Sons, New York, 718 p.

Hoffman, C., 1979: Augelite, a rare aluminum phosphate; first find in a metamorphic environment; N. Jb. Miner. Abh., v. 136, p. 1-9.

Holland, H.D., 1973: The oceans: a possible source of iron in iron-formations; Econ. Geol., v. 68, p. 1169-1172.

Hurlburt, C.S., 1950: Childrenite-eosphorite series; Amer. Min., v. 35, p. 793-805.

James, H.L., 1954: Sedimentary facies of iron-formation; Econ. Geol., v. 49, p. 236-240, 246-249, 272-275, 281-284.

Jeletzky, J.A., 1961: Eastern slope, Richardson Mountains: Cretaceous and Tertiary structural history and regional significance; Proc. 1st Intern. Symp. on Arctic Geology, Alberta Soc. Petrol. Geol., p. 578-582.

_____, 1971a: Stratigraphy, facies and paleogeography of Mesozoic rocks of northern and west-central Yukon; Geol. Surv. Canada Paper 71-1A, p. 203-221.

_____, 1971b: Marine Cretaceous biotic provinces and paleogeography of western and Arctic Canada; illustrated by a detailed study of ammonites; Geol. Surv. Canada Paper 70-22, 92 p.

_____, 1972: Stratigraphy, facies and paleogeography of Mesozoic and Tertiary rocks of northern Yukon and northwestern

District of Mackenzie; Geol. Surv. Canada Paper 72-1A, p. 212-215.

_____, 1975a: Sharp Mountain Formation (new): a shoreline facies of the Upper Aptian-Lower Albian flysch division, eastern Keele Range, Yukon Territory; Geol. Surv. Canada Paper 75-1B, p. 237-244.

_____, 1975b: Jurassic and Lower Cretaceous paleogeography and depositional tectonics of Porcupine Plateau, adjacent areas of northern Yukon and those of Mackenzie District; Geol. Surv. Canada Paper 74-16, 52 p.

Kimberley, M.M., 1978: Paleoenvironmental classification of iron formations; Econ. Geol., v. 73, p. 215-229.

_____, 1979: Origin of oolitic iron formations; Jour. Sed. Petrology, v. 49, p. 111-132.

Krauskopf, K.B., 1967: Introduciton to geochemistry; McGraw-Hill, New York, 721 p.

Langmuir, D., 1965: Stability of carbonates in the system $MgO-CO_2-H_2O$; Journal of Geology, v. 73, p. 730-754.

McConnell, D., 1973: Apatite: Its crystal chemistry, mineralogy, utilization, and geologic and biologic occurrences; Springer-Verlog, New York, 111 p.

McKelvey, V.E., 1967: Phosphate deposits; United States Geol. Surv. Bull. 1252-D, 21 p.

_____, 1973: Abundance and distribution of phosphorus in the lithosphere in E.J. Griffith, et al., eds., Environmental Phosphorus Handbook; Wiley and Sons, New York, p. 13-30.

Mandarino, J.A., and Sturman, B.D., 1976: Kulanite, a new barium iron aluminum phosphate from the Yukon Territory, Canada; Canadian Min., v. 14, p. 127-131.

_____, Sturman, B.D., and Corlett, M.I., 1977: Penikisite, the magnesium analogue of kulanite, from Yukon Territory; Canadian Min., v. 15, p. 393-395.

_____, Sturman, B.D., and Corlett, M.I., 1978: Satterlyite, a new hydroxyl-bearing ferrous phosphate from the Big Fish River area, Yukon Territory; Canadian Min., v. 16, p. 411-413.

Moore, E.S., and Maynard, J.E., 1929: Solution, transportation, and precipitation of iron and silica; Econ. Geol., v. 24, p. 272-303, 365-402, 506-527.

Moore, P.B., 1971: The Fe_3^{2+} $(H_2O)_n(PO_4)_2$ homologous series: Crystal-chemical relationships and oxidized equivalents; Amer. Min., v. 56, p. 1-17.

_____, 1973: Pegmatite phosphates: Descriptive mineralogy and crystal chemistry; Min. Record, v. 4, p. 103-130.

_____, and Ito, J., 1978: I. Whiteite, a new species, and a proposed nomenclature for the jahnsite-whiteite complex series. II. New data on xanthoxenite. III. Salmonsite discredited; Min. Mag., v. 42, p. 309-323.

_____, and Ito, J., 1979: Alluaudites, wyllieites, arrojadites: Crystal chemistry and nomenclature; Min. Mag., v. 43, p. 228-235.

Mrose, M.E., 1953: Palermoite and goyazite, two strontium minerals from the Palermo Mine, North Groton, New Hampshire (abst.); Amer. Min., v. 38, p. 354.

Murray, J.W., Grundmanis, V., and Smethie, W.M. (Jr.), 1978: Interstitial water chemistry in sediments of Saanich Inlet; Geochim. Cosmochim. Acta, v. 42, p. 1011-1026.

Norris, D.K., 1974: Structural geometry and geological history of the northern Canadian Cordillera in A.E. Wren and R.B. Cruz, eds., Proc. of the 1973 National Convention; Can. Soc. Explor. Geophysicists, p. 18-45.

Nriagu, J.O., 1972: Stability of vivianite and ion-pair formation in the system $Fe_3(PO_4)_2$-H_3PO_4-H_2O; Geochim. Cosmochim. Acta, v. 36, p. 459-470.

_____, 1976: Phosphate-clay mineral relations in soils and sediments; Can. Jour. Earth Sciences, v. 13, p. 717-736.

_____, and Dell, C.I., 1974: Diagenetic formation of iron phosphates in recent lake sediments; Amer. Min., v. 59, p. 934-946.

Palache, C., Berman, H., and Frondel, C., 1951: Dana's System of Mineralogy, 7th ed.; Wiley and Sons, New York, v. II, 1124 p.

Parker, R.J., 1975: The petrology and origin of some glauconitic and glauco-conglomeratic phosphorites from the South African continental margin; Jour. Sed. Petrology, v. 45, p. 230-242.

Pearson, M.J., 1979: Geochemistry of the Hepworth Carboniferous sediment sequence and origin of the diagenetic iron minerals and concretions; Geochim. Cosmochim. Acta, v. 43, p. 927-941.

Pecora, W.T., and Fahey, J.J., 1949: The Corrego Frio pegmatite, Minas Gerais: Scorzalite and souzalite, two new phosphate minerals; Amer. Min., v. 34, p. 83-93.

Pettijohn, F.J., 1975: Sedimentary Rocks, 3rd ed.; Harper and Row, New York, 628 p.

Pevear, D.R., 1966: The estuarine formation of United States Atlantic coastal plain phosphorite; Econ. Geol., v. 61, p. 251-256.

Pough, F.H., and Henderson, E.P., 1945: Brazilianite, a new phosphate mineral; Amer. Min., v. 30, p. 572-582.

Price, N.B., and Clavert, S.E., 1978: The geochemistry of phosphorites from the Namibian shelf; Chem. Geol., v. 23, p. 151-170.

Raade, G., 1970: Dypingite, a new hydrous basic carbonate of magnesium, from Norway; Amer. Min., v. 55, p. 1457-1465.

Riggs, S.R., 1979a: Petrology of the Tertiary phosphorite system of Florida; Econ. Geol., v. 74, p. 195-220.

_____, 1979b: Phosphorite sedimentation in Florida - a model phosphogenic system; Econ. Geol., v. 74, p. 285-314.

Ritz, C., Essene, E.J., and Peacor, D.R., 1974: Metavivianite, $Fe_3(PO_4)_2 \cdot 8H_2O$, a new mineral; Min. Mag., v. 59, p. 896-899.

Roberson, C.E., 1966: Solubility implications of apatite in sea water in Geological Survey research 1966; United States Geol. Surv. Prof. Paper 550-D, p. 178-185.

Rosenquist, I. Th., 1970: Formation of vivianite in holocene clay sediments; Lithos, v. 3, p. 327-334.

Rupke, N.A., 1972: Geologic studies of an Early and Middle Eocene flysch formation, south-western Pyrenees, Spain; Ph.D. dissertation, Dept. Geological and Geophysical Sciences, Princeton University.

Seyfert, C.K., and Sirkin, L.A., 1979: Earth History and Plate Tectonics, 2nd ed.; Harper and Row, New York, 600 p.

Smith, D.G.W., 1976: Quantitative energy dispensive microanalysis in Microbeam techniques, D.G.W. Smith, ed.; Min. Assoc. Canada, Short Course Handbook, v. 1, p. 63-106.

Sturman, B.D., and Mandarino, J.A., 1976: Baricite, the magnesium analogue of vivianite, from Yukon Territory, Canada; Can. Min., v. 14, p. 403-406.

_____, Mandarino, J.A., and Corlett, M.I., 1977: Maricite, a sodium iron phosphate, from the Big Fish River area, Yukon Territory, Canada; Can. Min., v. 15, p. 396-398.

Suess, E., 1979: Mineral phases formed in anoxic sediments by microbial decomposition of organic matter; Geochim. Cosmochim. Acta, v. 43, p. 339-352.

Van Hinte, J.E., 1976: A Cretaceous time scale; Amer. Assoc. Petrol., Geol. Bull, v. 60, p. 498-516.

Yorath, C.J., and Norris, D.K., 1975: The tectonic development of the southern Beaufort Sea and its relationship to the origin of the Arctic Ocean Basin in Canada's continental margins and offshore petroleum potential, C.J. Yorath, E.R. Parker, and D.J. Glass, eds.; Can. Soc. Petrol. Geol., Memoir 4, p. 589-612.

Young, F.G., 1972: Cretaceous stratigraphy between Blow and Fish Rivers, Yukon Territory; Geol. Surv. Canada Paper 72-1A, p. 229-235.

_____, 1974: Cretaceous stratigraphic displacements across Blow Fault Zone, northern Yukon Territory; Geol. Surv. Canada Paper 74-1B, p. 291-296.

_____, 1975: Upper Cretaceous stratigraphy, Yukon Coastal Plain and northwestern Mackenzie Delta; Geol. Surv. Can., Bull. 249, 83 p.

_____, 1977: The mid-Cretaceous flysch and phosphatic ironstone sequence, northern Richardson Mountains, Yukon Territory; Geol. Surv. Canada Paper 77-1C, p. 67-74.

_____, Myhr, D.W., and Yorath, C.J., 1976: Geology of the Beaufort-Mackenzie Basin; Geol. Surv. Canada Paper 76-11, 65 p.

APPENDIX I

The following are the sources of powder diffraction data used to identify mienrals in this study. Numbers refer to the Selected Powder Diffraction Data for Minerals (1st. ed.) published by the Joint Committee on Powder diffraction Standards.

Apatite 9-432

Aragonite 5-453

Arrojadite 6-370

Augelite 14-380

Brazilianite 14-379

Carbonate-apatite 21-145

Childrenite 11-621

Collinsite 14-314

Destinezite 12-209 (diadochite)

Dypingite 23-1218

Goethite 17-536

Gorceixite 19-535

Gordonite 14-313

Gormanite-souzalite (Sturman and Mandarino, in press)

Gypsum 6-46

Kryzhanovskite (Moore, 1971, Table 2)

Kulanite-penikisite (Mandarino and Sturman, 1976, Table 2)

Lazulite 14-137

Ludlamite 17-468

Maricite (Sturman et al., 1977, Table 2)

Metvivianite (Ritz et al, 1974, Table 1)

Nesquehonite 20-671

Satterlyite (Mandarino et al., 1978, Table 1)

Siderite 8-133

Varulite 6-487

Vivianite-baricite (Sturman and Mandarino, 1976, Table 3)

Wardite 13-403

Whiteite (Moore and Ito, 1978, Table 1, no. 2)

Wolfeite 5-612

APPENDIX II

Appendix II is a mineral by mineral compilation of data that has not been presented in greater detail in the text. Microprobe analyses were made with an Acton MS64 electron microanalyzer equipped with a Princton Gamma Tech 1000 Delta System processor. Operating conditions were; accelerating voltage, 15 Kv; incident beam current, measured with a Faraday cage, variable but generally in the range 5.0 to 0.5 microamps, depending on the minerals' stability. For thin section study the beam was focused to a diameter of 1 to 2 microns. For polished sections, the beam was defocused.

Analyses were made on an energy dispersive system using a program supplied by PGT which utilizes standard Bence-Albee correction factors for absorption and fluorescence.

Microprobe standards are listed below:

Maricite 170 - (Sturman et al., 1977, Table 3, ave. of 6)

Arrojadite 171 - (Moore and Ito, 1979, Table 6, no. 6)

Arrojadite 172 - (Moore and Ito, 1979, Table 6, no. 7)

Wyllieite 175 - (Moore and Ito, 1979, Table 3, no. 2)

Whiteite 176 - (Moore and Ito, 1978, Table 3, no. 5)

Garnet 105 - (Buddington, 1950, Table 2, no. 11)

Standards used for particular minerals are cited for each mineral in this appendix. The wyllieite and arrojadite proved to be the most homogeneous standards and produced satisfactory results consistently, even for unknowns of radically different composition.

Smith (1976) has given a detailed discussion of energy dispersive analysis, including source of errors. The topic will be treated only briefly here.

Several spectra were collected on five points for 40 seconds each. It was found that these spectra yielded poor and inconsistent analyses due to the low totals. Next, the five points were added to make a 200 second spectrum. This also proved to be inconsistant due to the likelihood of encountering impurities in one of the five points. Unknown sample and

standard spectra were then collected for 200 seconds on single points.

With the rare and new minerals involved in this study, standards of similar composition are not available. Also, most standards used in this study have a single wet chemical or microprobe analysis which may or may not be close to the actual composition of the points used for standard spectra and may introduce large errors in the determination of the unknown.

Perhaps the greatest source of error lies in the fact that most of the minerals studied have bonded $(H_2O)^0$ and $(OH)^{-1}$ which is volatilized under the electron beam. Even when the beam diameter is enlarged and beam current reduced, some water, and possibly sodium, is released which causes the determination to have a lower water content than the acutal composition. This was confirmed by analyzing the whiteite standard under normal operating conditions (for anhydrous silicates) and at reduced beam currents. It was observed that with the reduced currents apparent water content increased but never reached the ideal proportion. Therefore, many of the analyses reported here may actually contain more water than reported, even though no breakdown in the material was visually observed.

In all, plus or minus 2 percent is reasonable error for all elements reported except sodium, where the error may be somewhat higher. For all minerals, except kryzhanovskite, iron is reported as total FeO.

In the tables to follow, 'x-c' refers to Cross-cut Creek, 'FR' refers to Big Fish River and a number refers to an area (see fig. 24). 'i', 'm', and 'o' refer to inside (center), middle, and outside (edge) of a crystal.

Non-phosphate Minerals

Quartz

Quartz is found in almost all types of veins and areas and does not differ significantly between them, except in the Big Fish River area. There quartz occurs with a pronounced trigonal habit, i.e., pseudohexagonal prisms terminated by a single trigonal pyramid. This quartz generally has vianite-baricite overgrowths and is also usually somewhat etched or skeletal, indicating a period of dissolution before the precipitation of the latter mineral.

Siderite

Siderite is also ubiquitous which is not surprising considering the composition of the principal rock types. Its most striking feature is the variety of the habits it displays. These habits occur randomly and cannot be related to particular associations.

Siderite commonly displays evidence of dissolution where

Figure 24

Index map for figure to follow. Capital letters refer to figure 1. Numbers refer to areas on figure 6. Note that area 'C' is referred to as area 7 in the text.

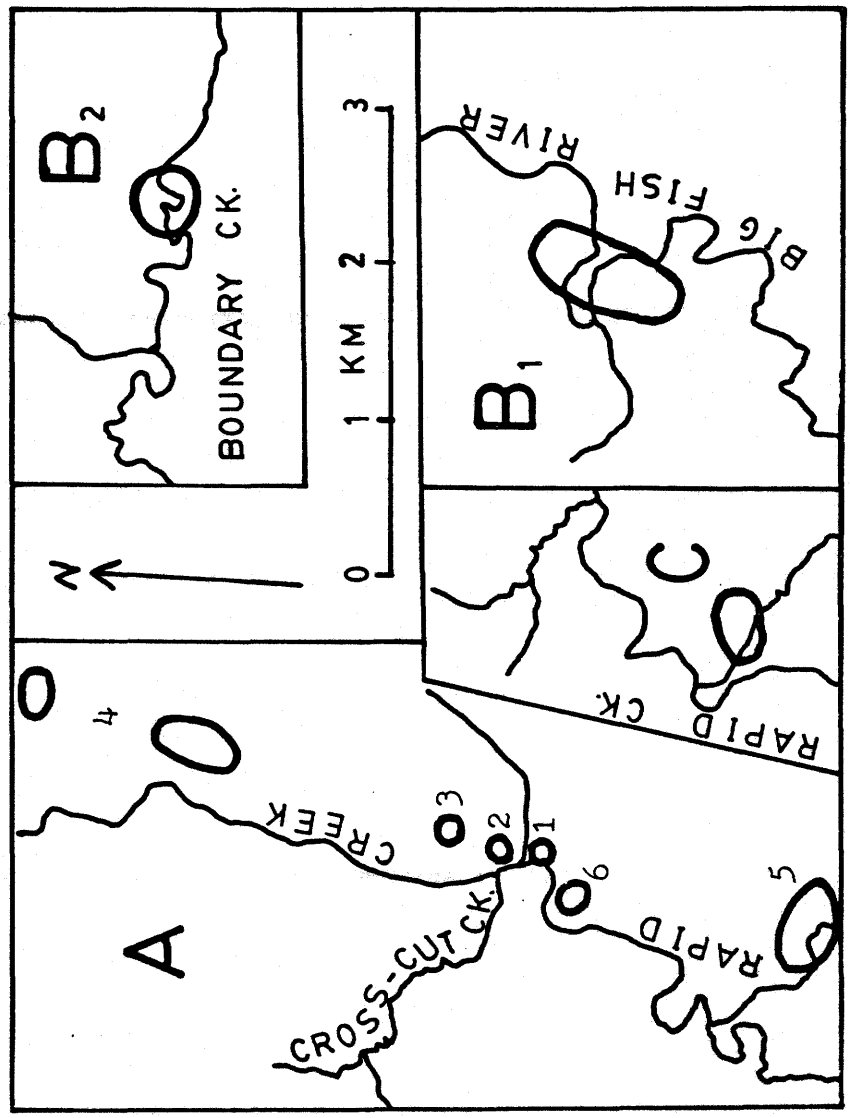
B2
BOUNDARY CK.
B1
BIG FISH RIVER
C
RAPID CK.
A
CREEK
CROSS-CUT CK.
RAPID
N
0
1 KM
2
3
1
2
3
4
5
6

edges of rhombs or tips of elongate crystals have been strongly etched. The degree of etching shows random variation, being best developed in area 2.

Qualitative microprobe investigation indicates little substitution of other cations for Fe. One sample from area 7 exhibits considerable substitution with a Mn-rich core and marked outward enrichment in Mg at the expense of Mn.

In veins that appear to have been intensively weathered, siderite has altered to goethite or limonite pseudomorphs.

Goethite and limonite

Goethite and limonite are the end-products of weathering of several iron-rich minerals, particularly siderite. Goethite samples produce recognizable diffraction patterns, although in many cases very weak, whereas limonite is amorphous and produces no diffraction lines. Both are common surface alterations in both the Big Fish River and Rapid Creek areas. Surface sample tend to contain limonite more frequently than goethite which is more common in samples from several feet below surface.

Aragonite

Aragonite was found as very small spherulitic bundles atop quartz crystals and, where it is very abundant, as a botryoidal

crust in a vein of the Ba-rich association in the slump deposit at the top of unit 4 in the Cross-cut Creek section.

Dypingite and Nesquehonite

In all areas studied, many outcrops are covered with patches of dypingite, ($Mg_5(CO_3)_4(OH)_2 \cdot 5H_2O$), a white surface alteration product. This encrustation is very fine grained and crystals cannot be seen with the unaided eye. SEM studies show the encrustation to be a botryoidal aggregate of radiating bundles of bladed crystals up to 0.01 mm long.

In area 2, particularly, thick coatings of dypingite contained small patches of colorless, coarsely crystalline (up to 10 mm) nesquehonite ($MgCO_3 \cdot 3H_2O$). In x-ray diffractogram, several small extra peaks were noted that may have been produced by lansfordite ($MgCO_3 \cdot 5H_2O$). This is expectable in other occurrences (coal mines and caves) where nesquehonite is a natural dehydration product of primary lansfordite.

Phosphate Minerals

Augelite - $Al_2PO_4(OH)_3$ - monoclinic

Augelite occurs only in veins of simple association and is relatively uniform in occurrence. It is generally colored some shade of light green but commonly grades from greenish to

colorless or from greenish to white and occasionally is tinted blue-green. Augelite usually occurs as pseudorhombohedral crystals with several smaller well developed faces bevelling edges. Twinned crystals are rare. Crystals up to 1 cm on a face have been found but more generally are 1-4 mm.

Qualitative microprobe analyses indicate the presence of trace amounts of Fe and Mn.

Augelite has been found previously in only ten localities (Hoffmann, 1979), usually in pegmatites or pneumatolytic veins. In its type locality, it occurs with other phosphates in an iron deposit (Hoffmann, 1979).

Childrenite - $(Fe,Mn)Al(PO_4)(OH)_2 \cdot H_2O$ - orthorhombic

Childrenite was found in several settings in the Rapid Creek area. Usually, it occurs alone as flattened prismatic crystals, up to 10 cm long by 1 cm wide, which are reddish brown to deep red in color, in thin veins 0.1 to 1 mm thick. In area 7, yellow childrenite occurs as stout to elongate prismatic crystals in 'bowtie' radial groups in veins dominated by quartz. In this occurrence individual crystals are similar to those shown by Hurlbut (1950, p. 794). Yellowish brown childrenite occurs as spherulitic bundles of flattened prismatic crystals in areas 2 and 4. One sample of vivianite-baricite from Cross-cut Creek contains a large euhedral crystal, 20x10x3 mm, of cream colored childrenite.

Figure 25. Augelite occurrences.

Figure 26. Childrenite occurrences.

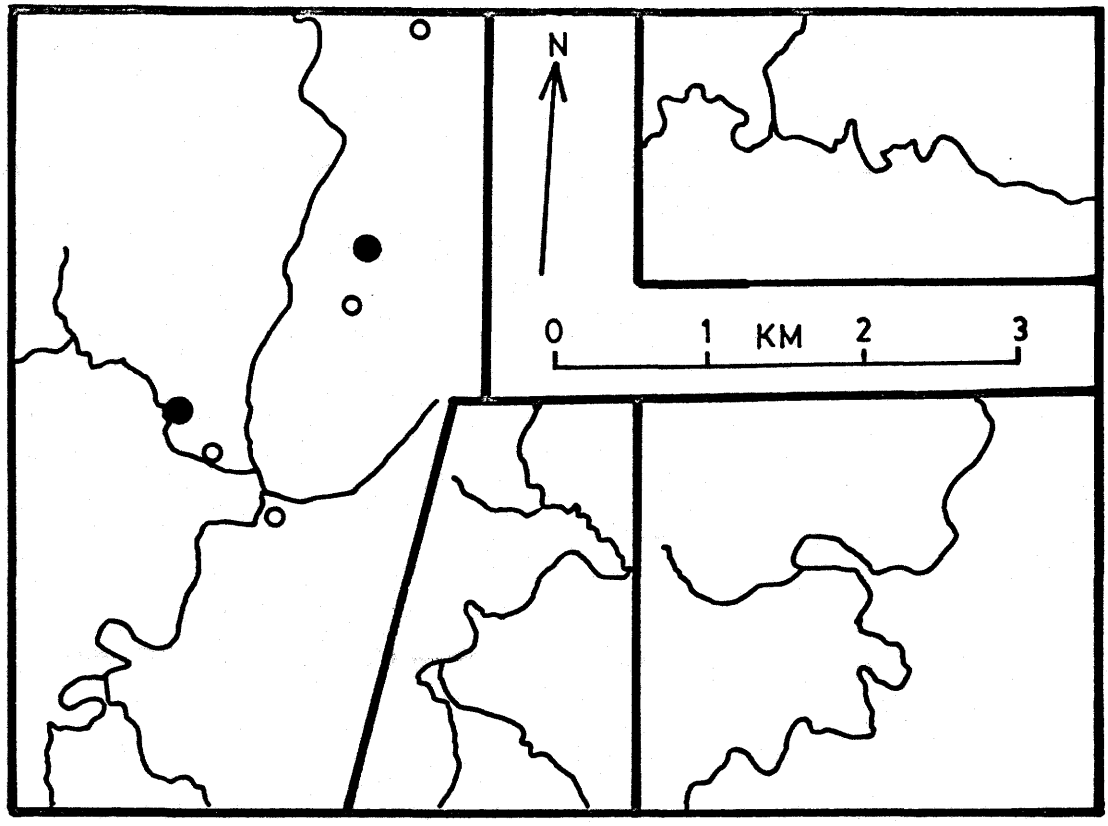

●=major ○=minor o=trace

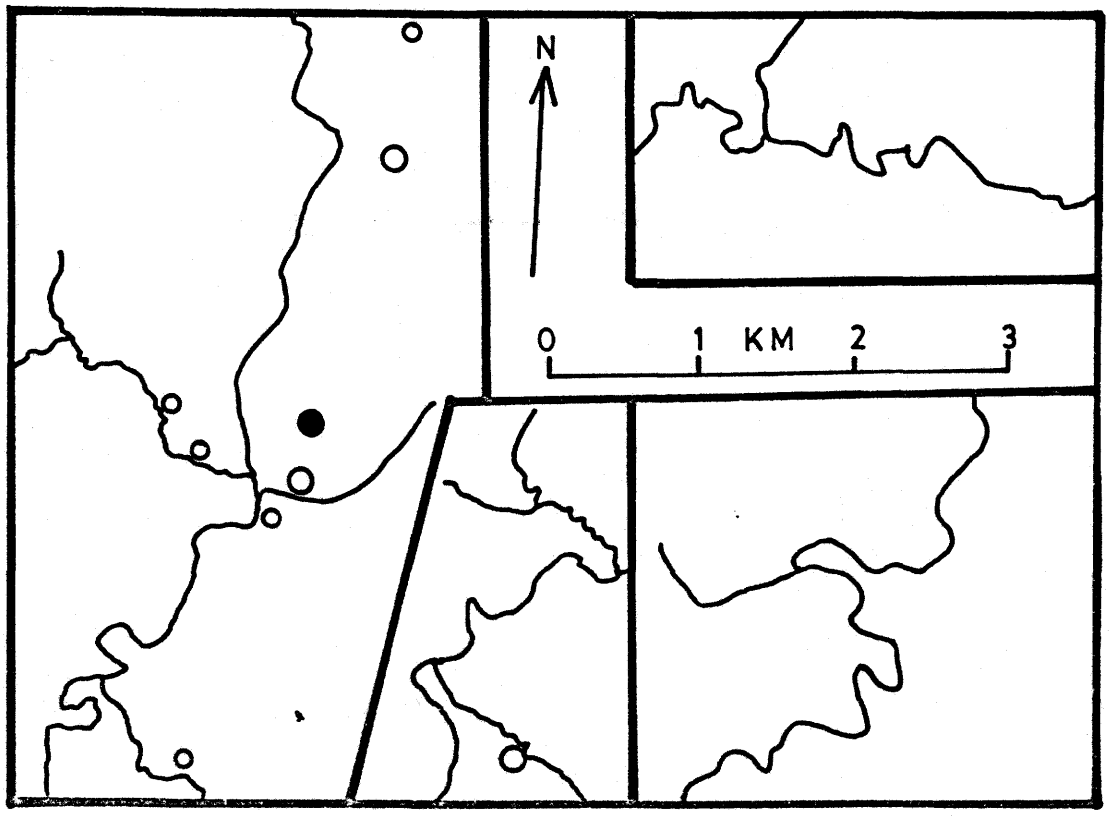

Childrenite is the iron-rich member of a solid solution series whose Mn end-member is esophorite. In it, small amounts of Ca and Mg substitute for Fe and Mn and minor amounts of trivalent Fe may be present due to partial oxidation. (Palache et al., 1951).

Microprobe analyses, using wyllieite 175 as a standard, indicate that Rapid Creek childrenites are relatively variable in composition (Table 10). The water content was calculated on the basis of an ideal composition. Sample x-c is from a Ca-rich association. The rest are all from veins in which childrenite is the only constituent. Fe:Mn ratios vary from 7.2:1 to 1.1:1 and most of the childrenites are unzoned. In those in which zoning was detected, it consists of slight outward enrichment in Mn and Ca. The low oxide totals may be due to the partial oxidation of iron which is apparent by the deep red color of many samples.

One notable feature of these analyses is the lack of any Mg while the amount of Ca present (up to 4.79 weight percent oxide) is the highest ever reported.

Destinezite - $Fe_2(PO_4)(SO_4)(OH)\cdot 5H_2O$ - triclinic (?)

Destinezite, the crystalline form of diadochite, occurs as equant microcrystalline lumps. The only specimen observed by the writer was 1 cm across and cream colored. This specimen was

Table 10. Childrenite analyses

Area	x-c_i	x-c_o	2-1	2-2	3-1	3-2	5	7_i	7_o
CaO	.37	1.77	2.30	4.79	1.96	3.11	2.81	1.14	1.17
MnO	5.40	7.34	3.32	8.39	9.58	8.47	5.02	13.73	14.60
FeO	23.48	20.76	25.30	16.01	18.69	17.34	22.31	17.10	15.85
Al_2O_3	21.53	22.30	20.59	21.36	21.11	21.39	20.51	21.02	19.89
P_2O_5	32.05	31.85	31.65	31.65	31.35	32.17	32.36	31.94	31.42
H_2O	15.68	15.68	15.68	15.68	5.68	15.68	15.68	15.68	15.68
Total	98.51	99.70	98.84	97.88	98.34	98.17	98.69	100.61	98.62
Atomic proportions based on 1.00 P:									
Ca	.01	.07	.09	.19	.08	.12	.11	.05	.05
Mn	.17	.23	.11	.27	.31	.26	.16	.43	.46
Fe	.72	.64	.79	.50	.59	.53	.68	.53	.50
Al	.94	.97	.91	.94	.94	.93	.88	.92	.88
P	1.00	1.00	1.00	1.00	1.00	1.00	1.00	1.00	1.00
Total-P	1.84	1.91	1.90	1.90	1.92	1.84	1.83	1.93	1.89

collected from talus in area 3 and its association with other minerals is not known.

Gordonite - $MgAl_2(PO_4)_2(OH)_2 \cdot 8H_2O$ - triclinic

Gordonite was found as small, white spherulites associated with wardite in area 4. Because of its extremely limited occurrence, it was not analyzed.

Lazulite - $(Mg,Fe)Al_2(PO_4)_2(OH)_2$ - monoclinic

Lazulite is ubiquitous in the Rapid Creek area where it is found in all major associations. It is deep blue to azure blue to greenish blue and well crystallized. Crystals up to 10 mm have been found but are more commonly 2-4 mm. Several samples from area 4 contain highly etched lazulite. Lazulite also occurs as a relatively rare component of pelletal and granular phosphate sandstone.

Microprobe analyses of lazulite (Table 11) were made using wyllieite 175 as a standard; water content was calculated on the basis of an ideal composition. These analyses are similar to the one reported by Cambell (1962) for lazulite recovered from the bed of Blow River.

No zoning was detected and compositional variation from area to area is limited. Mg:Fe ratios range from 5.9:1 to 3.1:1 and Mn and Ca substitute for Mg and Fe to a minor extent.

Table 11. Lazulite analyses

Area	x-c-1_i	x-c-1_o	x-c-2	1	4_i	4_o	6	7
MgO	10.90	10.88	11.17	11.23	9.60	9.56	11.26	11.27
CaO	.05	.01	.06	.05	-	-	-	.03
MnO	.21	.09	.03	.04	-	.20	.05	.04
FeO	3.99	2.94	4.18	3.37	5.88	5.58	3.53	3.42
Al_2O_3	32.70	32.64	32.14	33.00	32.79	32.33	32.54	32.35
P_2O_5	45.73	46.27	46.93	46.89	45.39	45.70	44.98	45.45
H_2O	5.96	5.96	5.96	5.96	5.96	5.96	5.96	5.96
Total	99.54	98.79	100.47	100.54	99.62	99.33	98.32	98.52
Atomic proportions based on 2.00 P:								
Mg	.84	.83	.84	.84	.74	.74	.88	.88
Ca	-	-	-	-	-	-	-	-
Mn	.01	-	-	-	-	.01	-	-
Fe	.17	.13	.18	.14	.26	.24	.16	.15
Al	1.99	1.96	1.91	1.96	2.01	1.97	2.01	1.98
P	2.00	2.00	2.00	2.00	2.00	2.00	2.00	2.00
Total-P	3.01	2.92	2.93	2.94	3.01	2.96	3.05	3.01

Figure 27. Lazulite occurrences.

Figure 28. Gormanite-souzalite occurrences.

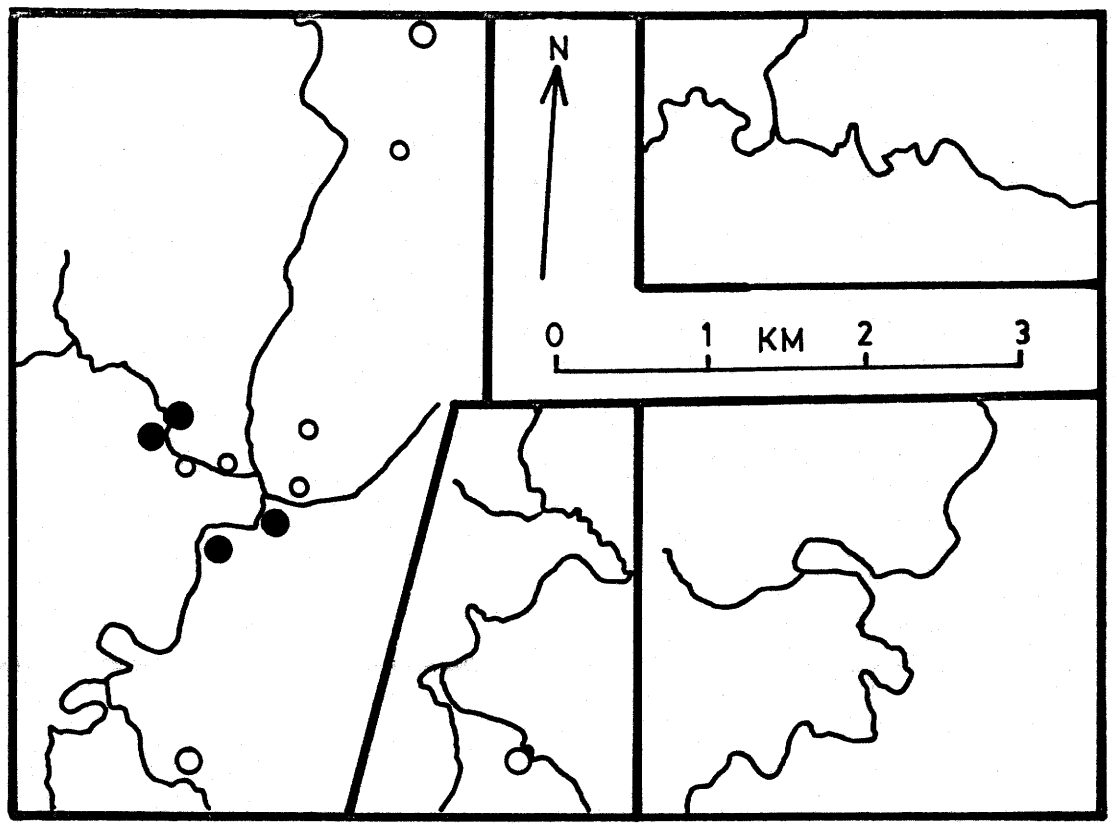

● = major ○ = minor ○ = trace

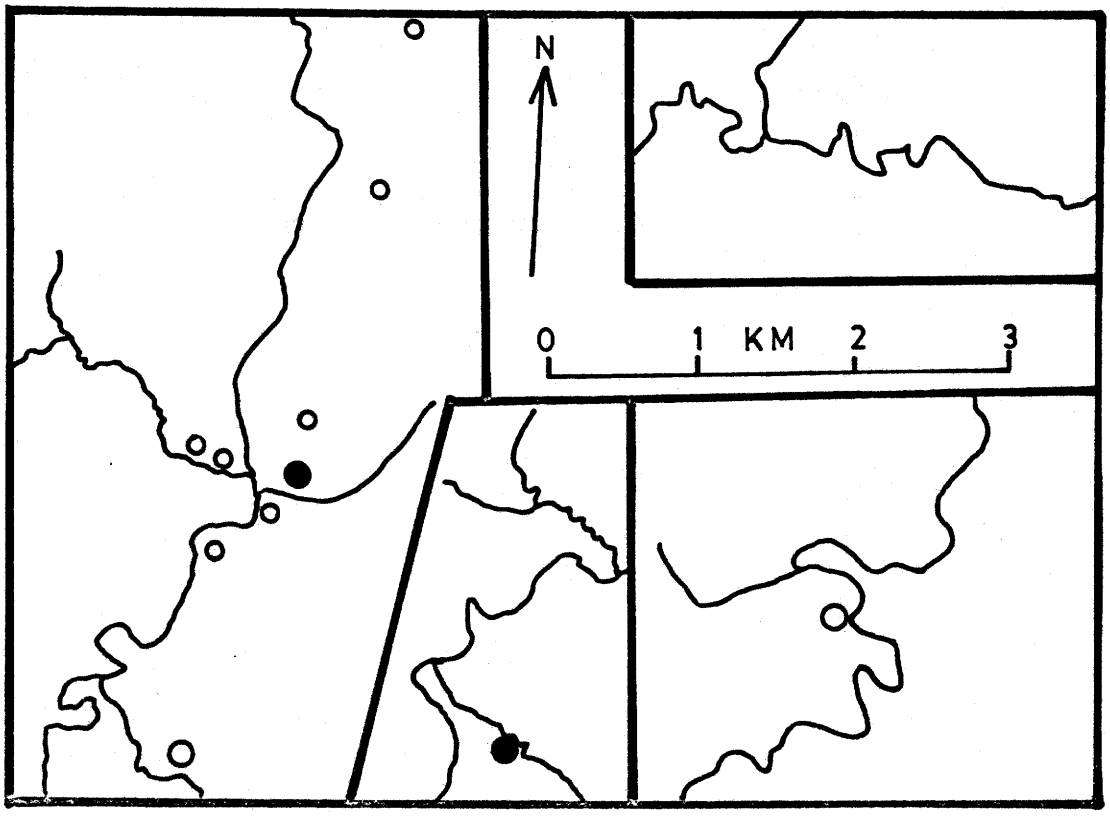

Gormanite-souzalite - $(Fe,Mg)_3(Al,Fe''')_4(PO_4)_4(OH)_6 \cdot 2H_2O$ - triclinic

Gormanite-souzalite occurs as hemispherulitic bundles alone or associated with other minerals in the Ca-rich and Fe-Mg-rich associations. It also occurs as coarse fibrous masses in veins in areas 2 and 4. Gormanite-souzalite is a major component of non-pelletal phosphate of mudstone and pelletal phosphate sandstone.

Gormanite is the Fe-analogue of souzalite (Sturman and Mandarino, in press) with which it forms a complete solid solution series. Microprobe analyses (Table 12) were obtained using wyllieite 175 as a standard with water content being calculated on the basis of a hypothetical composition in which Fe":Mg = 1:1.49 and Fe''':Al = 1:15.4. Samples 1, 2, 6, and 7 are from veins of the Fe-Mg-rich association; 4 and 5 are from simple associations.

The above analyses indicated substantial Fe/Mg solid solution. Since Fe"/Fe''' ratios have not been determined, reported ratios are on the basis of Fe as FeO. Fe:Mg ratios vary from 2.1:1 to 0.8:1 with gormanite being the dominant end-member in the Rapid Creek area.

Moderate zoning, becoming outwardly more Mg-rich, was detected in several samples. Manganese content appears to be independent of Fe and it also increases slightly outwards. The

Table 12. Gormanite-souzalite analyses

Area	1_i	1_o	2_i	2_o	4_i	4_o	5	6	7
MgO	7.56	8.35	5.41	6.86	6.66	7.56	6.31	9.26	6.51
CaO	.12	-	.47	-	-	-	.38	.06	.02
MnO	-	.19	.07	.21	.34	.89	-	.22	.16
FeO	16.30	14.15	20.50	17.60	18.77	16.70	19.08	13.70	18.38
Al_2O_3	25.50	25.65	23.12	24.33	23.90	24.51	23.51	25.21	23.74
P_2O_5	38.02	39.04	37.50	38.09	37.80	38.23	38.11	37.45	37.40
H_2O	12.11	12.11	12.11	12.11	12.11	12.11	12.11	12.11	12.11
Total	99.62	99.49	99.18	99.20	99.58	100.00	99.50	98.01	98.32
Atomic proportions based on 4.00 P:									
Mg	1.40	1.51	1.02	1.27	1.24	1.39	1.17	1.72	1.23
Ca	.02	-	.06	-	-	-	.05	.01	-
Mn	-	.02	.01	.02	.04	.09	-	.02	.02
Fe	1.69	1.43	2.16	1.83	1.96	1.73	1.98	1.45	1.94
Al	3.73	3.66	3.43	3.56	3.52	3.57	3.44	3.75	3.52
P	4.00	4.00	4.00	4.00	4.00	4.00	4.00	4.00	4.00
Total-P	6.84	6.62	6.68	6.68	6.76	6.78	6.64	6.95	6.72

variation in cationic ratios from area to area is greater than the limits of zoning for any individual specimen.

In the type locality, souzalite appears to be a hydrothermal alteration of scorzalite, the Fe-analogue of lazulite (Pecora and Fahey, 1949). Lazulite in this area is unaltered. Thus gormanite-souzalite is probably a later stage quasipolymorph of lazulite. It is interesting to note that lazulite was rarely found associated with gormanite-souzalite.

Apatite and carbonate-apatite

Apatite occurs as stout prismatic crystals in the Ca- and Ba-rich associations. It is usually white to colorless or faintly pink.

Carbonate-apatite was found in only two samples as a thin botryoidal crust lining solution cavities.

Qualitative microprobe analysis detected only Ca and P in these minerals, except for one sample of apatite which contains a trace amount of Na.

Pelletal and non-pelletal phosphate mudstone contains a large porportion of a member of the apatite group, but its identity was not determined.

Collinsite-messelite - $Ca_2(Mg,Fe,Mn)(PO_4)_2 \cdot 2H_2O$ - triclinic

Collinsite-messelite occurs as white to buff, hemispherulitic bundles in veins of the Ca-rich association in mineralized

Figure 29. Apatite and carbonate-apatite occurrences.

Figure 30. Collinsite-messelite occurrences.

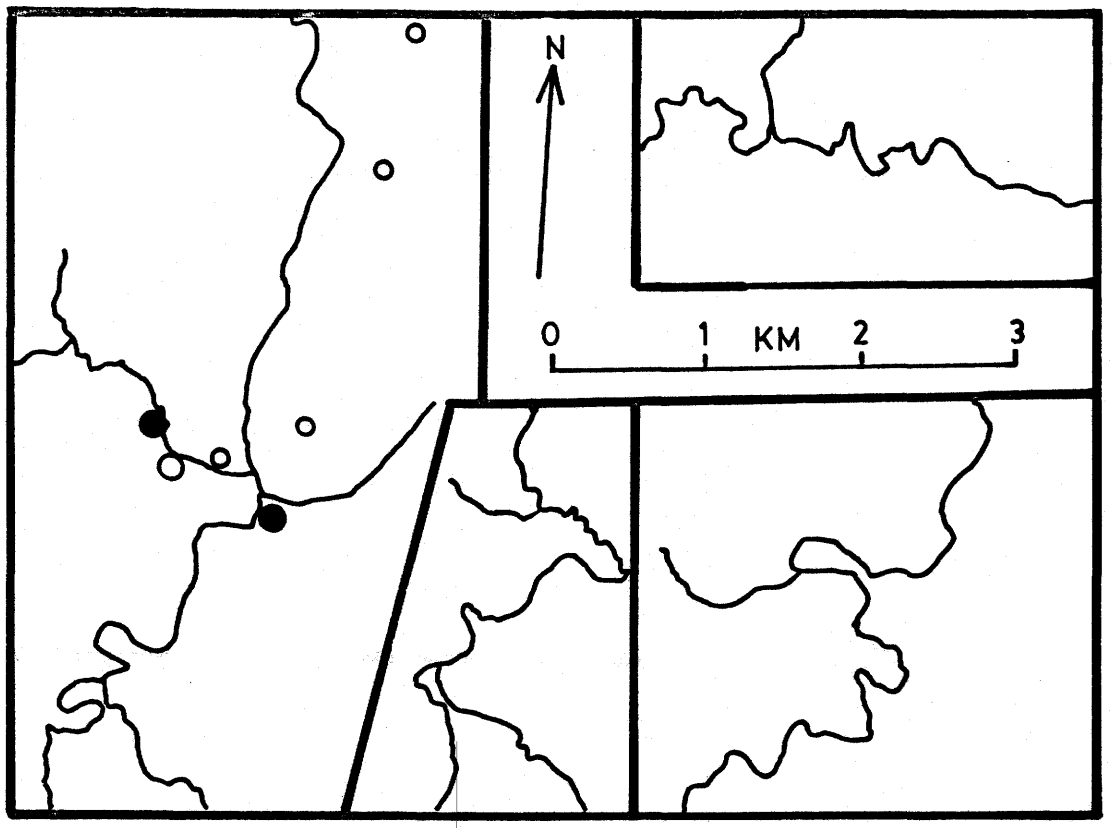

● = major ○ = minor o = trace

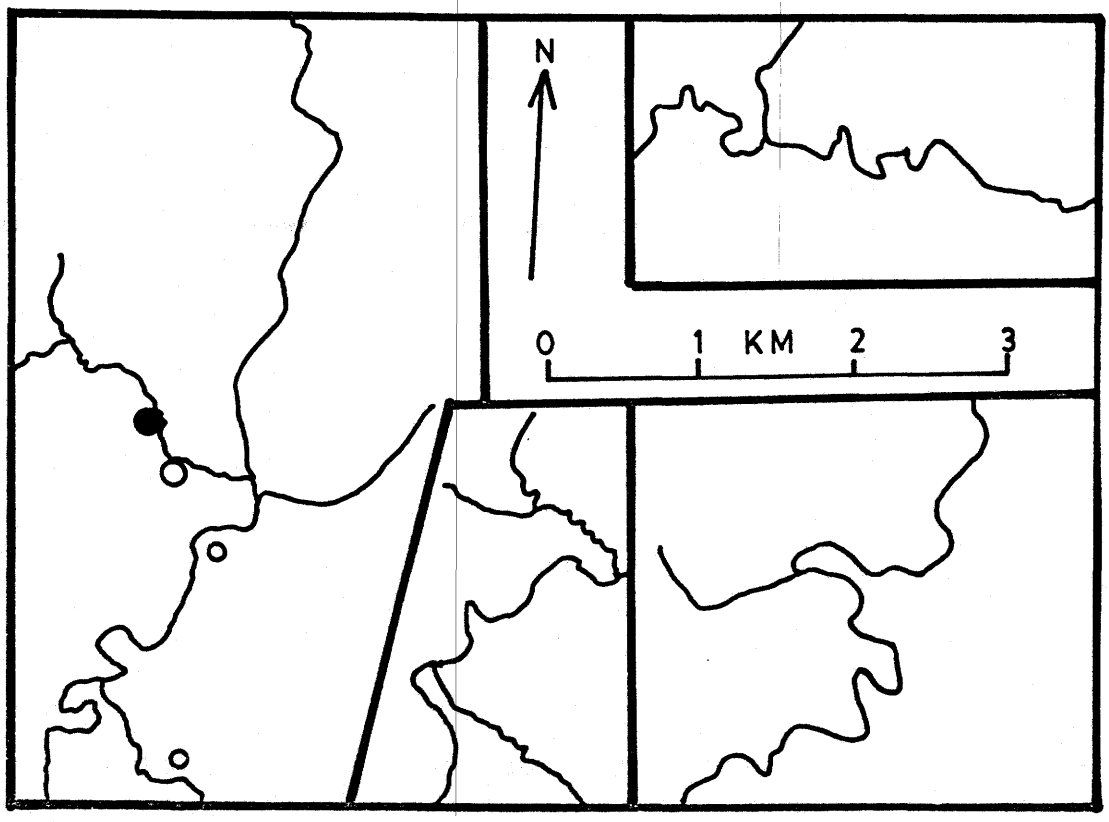

zone 1 of the Cross-cut Creek section and in veins of the Fe-Mg-rich association in area 6. Hemispherulites up to 2 cm in radius have been noted, but most are one half to one quarter that size. In area 5, a vein of the Fe-Mg-rich association contains rare blades, up to 3 cm long, of colorless collinsite which had crystallized around gormanite needles. Where it occurs in veins of the Ca-rich association, collinsite has been found on whiteite crystals.

Microprobe analyses (Table 13) were obtained using arrojadite 171, as a standard for Mg, Mn, Fe and P, and garnet 105, for Ca.

Water content was calculated using an ideal composition with Fe:Mg = 1:2.28. Sample x-c is from a Ca-rich association; the rest are from Fe-Mg-rich associations.

Rapid Creek collinsites are zoned with Mg decreasing in proportion outwards. Substitution for Mg is largely fulfilled by Mn and, to lesser extent, Fe and Ca. Cross-cut Creek samples are Fe-rich and therefore more properly designated as messelite. While the limits of solid solution are not known, the extent of zoning in the sample from area 6 suggests that there may be a comlete solid solution series between collinsite and messelite, and almost complete solid solution with fairfieldite ($Ca_2Mn(PO_4)_2 \cdot 2H_2O$).

Table 13. Collinsite-messelite analyses

Area	$x\text{-}c_i$	$x\text{-}c_o$	5-1	5-2	6_i	6_m	6_o
MgO	4.37	3.94	9.69	12.10	9.00	8.30	5.80
CaO	30.65	31.82	30.00	29.57	30.38	29.94	30.43
MnO	1.47	1.04	.26	-	1.92	2.53	4.57
FeO	12.08	11.88	7.80	4.44	6.01	6.71	6.72
P_2O_5	40.49	40.54	41.80	41.71	41.43	41.49	40.52
H_2O	10.60	10.60	10.60	10.60	10.60	10.60	10.60
Total	99.66	99.82	100.15	98.42	99.34	99.57	98.64

Atomic proportions based on 2.00 P:

Mg	.38	.34	.82	1.02	.77	.70	.50
Ca	1.92	1.99	1.82	1.79	1.86	1.83	1.90
Mn	.07	.05	.01	-	.09	.12	.23
Fe	.59	.58	.37	.21	.29	.32	.33
P	2.00	2.00	2.00	2.00	2.00	2.00	2.00
Total-P	2.96	2.96	3.02	3.02	3.01	2.97	2.96

Whiteite - (formula below) - monoclinic

Whiteite occurs as thin to thick, tabular to bladed, buff to white colored crystals, generally 1-3 cm across. It occurs rarely in a variety of rocks from area 3.

Whiteite is the Al-analogue of jahnsite (Moore and Ito, 1978) with the formula:

$XM(1)M(2)_2M(3)_2(H_2O)_8(OH)_2(PO_4)_4$

in which X accommodates Ca, Mn, and minor Na

M(1) accommodates Fe and Mn

M(2) accommodates Mg, Mn, and Fe

and M(3) accommodates Al and Fe"' and some Mg

Microprobe analyses (Table 14) of whiteite were made using whiteite 176 as a standard. Water content was calculated assuming composition with $X=Ca_{0.9}Mn_{0.1}$; $M(1)=Fe_{0.7}Mn_{0.3}$; $M(2)=Mg_{1.0}$; $M(3)=Al_{1.0}$. All whiteite samples come from veins of the Ca-rich association.

The compositions reported in Table 14 are similar to wet chemical analyses of whiteite from this locality reported by Moore and Ito (1978, Table 3, nos. 2-4) except that Al is slightly lower and no samples were very low in Ca (as with Moore and Ito, no. 4). CaO varies from 5.48 to 8.89 weight percent, the latter representing the maximum noted for any whiteite and suggesting partial filling of the M(2) or M(1) site by Ca.

Whiteite crystals are zoned from Ca-poor to Ca-rich outwards. In the samples from Cross-cut Creek ($x\text{-}c_i$ and

Table 14. Whiteite analyses

Area	x-c_i	x-c_o	1_i	1_o	3_i	3_o	7
MgO	12.27	11.50	10.11	10.26	11.33	11.11	10.98
CaO	5.48	6.65	6.27	8.89	5.69	7.47	6.09
MnO	.08	.23	2.40	1.94	4.81	4.10	2.15
FeO	11.65	11.74	11.85	10.33	8.71	7.80	10.30
Al_2O_3	10.07	10.65	11.00	10.24	10.66	10.65	10.82
P_2O_5	37.27	37.26	36.80	36.99	37.19	37.27	37.36
H_2O	21.40	21.40	21.40	21.40	21.40	21.40	21.40
Total	99.22	99.40	99.83	100.05	99.79	99.80	99.11
Atomic proportions based on 4.00 P:							
Mg	2.32	2.17	1.94	1.95	2.14	2.08	2.07
Ca	.75	.90	.86	1.22	.77	1.01	.83
Mn	.01	.02	.26	.21	.52	.44	.23
Fe	1.24	1.24	1.27	1.10	.93	.83	1.09
Al	1.66	1.59	1.66	1.54	1.60	1.59	1.61
P	4.00	4.00	4.00	4.00	4.00	4.00	4.00
Total-P	5.98	5.92	5.99	6.02	5.96	5.95	5.83

Figure 31. Whiteite occurrences.

Figure 32. Brazilianite occurrences.

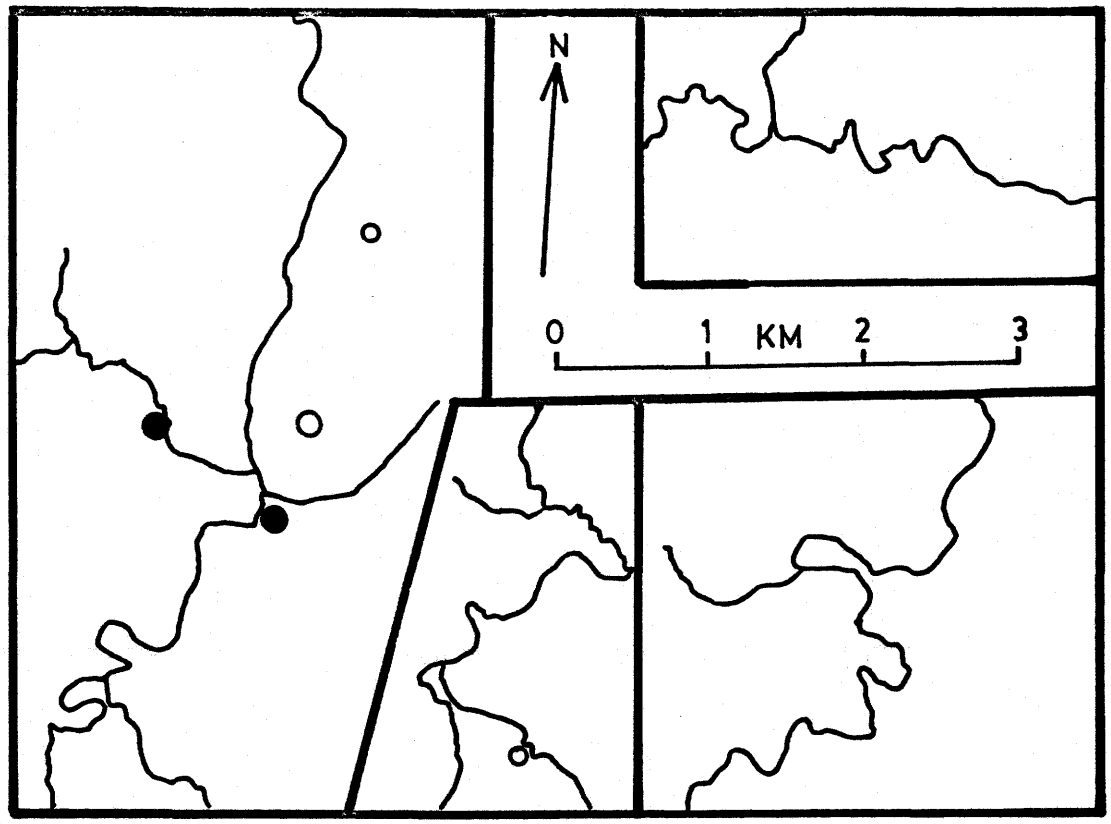

● = major ○ = minor o = trace

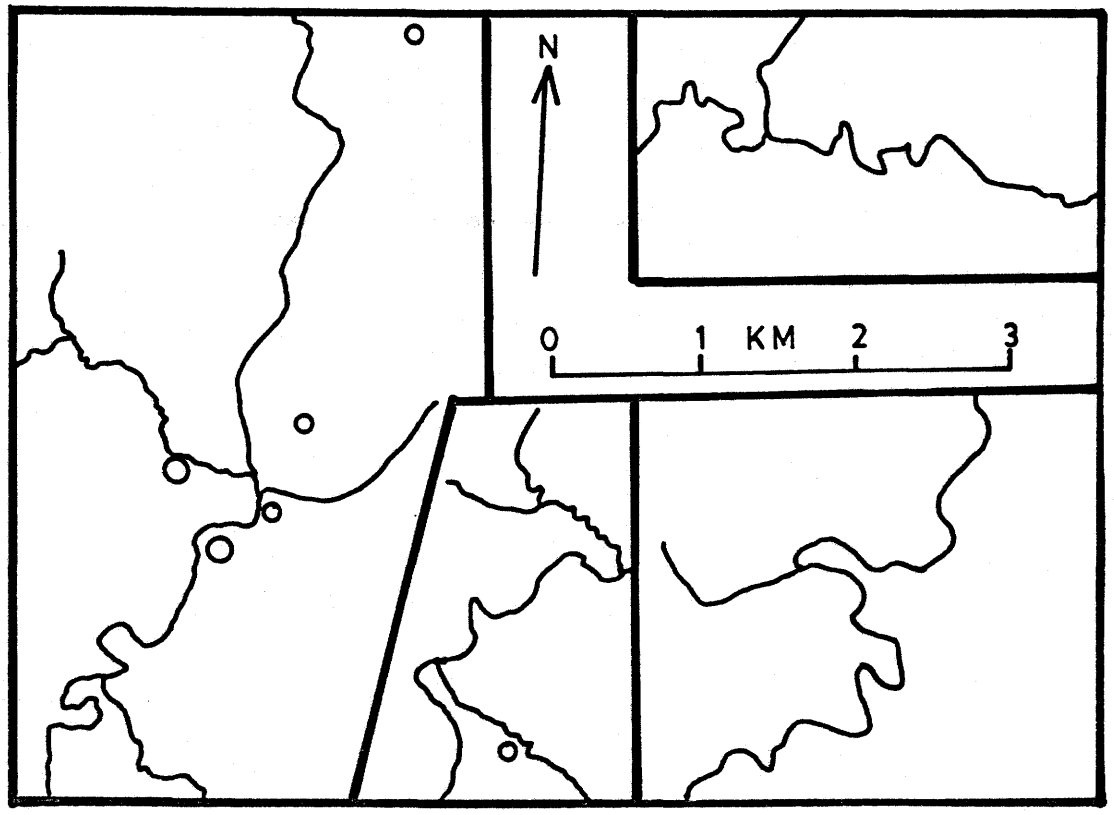

x-c_o), this Ca-enrichment is at the expense of Mg alone; in that form area 1 it is at the expense of Fe and Mn; and in that from area 3 it is at the expense of Fe, Mn, and Mg.

Brazilianite - $NaAl_3(PO_4)_2(OH)_4$ - monoclinic

Brazilianite occurs in veins of the Ba-rich and Na-bearing association. It is generally white to colorless but commonly displays a light blue or blue-green tint. Three distinct habits have been observed. In the first, it occurs as equant to short prismatic crystals which, at first glance, appear similar to apatite; in the second, it occurs with a pseudorhombohedral habit and was, at first, mistaken for augelite. In this habit it can be distinguished from augelite in that augelite crystals tend to have more and better developed faces and also two of the brazilianite faces are striated. In the third habit, it occurs as elongate crystals similar to those found in many other localities. These varieties are similar to those described by Pough and Henderson (1945). No brazilianite crystals in this area are larger than 10 mm and most are less than 3 mm.

Microprobe analyses (Table 15) of brazilianite were made using wyllieite 175 as a standard. Water content was calculated assuming an ideal composition. Samples x-c-1&2 and 7-1&2 come from Ba-rich associations; 1 and 3-1&2 are from Na-bearing associations.

Most samples contain trace amounts of Ca and Mn and minor

Table 15. Brazilianite analyses

Area	x-c-1	x-c-1	1	3-1	3-2	7-1	7-2
Na_2O	8.31	8.33	8.81	8.62	8.10	8.40	8.37
CaO	.04	.03	.03	.02	.01	.02	.02
MnO	.04	-	.15	.03	.10	-	-
FeO	.73	.69	-	.43	.38	.91	.41
Al_2O_3	42.24	42.09	43.44	42.48	42.33	42.09	41.97
P_2O_5	38.93	38.53	38.26	38.41	38.71	38.10	39.14
H_2O	9.96	9.96	9.96	9.96	9.96	9.96	9.96
Total	100.25	99.63	100.64	99.95	99.59	99.48	99.77
Atomic proportions based on 2.00 P:							
Na	.98	.99	1.05	1.03	.96	1.01	.98
Ca	-	-	-	-	-	-	-
Mn	-	-	.01	-	.01	-	-
Fe	.04	.04	-	.02	.02	.05	.02
Al	3.02	3.04	3.16	3.08	3.04	3.08	2.99
P	2.00	2.00	2.00	2.00	2.00	2.00	2.00
Total-P	4.04	4.07	4.22	4.13	4.03	4.14	3.99

amounts of Fe. Brazilianite is unzoned and relatively consistent in composition from area to area.

Wardite - $NaAl_3(PO_4)_2(OH)_4 \cdot 2H_2O$ - tetragonal

Wardite occurs in simple, Na-bearing, and Ba-rich associations. In most occurrences it is colored in shades of light greenish yellow but, in places, is also light blue to grey and white and, in very small crystals, is generally colorless. In all areas, wardite occurs in well-developed dipyramidal (pseudooctahedral) crystals with horizontally striated faces similar to those described by Fisher and Runner (1958). Occasionally, other small faces are developed which tend to bevel corners. Wardite crystals have been found up to 2 cm across, but ones larger than 5 mm are relatively uncommon, except in area 4.

Wardite proved too unstable under an electron beam to permit quantitative microprobe analysis. Qualitative analysis indicates the presence of Na, Al, and P with only minor or trace amounts of Ca and Fe.

Arrojadite - $K(Na,Ca)_5(Fe,Mn,Mg)_{14}Al(OH,F)(PO_4)_{12}$ - monoclinic

Arrojadite occurs in simple and Fe-Mg-rich associations, where it is generally orange-brown to deep green and occurs as flattened diamond-shaped crystals or as curved lamellar aggregates up to 1 cm long. This is the first reported

Figure 33. Wardite occurrences.

Figure 34. Arrojadite occurrences.

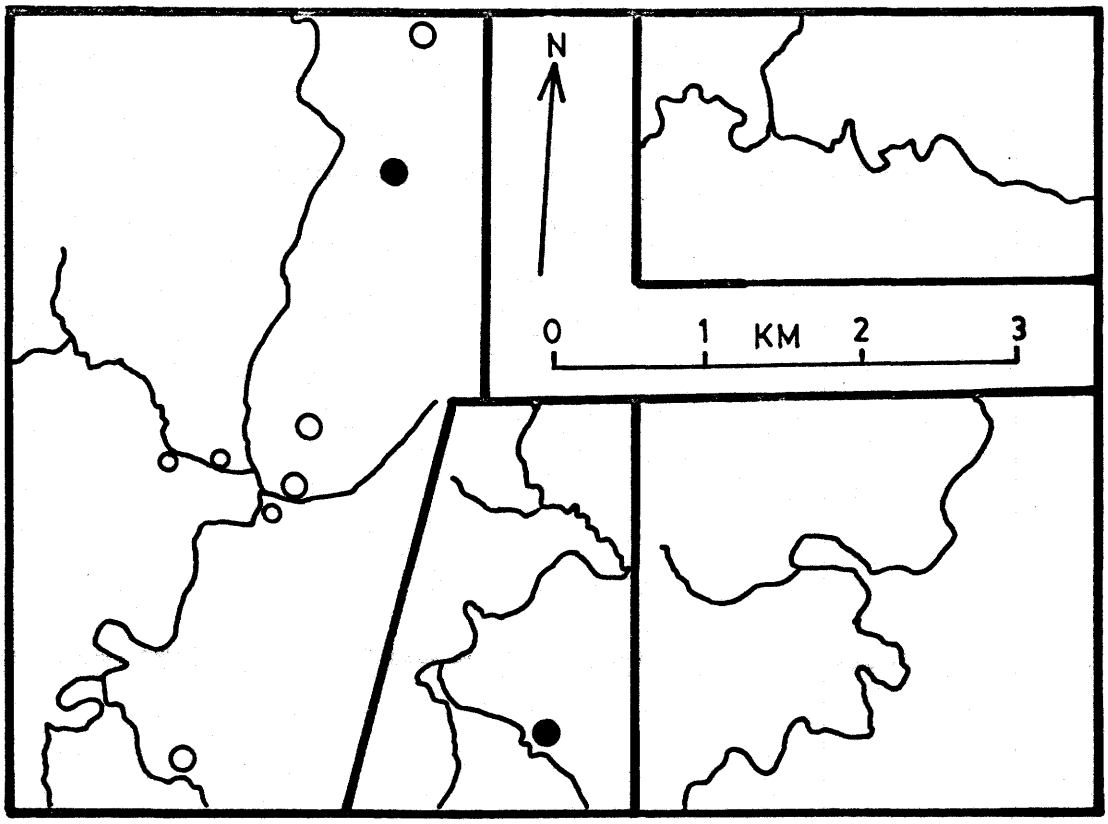

● = major ○ = minor o = trace

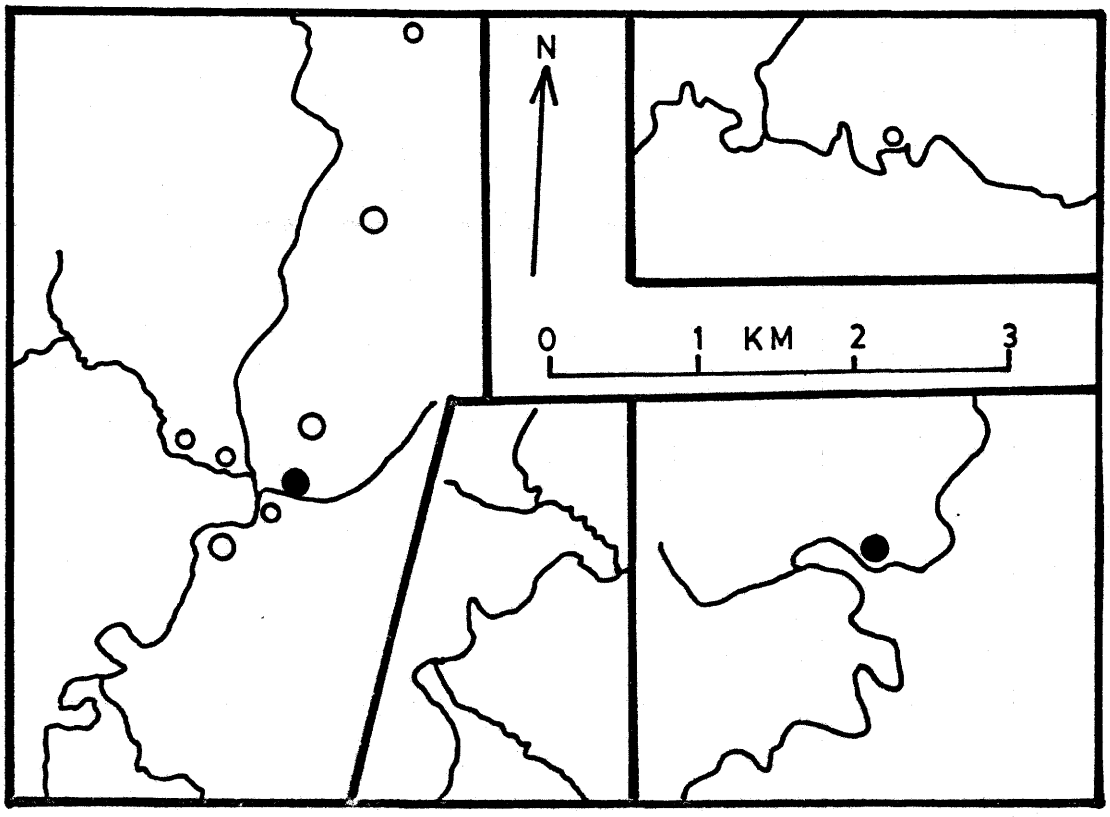

occurrence of arrojadite crystals (Sturman, pers. comm.). Their habit is similar to that depicted by Palache et al. (1951) for dickinsonite. Arrojadite is a major constituent of pelletal phosphate and siderite sandstone in the Rapid Creek area.

Microprobe analyses (Table 16) were made using a sample of arrojadite from Big Fish River as a standard. All samples are from veins of the Fe-Mg-rich association.

These analyses indicate only minor compositional variation from area to area, except at Big Fish River where arrojadite is Mn-rich.

Kryzhanovskite - (Fe,Mg,Mn) $Fe^{3+}_2 (PO_4)_2(OH)_2 \cdot H_2O$ - orthorhombic

Kryzhanovskite occurs as large cleavable masses in veins of the Fe-Mg-rich association. It is brown to red-brown in color with the one cleavage direction showing a distinct bronze color. Poorly developed prismatic crystals were found in area 5.

Microprobe analyses (Table 17) were made using maricite 170, as a standard for P and Fe, and wyllieite 175, for Mg, Al, Ca, and Mn. Water content was calculated assuming a composition of $MgFe^{3+}_2(PO_4)_2(OH)_2 \cdot H_2O$. Fe is reported as total Fe_2O_3.

Compositions are quite variable with Fe:Mg ratios ranging from 1.3:1 to 3.6:1 with up to 5.40 weight percent MnO substituting for Fe and Mg. Minor amounts of Ca and Al are also present.

Zoning in kryzhanovskite was determined qualitatively on a

Table 16. Arrojadite analyses

Area	FR*	2-1	2-2	2-3	3	4-1	4-2	6_i	6_o
Na_2O	7.37	6.17	6.65	5.62	6.67	3.45	5.69	6.61	5.89
K_2O	1.81	2.35	2.06	2.07	2.22	3.06	2.06	2.14	2.19
MgO	3.27	5.31	5.05	4.43	5.33	4.92	4.07	4.26	4.56
CaO	2.53	2.27	2.45	2.47	2.54	2.19	2.31	2.45	2.75
MnO	4.60	1.36	1.44	3.12	2.11	1.68	1.77	1.57	1.60
FeO	34.32	35.92	35.41	36.97	35.65	39.79	38.25	39.23	37.25
Al_2O_3	2.49	2.61	2.58	3.09	2.47	2.05	2.51	2.64	2.54
P_2O_5	40.79	42.62	42.25	40.74	40.67	40.79	40.80	40.85	40.73
Total	97.18	98.61	97.98	98.51	97.66	97.92	97.46	99.75	97.51
Atomic proportions based on 12.00 P:									
Na	4.97	3.98	4.32	3.79	4.51	2.33	3.83	4.45	3.97
K	.80	1.00	.88	.92	.98	1.35	.91	.95	.97
Mg	1.69	2.63	2.53	2.29	2.77	2.55	2.11	2.20	2.37
Ca	.94	.81	.91	.92	.95	.82	.86	.91	1.03
Mn	1.36	.38	.41	.92	.62	.49	.52	.46	.47
Fe	9.97	9.99	9.93	10.76	10.39	11.56	11.11	11.38	10.84
Al	1.02	1.02	1.02	1.27	1.02	.84	1.03	1.08	1.04
P	12.00	12.00	12.00	12.00	12.00	12.00	12.00	12.00	12.00
Total-P	20.75	19.81	20.00	20.87	21.24	19.94	20.37	21.43	20.69

*probe analysis by M. Corlett, used as a standard

Table 17. Kryzhanovskite analyses

Area	ideal	2-1	2-2	4-1	4-2	4-3	5
MgO	10.66	8.48	6.47	10.46	13.03	8.18	10.55
CaO	-	.43	.13	.30	.18	.50	.53
MnO	-	.93	1.13	5.40	4.57	1.51	1.24
Al_2O_3	-	.40	.41	.46	.38	.35	.82
Fe_2O_3	42.25	43.43	46.74	34.96	33.08	43.26	39.28
P_2O_5	37.55	37.45	36.79	38.37	38.68	37.28	37.97
H_2O	9.54	9.54	9.54	9.54	9.54	9.54	9.54
Total	100.00	100.23	101.18	99.52	99.46	100.62	99.93
Atomic proportions based on 2.00 P:							
Mg	1.00	.80	.62	.97	1.19	.78	.98
Ca	-	.03	.01	.02	.02	.04	.04
Mn	-	.06	.07	.29	.24	.09	.07
Al	-	.04	.04	.04	.03	.03	.06
Fe	2.00	2.07	2.26	1.63	1.53	2.07	1.84
P	2.00	2.00	2.00	2.00	2.00	2.00	2.00
Total-P	3.00	3.00	3.00	2.95	3.01	3.01	2.99

Figure 35. Kryzhanovskite occurrences.

Figure 36. Ludlamite occurrences.

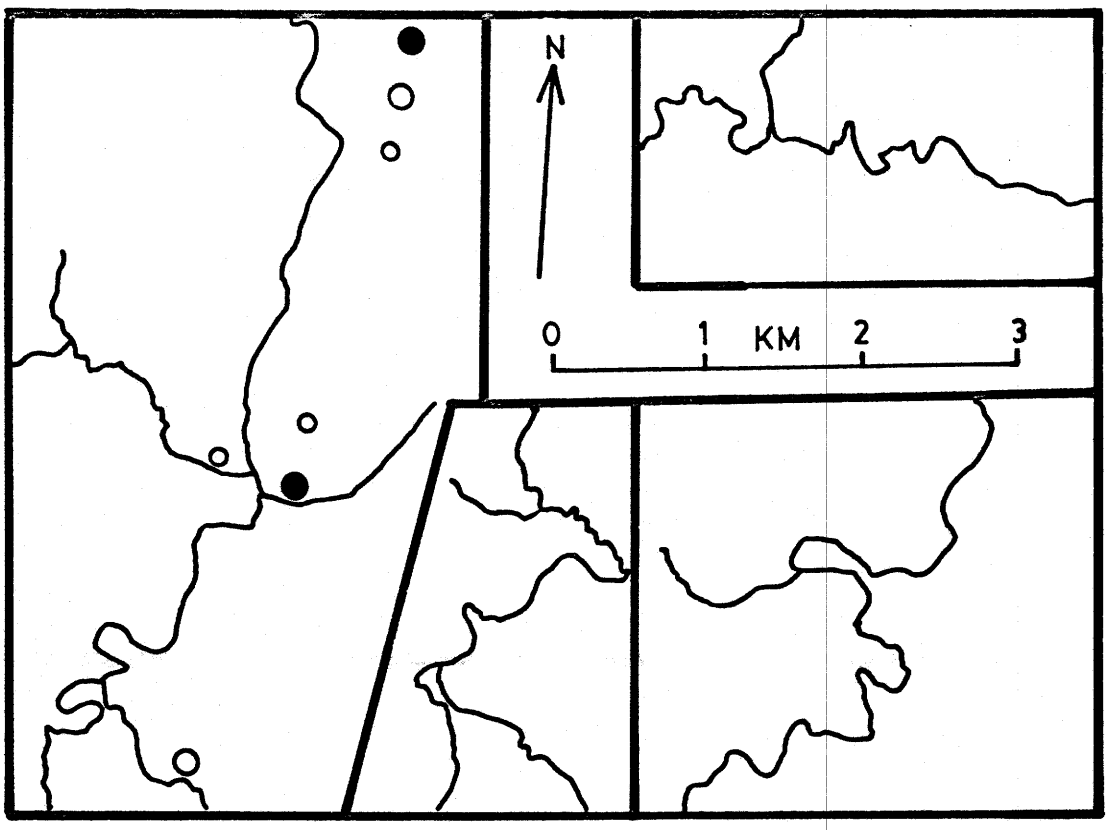

● = major ○ = minor ○ = trace

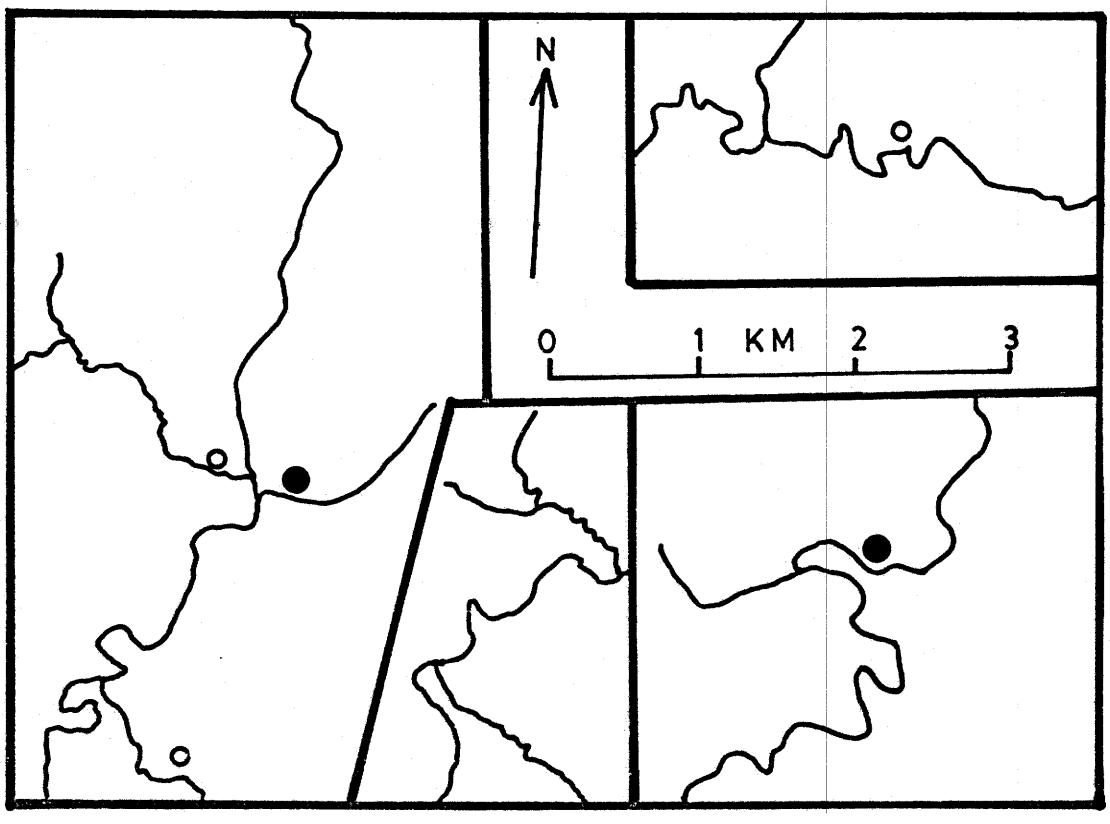

crystal from area 5 and consists of Mg-enrichment outwards. There is also a slight tendency for Mn to increase outwards.

Ludlamite - $(Fe,Mg,Mn)_3(PO_4)_2 \cdot 4H_2O$ - monoclinic

Ludlamite occurs as large, green, cleavable masses in veins of the Fe-Mg-rich association. It occurs alone as bright green, parallel to curved, fibrous masses or as a light brown alteration product of various minerals in nodules in the Big Fish River area. It also occurs as an alteration product in pelletal and granular phopshate sandstone in area 3.

Microprobe analyses (Table 18) were made using wyllieite 175 as a standard.

Ludlamite is not zoned and Mg and Mn substitute for Fe to a small degree. The reported Al may be due to contamination during specimen polishing.

Vivianite-baricite - $(Fe,Mg)_3(PO_4)_2 \cdot 8H_2O$ - monoclinic

Vivianite-baricite occurs as large plates and micaceous masses in veins of simple, Fe-Mg-rich or Ca-rich association. It occurs as elongate crystals associated with arrojadite in the Big Fish River and where it also occurs as an alteration of wolfeite, satterlyite, and maricite in nodules. Vivianite-baricite is a common, but minor, component of various rock types in the Rapid Creek area where it occurs as a pore filling and alteration product. When fresh, vivianite-baricite is colorless

Figure 37. Vivianite-baricite occurrences.

Figure 38. Metavivianite occurrences.

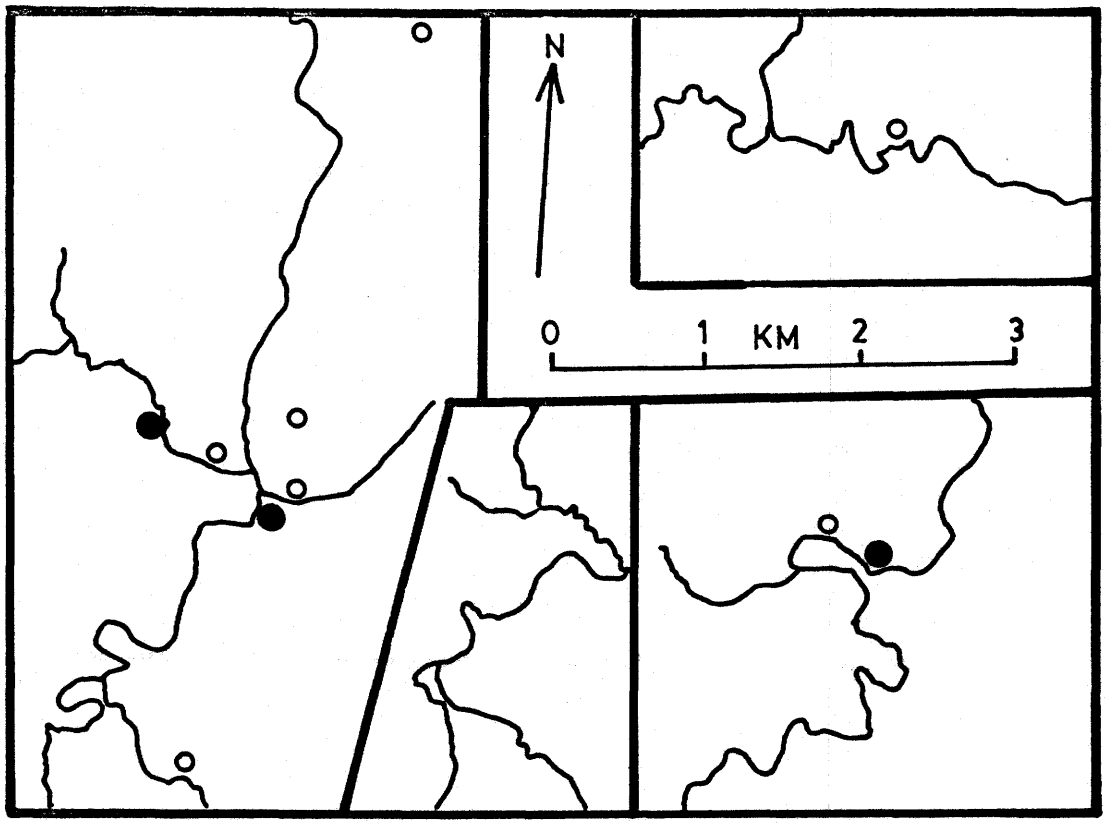

● = major ○ = minor o = trace

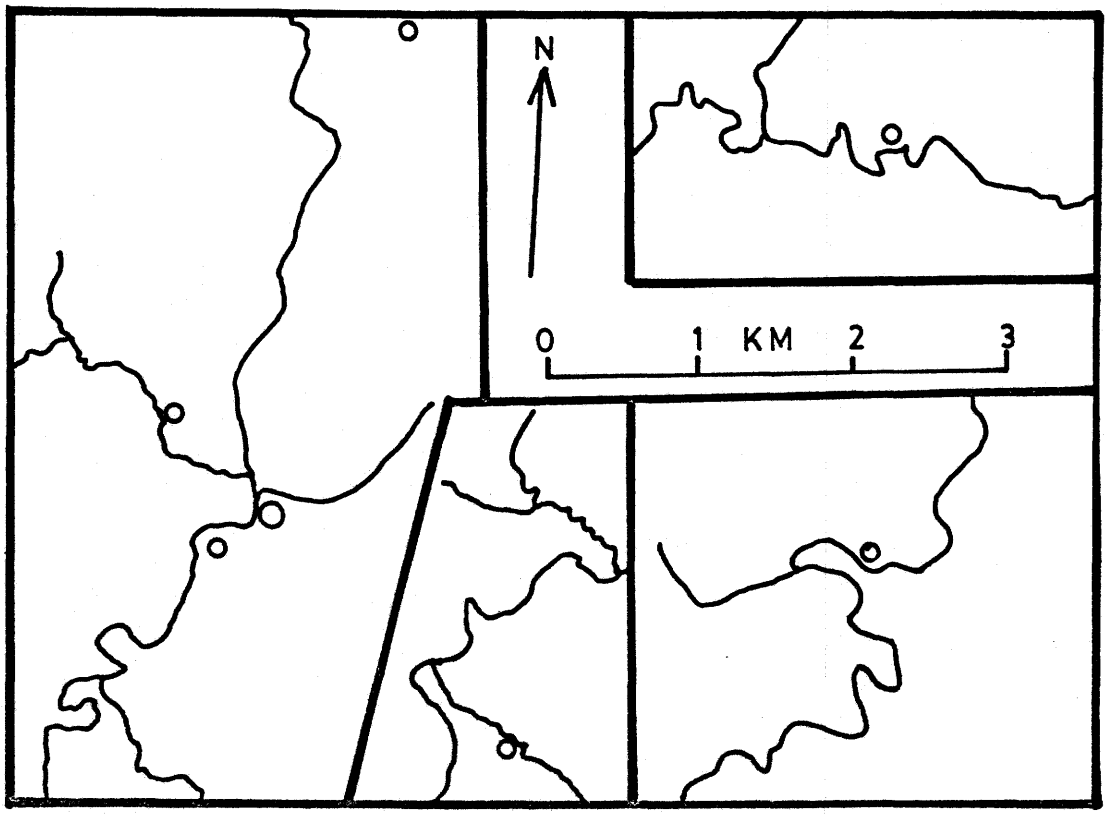

but it quickly oxidizes and turns blue on exposure to air. With prolonged exposure, it breaks down to a yellowish earth alteration product.

Microprobe analyses (Table 18) of samples from four localities (including the type locality for baricite (Sturman and Mandarino, 1976) were made using wyllieite 175 as a standard. Water contents are apparently quite variable due to partial oxidation of Fe. Sample x-c is from a Ca-rich association; the rest are from Fe-Mg-rich associations.

The analyses indicate considerable variation in composition, particularly with respect to Mg and Fe. The Al reported may be due to contamination during polishing. Manganese substitutes for Mg and Fe, but has an observed maximum of 1.57 weight percent oxide. The reported Ca may also be due to contamination.

While strong zoning from vivianite towards baricite was observed in the material from the baricite type locality (sample x-c), none of the materials analyzed during this study can be properly called baricite because all have Mg/Fe ratios less than 1.0.

Metavivianite - $Fe_3(PO_4)_2 \cdot 8H_2O$ - triclinic

Metavivianite occurs as dark to light green, cleavable to micaceous masses alone or in veins of the Fe-Mg-rich and Na-bearing association. It also occurs as an alteration product

Table 18. Vivianite-baricite and ludlamite analyses

Area	vivianite-baricite x-c_i	vivianite-baricite x-c_o	vivianite-baricite 1	vivianite-baricite 3	vivianite-baricite 4	ludlamite 2-1	ludlamite 2-2	ludlamite 2-3
MgO	5.61	12.66	4.99	8.57	11.71	3.92	4.08	4.64
CaO	.03	.04	-	.07	-	-	-	-
MnO	.42	.53	1.39	1.29	1.57	.55	.69	.88
FeO	34.45	23.97	34.07	30.59	24.89	42.02	42.21	41.13
Al_2O_3	-	.17	.11	.21	.10	.31	.16	.09
P_2O_5	29.67	31.30	29.43	31.18	31.34	33.41	33.57	33.53
Total	70.18	68.67	69.99	71.91	69.61	80.21	80.71	80.26
Atomic proportions based on 2.00 P:								
Mg	.67	1.43	.60	.97	1.32	.42	.44	.49
Ca	.01	.01	-	.01	-	-	-	-
Mn	.03	.04	.10	.09	.10	.04	.05	.06
Fe	2.32	1.52	2.29	1.94	1.57	2.49	2.50	2.43
Al	-	.02	.02	.02	.01	.03	.02	.01
P	2.00	2.00	2.00	2.00	2.00	2.00	2.00	2.00
Total-P	3.03	3.02	3.01	3.03	3.00	2.98	3.01	2.99

of other phosphates in nodules in the Big Fish River and Boundary Creek areas.

Metavivianite is the triclinic dimorph of vivianite (Ritz et al., 1974). Material of this study is too soft and altered to allow polishing for quantitative microprobe analysis. Qualitative analysis indicates major amounts of Fe and P are present with only very minor amounts of Mg and Mn. Slight zoning, with Mg-enrichment outwards, was also detected.

Gorceixite - $BaAl_3(PO_4)_2(OH)_5 \cdot H_2O$ (?) - trigonal

Gorceixite is found only in the Ba-rich association where it occurs as tabular rhombohedral to psuedocubic crystals which are orange-brown to white in color. This is the first reported occurrence of gorceixite crystals (Sturman, pers. comm.). Their habit is similar to that depicted in Palache et al. (1951) and described by Mrose (1953) for goyazite.

Quantitative microproble analyses were not made because of the mineral's scarcity. Qualitative analysis indicates the presence of Ba, Al, and P with a minor or trace amount of Ca.

Goyazite, the Sr-analogue of gorceixite, has been reported from area 7 (H. G. Ansell, pers. comm.) but was not observed by the writer.

Figure 39. Kulanite-penikisite occurrences.

Figure 40. Gorceixite occurrences.

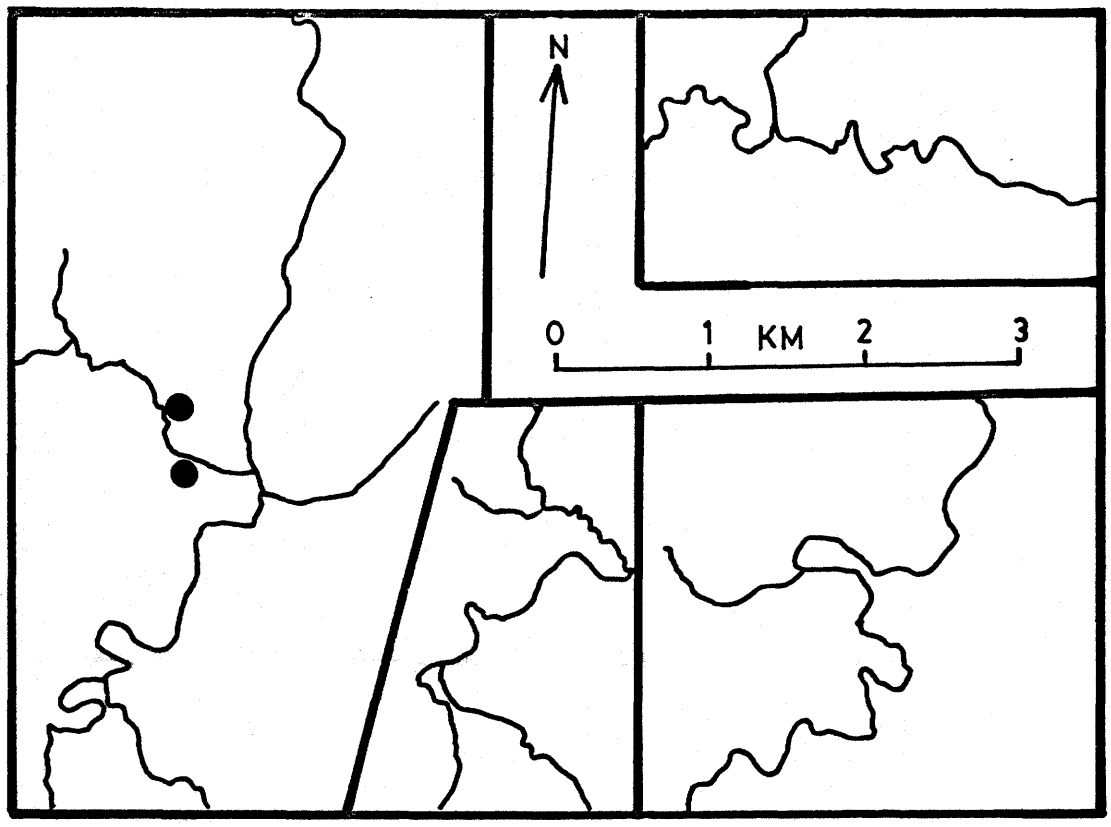

● = major ○ = minor o = trace

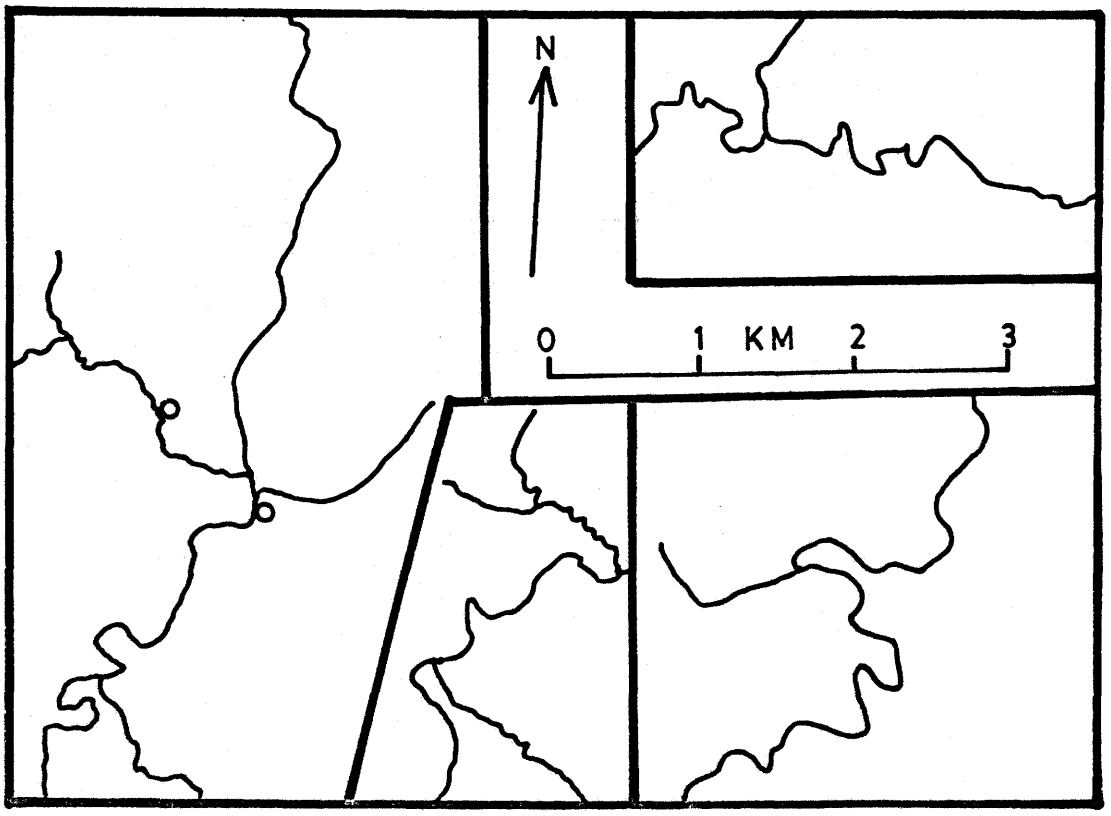

Kulanite-penikisite - $Ba(Fe,Mg,Mn,Ca)_2(Al,Fe)_2(PO_4)_3(OH)_3$ - triclinic

Kulanite (Mandarino and Sturman, 1976) and penikisite (Mandarino et al., 1977) are new minerals from this locality and have been adequately described in these papers. Qualitative microprobe analysis during this study confirms an uneven outward enrichment of the Mg-rich member of this series as is reported by Mandarino et al. (1977) for material from mineralized zone 2 in the Cross-cut Creek section.

Maricite - $NaFePO_4$ - orthorhombic

Maricite is a new mineral reported first from this locality and has been fully described by Sturman et al. (1977).

Satterlyite - $(Fe,Mg,Fe''',H,Na,Mn)_2PO_4(OH)$ - hexagonal

Satterlyite (Mandarino et al., 1978) is a new mineral reported first from the Big Fish River area where it occurs with other phosphates in spherulitic nodules. A new occurrence of it was discovered by the writer on Boundary Creek where satterlyite nodules are even more abundant than in the type locality. Satterlyite is also the principal phosphate component of pelletal and granular phosphate sandstone in the Rapid Creek area.

Varulite - $(Na,Ca)(Mn,Fe)_2(PO_4)_2$ - orthohombic (?)

Varulite is a rare component in nodules in the Big Fish River area. Here it occurs in patches between radial blades of other phosphates, usually satterlyite or maricite, and is apparently an alteration of these minerals.

Wolfeite - $(Fe,Mn,Mg)_2PO_4(OH)$ - monoclinic

Wolfeite has the same general occurrence as maricite and satterlyite but is far more abundant. It is reddish brown to deep red in color.

Wolfeite is the monoclinic dimorph of satterlyite and has the same chemical composition. It generally contains slightly less Mn and Mg than does satterlyite.

Nahpoite - Na_2HPO_4 - monoclinic

This is the first reported natural occurrence of disodium hydrogen orthophosphate, which has been named nahpoite. Detailed description of nahpoite will be published at a later date.

Nahpoite occurs as a microscopically-grained, white alteration product of maricite in fractured nodules in the Big Fish River area.

The x-ray powder diffraction data are in good agreement with Inorganic Powder Diffraction File Card no. 10-184 and with synthetic material prepared in this study. The first routine

diffraction made on this material could not be positively identified. A second pattern run on the same sample two weeks later was very different from the first and was identified as anhydrous disodium hydrogen orthophosphate. By comparing the first diffractogram with various hydrated forms of this compound, a relatively good match was obtained with the septahydrate (file card nos. 12-445 and 10-191). This indicates that this compound is unstable with respect to water content.

Nahpoite proved to be too soft for polishing for microprobe analysis. A two milligram sample was dissolved in water and analyzed by atomic absorption spectrometry by Dr. Smithson of the Saskatchewan Research Council. Results indicated a relatively pure sample with Na and P as major constituents and a trace amount of K. However, the error associated with such a small sample made the results unreliable and, in fact, in contradiction to the compound indicated by x-ray diffraction.

A thirteen milligram sample was analyzed for P, by colorimetry, and Na, by atomic absorption spectrometry, by E. Bailey of the Chemistry Department, University of Saskatchewan. This analysis gave a Na/P ratio of 1.998 for the natural material which is consistent with the formula Na_2HPO_4.